TRIBOLOGY OF POLYMERIC COATINGS FOR AGGRESSIVE BEARING APPLICATIONS

BY

SEUNG MIN YEO

DISSERTATION

Submitted in partial fulfillment of the requirements
for the degree of Doctor of Philosophy in Mechanical Engineering
in the Graduate College of the
University of Illinois at Urbana-Champaign, 2013

Urbana, Illinois

Doctoral Committee:

Professor Andreas A. Polycarpou, Chair and Director of Research
Professor Emeritus Thomas F. Conry
Professor Pascal Bellon
Assistant Professor Seok Kim

ABSTRACT

To meet the higher performance requirements of today's air-conditioning and refrigeration (ACR) compressors, their operating conditions have been getting harsher under higher speed and load, thus making tribological characteristics of interacting surfaces playing a significant role in compressor's reliability. However, the capabilities of conventional fluid lubricants are limited such that the state of lubrication is usually unknown, and, at best, in the boundary/mixed lubrication regimes. Therefore, it becomes necessary to implement some type of advanced protective coatings on the interacting surfaces to withstand stringent contact conditions. Due to favorable tribological performance, polytetrafluoroethylene (PTFE)- and polyetheretherketone (PEEK)-based polymeric coatings have received interest in ACR compressor applications, as a potential solution to supplement and potentially replace conventional oil lubricants. However, compared to a great amount of research and experiments done so far for bulk of polymers, there is limited literature on the tribological performance of PTFE- and PEEK-based polymeric coatings.

In this work, several PTFE-, PEEK-, resin- and fluorocarbon-based polymeric coatings, coated on gray cast iron were tribologically evaluated using a specialized tribometer under compressor specific conditions. The coatings showed good to excellent tribological performance, and in general PTFE-based coatings exhibited better friction and wear behavior than the rest of the coatings, including PEEK-based coatings.

The micromechanical properties of polymeric coatings were examined using instrumented microindentation. The load-unload responses were used to measure the

load-bearing properties of the coatings, as well as to extract their elastic modulus and hardness values. Induced structural differences between the PTFE- and PEEK-based coatings were confirmed using scanning electron microscopy. These measurements were used to explain the difference in the tribological performance between PTFE- and PEEK-based coatings.

Additionally, the polymeric coatings were tested under elevated (aggressive) temperature conditions to investigate the effect of increasing temperature on their tribological behavior. The friction coefficient of the polymeric coatings usually increased with temperature, reaching a maximum value in the vicinity of their glass transition temperature, and then dropped significantly with further increase of temperature. A measured property called "recovery" was investigated as a key factor affecting the frictional behavior of these coating surfaces using scratch testing, showing that surfaces with higher recovery exhibited lower friction coefficient.

Finally, the tribological performance of two representative PTFE- and PEEK-based polymeric coatings was evaluated under fretting motion testing. The effect of oil on the friction and wear behavior of the coatings was also studied under fretting test conditions. It was found that the eventual tribological behavior of a polymeric coating depended greatly on the transfer film formed on the counterface. Coating tested with oil showed worse performance than dry condition because the oil prevented the formation of transfer film on the counterface. The morphology of the transfer films on the counterface was observed using SEM and profilometer measurements along with detailed discussion of mechanism of transfer film development and its effect on polymer tribology.

ACKNOWLEDGEMENTS

First of all, I would like to sincerely thank my advisor, Professor Andreas. A. Polycarpou. My gratitude for his friendly and valuable advice and guidance not only on the research but also on my life cannot be overemphasized. From the first day we met in 2007 summer, he has always trusted and supported me and my work, and without such entire trust and respect of his, the completion of this dissertation wouldn't have been possible.

I would like to thank my mother, Hoo Nam Kim and father, Kyoo Yub Yeo in South Korea. Their endless love for me has always been one of the strongest motives of my life and during my graduate study as well.

I have always been proud of being a member of MicroTriboDynamics Lab., and there were many Lab. mates that I would like to thank. Especially, I would like to give special thanks to Wasim Akram and Shahla Chowdhury who sincerely cheered me to overcome the hard time especially at the end of my PhD life.

This research work was supported by the 28 member companies of the Air Conditioning and Refrigeration Center (ACRC), an Industry-University Cooperative Research Center at the University of Illinois at Urbana-Champaign. I would like to thank these sponsoring companies for their insightful discussions, input, support, and donation of samples. SEM, scratch and indentation measurements were carried out in the Materials Research Laboratory, University of Illinois, which is supported by the Department of Energy's Office of Basic Energy Sciences, Materials Sciences and Engineering Division (DOE BES\DMS); Department of Defense (DOD) agencies and

DARPA; the National Science Foundation (NSF); other federal agencies; industry; and the University of Illinois.

TABLE OF CONTENTS

CHAPTER 1: INTRODUCTION

1.1 Background and motivation

Traditionally liquid-type lubricants have effectively served in reducing the friction and wear of rolling and sliding bearings inside the air-conditioning and refrigeration compressors to prolong their lifetime. Similarly liquid lubricants have been used since antiquity for friction and wear reduction. However, in order to meet higher performance requirements, modern air-conditioning and refrigeration compressors (and other mechanical components and engines in general) need to function at harsher operating conditions, including higher speeds and loads. Such severe conditions could cause higher temperature, friction, excessive wear and catastrophic failures of critical interacting components, thus the tribological performance of interacting surfaces plays a significant role in compressor's reliability. A further complexity in the operation of such devices is that the state of liquid type lubrication is usually unknown, and is considered (at best) to be in the boundary/mixed (or starved) lubrication regimes (Pergande *et al.*, 2004).

Moreover, there were two international agreements (Table 1.1) regulating the usage of conventional HCFC- (Montreal Protocol) and HFC-based refrigerants (Kyoto Protocol). The Montreal Protocol is designed to protect the ozone layer by phasing out the production of numerous substances believed to be responsible for ozone depletion, including CFCs, HCFCs, HBFCs and Halons which are mainly man-made chlorines. Consequently, refrigerants based on CFCs (R12), HCFCs (R22) were replaced by HFC-based such as R134A and R404A. In 2005, however, these HFC-based refrigerants were

again regulated by Kyoto Protocol due to their high global warming potentials (Table 1.2). Nowadays, therefore, more environmentally friendly refrigerants based on natural gases such as CO_2 (R744) are of great interest to compressor companies. Even though CO_2 is also regulated by the Kyoto Protocol, CO_2 is still the best solution replacing HFC-refrigerants, because CO_2 has no ODP and a negligible GWP of 1 as seen in Table 1.2. Unfortunately, however, this CO_2 based refrigerants had miscibility issues with conventional refrigeration oils, and also the properties of oils were significantly affected under CO_2 environment, in addition of their need to operate at very high pressures, which renders direct replacement of current refrigerants (in the same compressors) impossible.

Table 1.1 Two protocols regulating the usage of refrigerants

Protocol	**Montreal Protocol**	**Kyoto Protocol**
Year	September 1987 (UNEP)	February 2005 (UNFCCC)
Objective	Reduce emission of **ODC** (Ozone-Depleting-Chemicals)	Reduce emission of **GHG** (Green-House-Gases)
Regulating Gases	**CFCs, HCFCs**, HBFCs, Halons (mainly man-made chlorines)	**CO_2, HFCs**, PFCs, CH_4, N_2O, SF_6
Result	**HCFCs** have been replaced by **HFCs**.	**HFCs** have been replaced by **natural gases**.

Table 1.2 Refrigerant Characteristics

Type	**Refrigerant**	**ODP**	**GWP**	**Flammability**	**Toxicity**
HCFC	R22	0.055	1700	NO	NO
HFCs	R134A	0	1300	NO	NO
	R407C	0	1530	NO	NO
	R404A	0	3260	NO	NO
Natural Refrigerants	**CO_2 (R744)**	**0**	**1**	**NO**	**NO**
	HC	0	3	YES	NO
	NH_3	0	~ 0	NO	YES

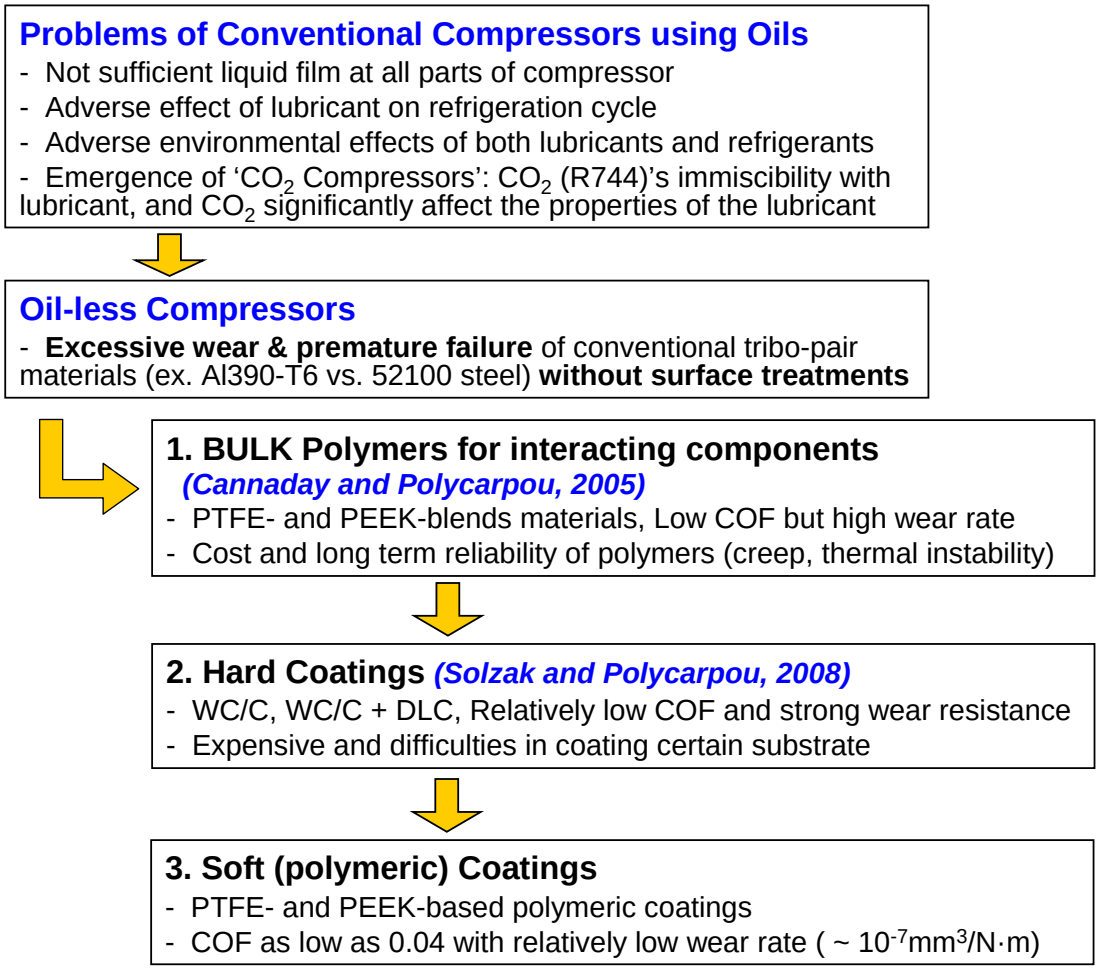

Figure 1.1 Motivation and development of advanced coating materials for oil-less compressor applications.

Lastly, due to thermodynamically negative effects of lubricants on the refrigeration cycle of typical refrigeration and air conditioning compressors (Solzak and Polycarpou, 2006), recent research interest has focused on oil-less type compressors. Under these oil less and new refrigerant conditions, some form of surface treatments become necessary on the interacting surfaces for reliable operation of compressors. As described in Figure 1.1, extensive tribological studies have been performed by Prof. Polycarpou's group using different method of surface treatments, namely bulk polymers

(Cannaday and Polycarpou, 2005) and hard coatings (Solzak and Polycarpou, 2006), in the presence of different refrigerants, sliding velocities and temperatures typical to compressor surfaces.

Sheiretov *et al.* (1995) conducted a tribological study of polymer materials (polyimide and poly(amide-imide) polymers) for ACR compressor-specific applications for the first time. Then, Cannaday and Polycarpou (2005) characterized the tribological performance of bulk form of unfilled and filled polymers based on polytetrafluoroethylene (PTFE) and polyetheretherketone (PEEK) for compressor applications. Even though these bulk polymers showed promising tribological performance, their cost issues and especially thermal instability under high temperature were still significant barriers for actual industrial applications. Recently, therefore, tribologically advanced coatings are getting attention for new type of surface treatments of sliding/bearing contact parts of compressors. A further advantage of polymeric coatings on engineering surfaces is that their cost low, compared to advanced hard coatings.

Coatings can be broadly classified as either “hard” or “soft” coatings, with one category of soft coatings being polymer-based coatings. Conventionally, hard coatings such as diamond-like carbon (DLC), Ti-N and WC/C synthesized through physical vapor deposition (PVD) techniques are thought to be effective in preventing both abrasive and adhesive wear of metal sliding contacts (Bloyce, 2000). DLC is one of the most researched tribological coatings, and is found in commercial applications such as magnetic storage hard disk drives (Suh and Polycarpou, 2006) and in automotive applications. These coatings are in the form of a hard film on the surface that are able to

reduce scratching, and offer good load-carrying capacity. Tribological coatings also have the ability to form low shear strength reaction layers and transfer layers on the top surface and the counterface, resulting in weak shear planes and thus low friction (Holmberg and Matthews, 2009). Another type of hard coatings, WC/C-based coatings were also shown to have superior tribological properties not only as far as wear resistance, but also low friction coefficient values as low as 0.05 under dry unidirectional pin-on-disk sliding conditions (Solzak and Polycarpou, 2008). Hard coatings are relatively expensive and exhibit difficulties in coating them on substrates with low surface energy or high roughness (Zhao *et al.*, 2002). Moreover, hard coatings sometimes could wear out the counterface they slide against, due to their relatively high hardness (Sung, 1998), and alternative solutions need to be explored.

Recent attention has focused on soft, thermoplastic-based polymer materials such as PTFE and PEEK. As already mentioned in Cannaday and Polycarpou (2005), the bulk form of these materials shows relatively low friction coefficient and self-lubricating properties (Fusaro, 1990), and are also inexpensive and easy to fabricate (Holmberg and Matthews, 2009). PTFE has been used extensively since its discovery because of its desirable tribological properties such as chemical inertness and superb lubricity (Yamane *et al.*, 2007). However, bulk PTFE suffers from poor resistance to wear and creep, because it easily yields in shear due to its relatively low intermolecular strength (Suh, 1986). Thus, PTFE is typically used in the form of composites, either 1) as a matrix filled with various hard fillers and micro/nano particles such as glass fibers, ceramics, MoS_2 and carbon nanotubes (CNTs) to enhance its wear resistance, or 2) as a filler into polymeric materials which have good wear resistance but poor frictional properties, such

as PEEK, in which case it lowers its friction while retaining high wear resistance (Hufenbach *et al.*, 2003 and Lal *et al.*, 2007). In fact, PEEK composites have been investigated as bearing and sliding materials for use in industrial applications due to their favorable tribological characteristics (Lu and Friedrich, 1995 and Stolarski, 1992).

PEEK is a semi-crystalline high performance engineering polymer with good thermal properties (glass transition temperature, T_g = 143 °C, melting temperature, T_m = 338 °C, continuous service temperature = 250 °C, and heat distortion temperature often in excess of 300 °C), as well as good mechanical properties (strength, modulus, toughness, and resistance to creep, abrasion, and fatigue) (Stolarski, 1992 and Stening, 1982).

Despite these promising polymer tribological properties, the majority of studies were performed for bulk materials, and there is little information in the open literature about the behavior of polymer-based coatings, especially under compressor-specific conditions.

1.2 Objective and research outline

1.2.1 Questions and objectives

In the context that the main goal of this work is the development and assessment of polymer-based coating materials for reliable compressor operation, the following research objectives, questions and plans could be addressed.

(a) Evaluate the tribological performance and applicability of PTFE- and PEEK-based polymeric coatings under actual compressor operating conditions. → Chapters 3, 5, 6

Extensive tribological testing of various commercially available PTFE- and PEEK-based polymeric coatings was performed under conditions simulating actual compressor operations including both rolling-piston (reciprocating motion), swash-plate type, and scroll type (unidirectional motion) compressors. Testing was performed under both dry (no liquid lubricant) and lubricated conditions (in all cases in the presence of a refrigerant). Tribological performance such as friction coefficient, wear rate and thermal stability were directly compared between PTFE- and PEEK-based coatings to show which coating performed better under specific conditions. Also, the behavior of polymeric coatings was compared to those of bulk form of polymers.

(b) If a specific coating performs better than others, why does it? Which property of polymeric coatings affects their tribological performance? → Chapters 4, 5, 6

To answer the above questions, material characteristics of polymeric coatings such as micromechanical and microstructural properties were examined using various techniques including indentation, scratch, SEM, and profilometric measurements. These coating properties were correlated to their tribological performance to find out the key factors determining the tribological behavior of polymeric coatings.

(c) Evaluate newly developed coating materials for compressor applications. → Chapter 5, Appendix A

Newly developed polymeric coating materials, namely, Aromatic Thermo-Setting Copolyesters (ATSP®) and its blends with PTFE were tested under various compressor specific conditions, and then directly compared to the commercial PTFE-based coatings.

Also, surface material properties of these coatings were characterized and compared with commercial polymeric coating materials.

1.2.2 Research outline

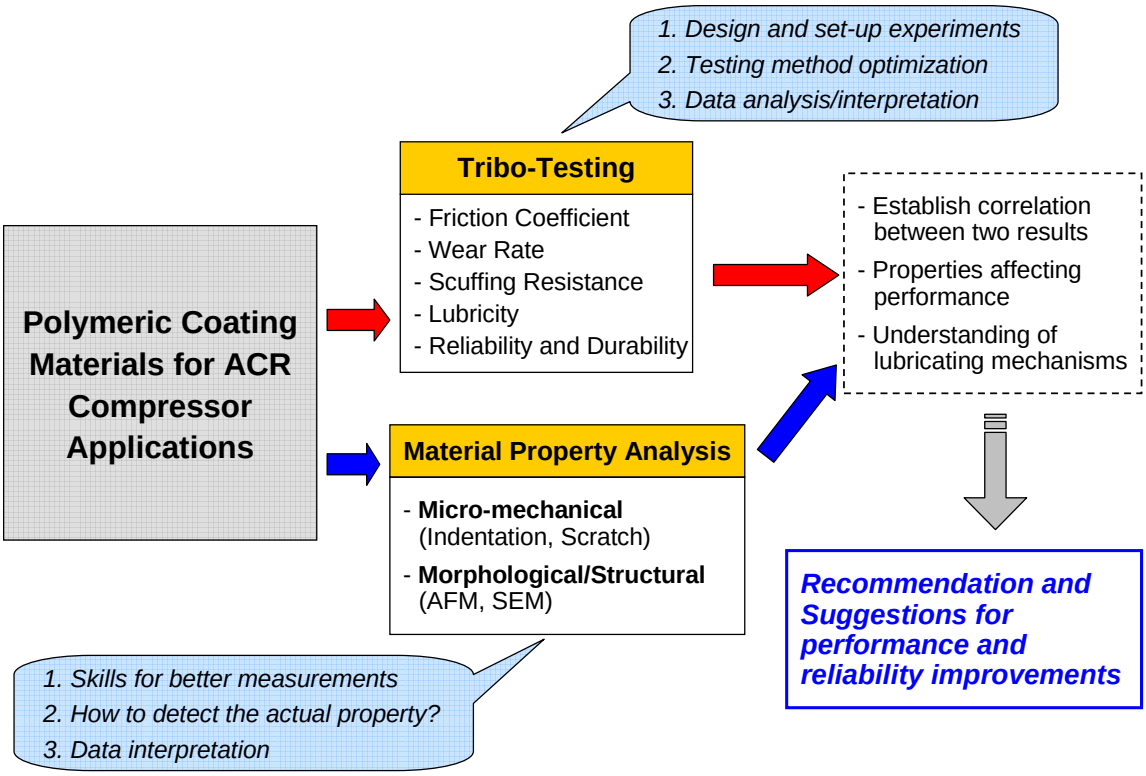

Figure 1.2 Two main research approaches to tackle the tribology of polymeric coating materials for compressor applications.

As described in Figure 1.2, the two research approaches could be broadly classified as either experimental tribo-testing or material property analysis of coating materials. Through tribological testing, various surface performance and behaviors of polymer coating materials, namely friction coefficient, wear rate, scuffing resistance, and durability are usually examined under various testing conditions. During this process,

significant amount of time is usually spent on testing methods and parameter optimization to better characterize and differentiate the performance of polymer coating samples. After tribological testing, polymeric coating materials are examined using various material property characterization tools such as indentation, scratch, SEM and profilometer, to determine their mechanical, structural and morphological surface properties. During this step of property characterization, significant amount of effort was placed on data analysis and interpretation to extract the exact and pure (actual) properties of the polymer coating layers decoupled from substrate effects. Once the tribological performance and material properties of the polymer coatings are measured, both results are correlated to better understand the tribological behavior and mechanism of polymer coatings on the contact interface.

Chapter 2 reviews the fundamentals of polymer and polymer coating tribology based on the open literatures, which gives an insight on the tribological study of polymeric coatings for actual industrial applications in this work. In Chapter 3, seven different polymeric coatings were tribologically tested under conditions simulating both rolling-piston and swash-plate type compressors in CO_2 refrigerant environment. Friction and wear behavior of different polymeric coatings were directly compared to select the best potential coatings for compressor applications. In Chapter 4, micro-mechanical and structural properties of these polymeric coatings were characterized using the indentation technique. Especially, two representative PTFE- (PTFE/Pyrrolidone-2) and PEEK-based coatings (PEEK/PTFE) were directly compared to find out the key factors determining the tribological performance differences between these two coatings. In Chapter 5, the tribological behavior of polymeric coatings under elevated temperature

conditions was studied. At the same time, the elastic recovery property of polymer coatings which was greatly affected by temperature was measured using scratch tests, and correlated with their frictional behavior. In Chapter 6, the tribological performance of the polymeric coatings tested under specific fretting motion was characterized. Especially, under this fretting conditions, the effect of oil lubricants and the interaction between polymeric coatings and oils were studied. Through SEM and profilometric measurements, the transfer film effect of the polymer coatings was characterized in the context of overall tribological behavior of polymer-to-metal contact.

CHAPTER 2: FUNDAMENTALS OF POLYMER TRIBOLOGY

2.1 Introduction

Polymers play an important part in materials and mechanical engineering, not just for their ease in manufacturing and low unit cost, but also for their potentially excellent tribological performance in engineered forms. Recently, with improvement of coating processing technology, polymeric-based coatings are increasingly used not only for aesthetic reasons, but more importantly for improving component functional performance, such as improving lubricity, corrosion, and wear, which will be studied in detail in this work. Polymers have various tribological advantages such as, 1) relatively low friction coefficient (0.1 to 0.3 during unlubricated sliding against either themselves or metals), 2) dispensable periodic maintenance (self-lubricating properties), 3) high resistance to chemical attack such as acids and alkalis, and 4) low noise emission (Holmberg and Matthews, 2009). However, polymers also have such limitations as, 1) poor wear resistance, 2 visco-elastic and creep behaviors, 3) lower ultimate strength and elastic modulus than metals, typically by a factor of ten, 4) relatively high thermal expansion coefficient (dimensional stability problem), 5) very low thermal conductivities (poor dissipation of frictional heat), and 6) low limiting temperatures (< 300°C, thus easy softening, melting, oxidation and thermal degradation). Usually, therefore, single component polymers are weak for external load and hardly meet most of the tribological requirements. However, in the composite and hybrid forms these days, polymers satisfy performance requirement for specific applications, often surpassing other traditional materials such as metals and ceramics in tribological point of view.

2.2 Applications and performance determining factors

2.2.1 Applications of polymer surfaces

Due to their unique properties such as self-lubricity, resistance to impact, corrosion, chemicals, solvents, nuclear radiation, contamination with oils, etc., apart from easy processibility in complex shapes and capacity to absorb vibrations leading to quiet operation, tribological applications of polymers include gears, a range of bearings, bearing cages, and also conventional macro-scale automotive and marine applications. With recent technological advances in composite materials and coating process, the application of polymeric coatings has expanded to include biomedical, food processing and sports devices such as tennis racquets. Especially, these polymer-based tribo-components can be used in extreme conditions of temperatures (up to 300 ◦C) and pressures (vacuum to high), where liquid lubricants cannot be considered. Such tribo-components fabricated from the polymer composites are used in typical situations where either hydrodynamic lubrication is not possible because of frequent starts and stops or low PV (pressure–velocity) conditions. Therefore, polymeric bearing surfaces are the unique solution in the following situations where (Bijwe *et al.*, 2009),

- lubrication is a problem (tribological components in inaccessible equipment; for example, in nuclear reactors and in hazardous conditions in chemical plants or in vacuum or space);
- conventional lubricants cannot be employed (in space or cryogenic temperatures where liquid lubricants will either freeze or evaporate);

- lubrication is unacceptable because of the possibility of contamination of lubricant with product (plain bearings or gears in industries, such as food, paper, pharmaceutical and textile);
- maintenance is spasmodic or impossible (bushes and seals in domestic appliances, toys and instruments); and
- lubrication is sparse (aircraft linkage bearings) or as a safeguard in the event of failure of the lubrication systems (e.g. gears in train).

2.2.2 Determining factors of tribological performance

Today, more and more advanced technical applications of polymeric materials involve friction and wear, often under challenging environments such as elevated operation temperatures. To further exploit the economical advantages of polymers and also to satisfy the expected tribological performance of devices or components, a fundamental assessment not only of the intrinsic material properties but of the complete tribosystem is also required. On the one hand, material properties such as crystallinity, glass transition temperature, mechanical properties, molecular weight, orientation, hardness, and surface energy are factors that have been shown to influence both the friction and wear behavior of polymers under various experimental conditions. On the other, the tribological system itself, more precisely the loading characteristics, the counterpart material, as well as the external conditions including the temperature or the presence of lubricants play a major role in wear mechanism and, subsequently, for the overall wear performance. An overview of the various factors influencing the wear behavior of polymers is shown in Figure 2.1 (Friedrich *et al.*, 1993).

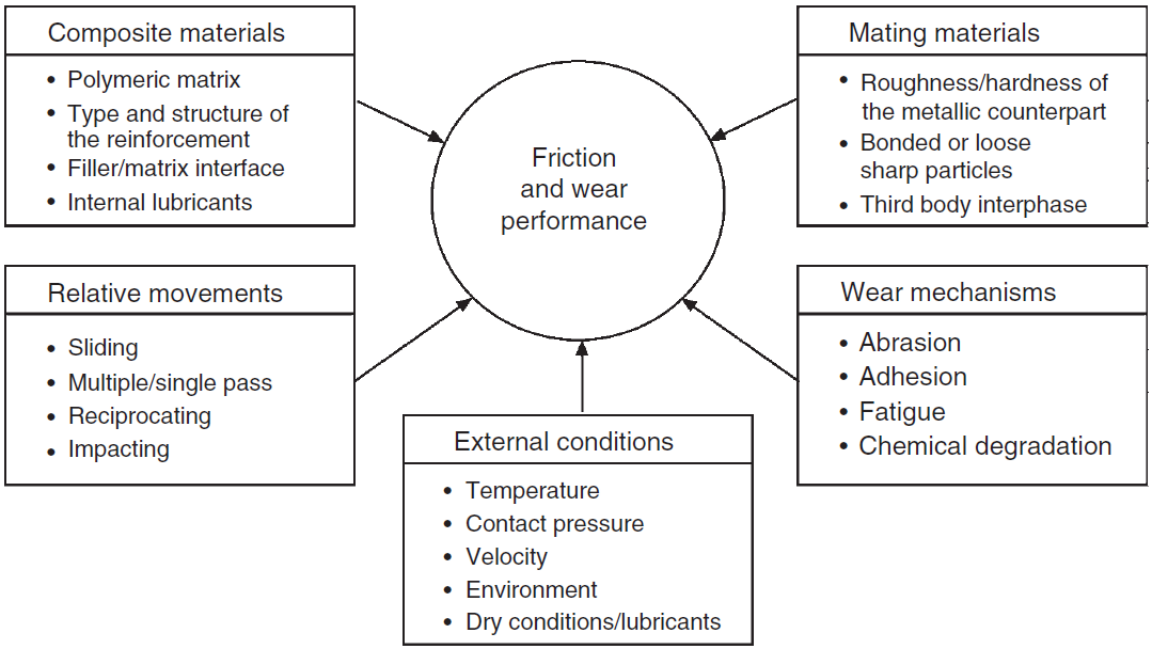

Figure 2.1 Factors determining the wear and friction behavior of polymers (Friedrich *et al.*, 1993)

As described in Figure 2.1, the tribological characteristics of polymers are greatly influenced by the effects of temperature, relative speed of the interacting surfaces, normal load and the environment. However, industrial application conditions greatly vary, thus requiring performance additives for each corresponding application conditions. Therefore, to deal with these effects and for better control of the responses, polymers are usually modified by adding appropriate fillers to suit a particular application. Thus, they are invariably used in composite or, at best, in blended form for an optimum combination of mainly friction and wear performances. Also, pragmatically fillers may be less expensive than the polymer matrix. Therefore, for the past few decades, the majority of research efforts of polymer tribology have been focused on 1) the characteristics of polymer composite materials such as optimized amount and size of various fillers, along with 2) friction and wear mechanisms of polymer surfaces.

2.3 Polymer composite tribology

In author's knowledge, except for only ultra-high-molecular-weight polyethylene (UHMWPE) and probably nylons, no other polymer is currently being used in its pristine form for a tribological application. The reason is that no polymer can provide a reasonable low wear rate with optimum coefficient of friction required. Hence, there is a need to modify most polymers by a suitable filler that can reduce the wear rate and, at the same time, either increase or decrease the coefficient of friction depending on the design requirement. The filler can perform a variety of roles depending on the choice of the matrix and the filler materials. Some of these roles are strengthening of the matrix (high load-carrying capacity), improvement in the sub-surface crack arresting ability (better toughness), lubricating effect at the interface by decreased shear stress and the enhancement of the thermal conductivity of the polymer (Burris *et al.*, 2008). The entire aspects of the tribology of polymer composites can be quite complex, and thus, a simple and efficient way to handle this topic is to classify the composites according to the role of the filler material in the composite, by modifying either the bulk or the interface (Briscoe, 1993).

2.3.1 Hard (strong) fillers in a softer matrix: Bulk modification

PTFE, most well known self-lubricating polymer, is usually weak to external load, thus showing poor wear resistance. However, these kind of soft polymers with exceptional frictional property can be made also wear resistant by strengthening the bulk with hard or strong filler material such as particles of ceramics/metals or a suitable strong

fiber (carbon, aramid or glass fibers). The main function of the filler here is to strengthen the polymer matrix and thus increase the load-bearing capacity of the composite. The coefficient of friction remains low or sometimes increases marginally but the wear resistance can be increased up to an order of magnitude (Burris and Sawyer, 2006 and Briscoe and Sinha, 2005). Cannaday and Polycarpou (2005) showed that PTFE blended with PEEK had superior tribological characteristics to unfilled polymers and metals under specific compressor operating conditions.

These days, the use of nano size particles in polymers has become quite promising. Superior mechanical properties of a polymer nanocomposite are attributed to its significantly high interface area between the filler (nano-particles or nano-fibers) and the matrix (a polymer). High interface leads to a better bonding between the two phases and hence better strength and toughness properties over unfilled polymer or traditional micro-composites. For all polymer/nano-particle systems, there will be an optimum amount of the nanoparticles beyond which there will be a reduction in the toughness as the stiffness and strength increase. Chen *et al.* (2003) showed that carbon nanotubes (CNTs) significantly increased the wear resistance of PTFE composites and decreased their coefficient of friction with optimum 15-20 vol.%. The CNTs greatly reinforced the structure of the PTFE-based composites and thereby greatly reduced the adhesive and plough wear of CNT/PTFE composites.

The disadvantage of using fillers (especially the particulate type) is that the composite material may become somewhat less tough compared to the pristine polymer and thus induce wear by fatigue. However, this can be avoided by proper optimization of the mechanical and tribological properties.

2.3.2 Soft lubricating fillers in a hard (strong) matrix: Interface modification

This type of composite utilizes the low shear strength and self-lubricating properties of the filler to reduce the coefficient of friction and, as a result, wear and frictional heating is drastically reduced. The main requirement is the availability of the filler at the interface in sufficient amount such that a reduction in the coefficient of friction and an increase in the wear resistance can be realized. Most common filler and matrix in this type of composites are PTFE filler and PEEK matrix (Cannaday and Polycarpou, 2005, Hufenbach *et al.*, 2003, Bijwe *et al.*, 2005, and Lal *et al.*, 2007). Hufenbach *et al.* (2003) showed that the inclusion of PTFE powder in PEEK matrix significantly improved the tribological performance of the PEEK composite without showing any scuffing behaviors. An improvement of 30 times in the wear rate at 7.5 wt.% and 5 times in friction coefficient at 30 wt.% was observed due to blending. Also, Lal *et al.* (2007) showed that PTFE filled PEEK diminished stick-slip tendency of PEEK and fluctuations in COF with very low and stable values.

The disadvantage of this type of composite is obviously the reduction in the strength and load-carrying capacity of the material in the composite form. Hence, adding this type of filler beyond a certain percentage by volume or by weight would be counterproductive for tribological performance due to a drastic decrease in the bulk strength as mentioned above in Hufenbach *et al.* (2003). Therefore, majority of recent researches have focused on finding an optimum ratio of the filler and the matrix to achieve maximum wear resistance and at the same time, lowest friction coefficient.

For both types of composites, the properties of the transfer film formed on the counterface will define whether the composite can have low wear rate or not as will be discussed in detail in Chapter 6. A strongly adhering and tenacious, yet lubricating, transfer film would reduce wear after the formation of the film during the running-in period. Bulky and thick film has the tendency to detach itself from the counterface, which may increase the wear rate due to a continuous film formation and detachment mechanism (transfer wear).

2.4 Friction and wear mechanisms of polymer surfaces

Along with polymer composites, another major research area of polymer tribology is to shed light on the mechanism of friction and wear of polymeric surfaces. To better understand the overall tribological behavior, we need to investigate how the frictional force is determined for sliding wear of a polymer surface against a metallic counterpart.

From the most well-known two-term model by Briscoe (Briscoe and Sinha, 2002), the surface layer of the polymer involved in the frictional process can be classified into two zones: the interfacial zone with a depth of about 100 nm and the cohesive (subsurface) zone corresponding to the depth of the coating thickness. Therefore, the frictional force resulting from the adhesion equals the product of the "real contact area" of the interfacial zone (with the counterpart) and the "shear stress" of the subsurface zone. This is assuming that the counterface is sufficiently hard in comparison to the polymer-mating surface and undergoes only mild or no elastic deformation. Figure 2.2 shows a schematic diagram of the two-term friction model of polymeric surface.

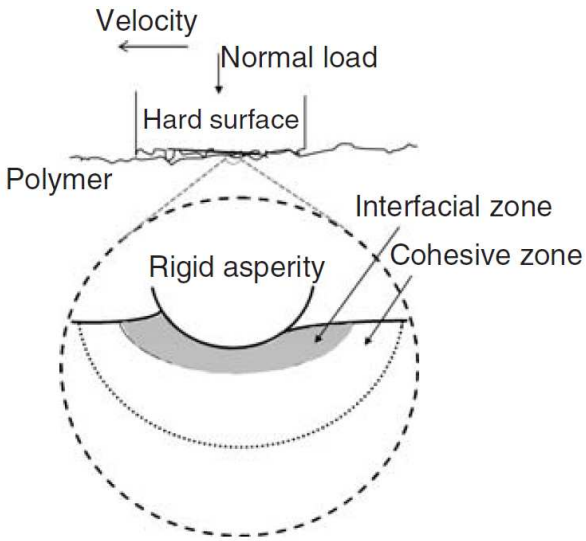

Figure 2.2 Briscoe's two-term model of polymer interface showing interfacial and cohesive zones (Briscoe and Sinha, 2002).

The interfacial frictional work is the result of adhesive interactions between the polymer surfaces and the rigid asperities which depend on factors such as the hardness of the polymer, molecular structure, glass transition temperature, crystallinity of the polymer, surface roughness of the counterface and chemical/electrostatic interactions between the counterface and the polymer. For example, an elastomeric solid, which has its glass transition temperature below the room temperature and hence very soft, would have very high adhesive component leading to high friction. Beyond interfacial work is the contribution of the cohesive term, which is a result of the plowing actions of the asperities of the harder counterface into the polymer. The energy required for the plowing action will depend primarily on the tensile strength and the elongation before fracture (or toughness) of the polymer and the geometric parameters (height and the cutting angle) of the asperities on the counterface (Briscoe and Sinha, 2002). In a normal

sliding experiment, however, it is hard to completely decouple the two terms (interfacial and cohesive) and therefore most of the data available in the literatures generally include a combined effect.

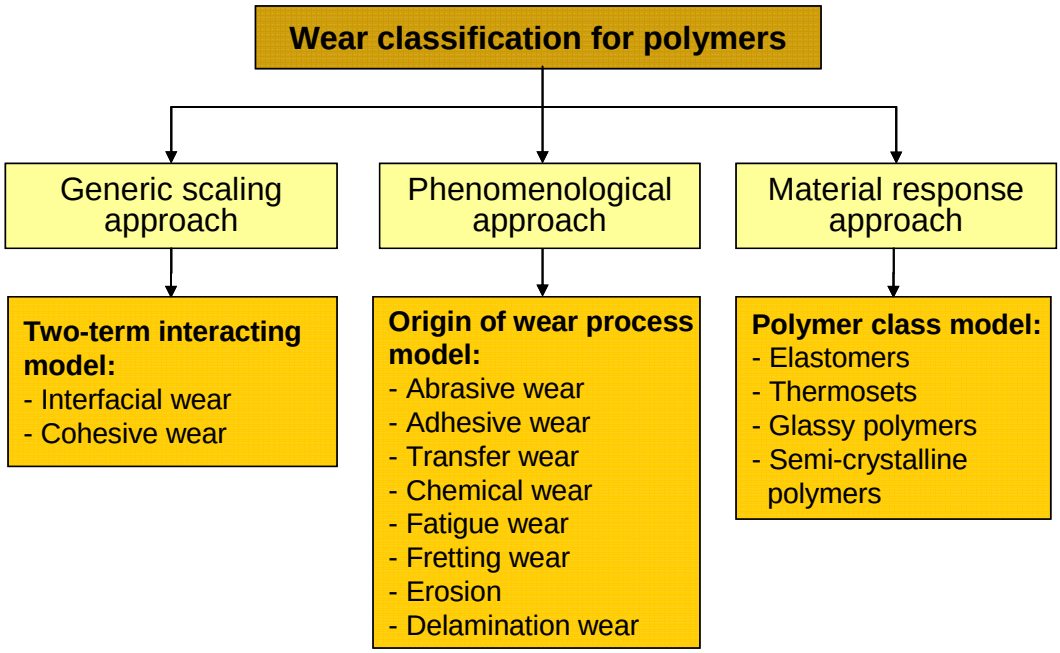

Figure 2.3 Briscoe's two-term model of polymer interface showing interfacial and cohesive zones (Briscoe and Sinha, 2002).

Wear is an avoidable consequence of friction in a sliding contact of polymer surfaces. Wear of polymers is extremely complex process, and thus the explanation of the wear mechanism can be most efficiently given when we follow one of the three systems of classification as shown in Figure 2.3 (Briscoe and Sinha, 2002). It should be noted that, similar to the case of friction, polymer wear is also greatly influenced by the type (elastomer, amorphous, semi-crystalline) of the polymer. Of particular importance are the properties such as the elastic modulus, tensile strength and the percentage

elongation at failure (toughness), which changes drastically as we move from one type of polymer to another.

2.5 Summary

The tribological applications of polymers and their composites have steadily increased. Especially, the self-lubricating property of many linear thermoplastics such as PTFE, both in pristine and composite forms, has been well exploited for many industrial applications such as gears, bearings, human hip/knee joints, non-stick cooking pans, etc. These days, the newly emerging area of polymer nanocomposites is getting a great interest from young tribologists. However, the tribological research on these polymer nanocomposites is still at a relatively early stage.

Along with this polymer nanocomposite research, the study of polymer coating (film) tribology is being increasingly performed. Many tribological problems associated with metals or other materials, such as silicon, can be eliminated by having a mechanically robust polymer coating. High-performance (strength and thermal stability) polymers, such as PEEK and PI, when mixed with nano-particles or nano-fibers can be used as a thin film on a substrate for high wear resistance, which is thoroughly discussed in this dissertation. Research papers currently available in this area are still very few, and hence this could be another major growth area for future polymer tribology research.

CHAPTER 3: TRIBOLOGICAL TESTING OF PTFE- AND PEEK-BASED POLYMERIC COATINGS FOR COMPRESSOR APPLICATIONS

3.1 Introduction

Compared to the abundance of research on the tribology of bulk polymers as discussed in Chapter 2, there is little work on the tribological behavior of polymeric-based coatings (with thicknesses in the 10's of micrometers). The tribological behavior of polymeric coatings may not necessarily follow the same behavior as that of their bulk counterparts. This is partly due to the fact that the structure of the polymer materials changes during the coating process, which is known to affect the tribological performance, e.g., being amorphous or crystalline (Zhang *et al.*, 2007). Research examining the tribological behavior of polymeric coatings (Zhang *et al.*, 2006 and McCook *et al.*, 2005), under mild conditions of 1 ~ 10 N normal load and 0.25 ~ 2.5 m/s sliding speed have been reported. Tribological testing of commercially available PTFE- and PEEK-based polymeric coatings under realistic compressor operating conditions (4.5 m/s sliding speed and normal loads of 400 N ~ 2,000 N) has also been reported. Demas and Polycarpou (2008) evaluated the tribological performance of two different PTFE/Pyrrolidone coatings and a Resin/PTFE/MoS_2 coating under unlubricated and carbon dioxide (CO_2) refrigerant environments with reciprocating motion, simulating the wrist pin in a piston-type compressor. The PTFE-based coatings showed excellent frictional characteristics, with friction coefficient values as low as 0.1, and good wear resistance attributed to the beneficial effects of the generated wear debris at the interface. Escobar Nunez *et al.* (2011) performed a comparative testing of PEEK-based coatings

under starved lubricated (mixture of R-134A refrigerant and polyalkylene glycol lubricant) and unidirectional sliding conditions simulating swash plate compressors. A study of a newly developed Aromatic Thermosetting Copolyester applied as a coating, has showed exceptionally low wear performance and reasonable friction behavior, and is under further development (Zhang *et al.*, 2010).

A research question that still remains unanswered is which of the two families of coatings; PTFE-based or PEEK-based offer superior tribological performance under either piston-type (reciprocating) or swash plate (unidirectional) compressor conditions, as well as their comparison with their bulk counterparts. In this chapter, therefore, seven different PTFE- and PEEK-based coatings are tribologically evaluated under different operating conditions, simulating both unidirectional and oscillatory motions, and compared to bulk polymers. Additionally, newly developed ATSP-based coatings were also tested under identical conditions as commercial coatings, and discussed in detail in Appendix A.

3.2 Experimental

Oscillatory and unidirectional testing conditions (simulating piston-type and swash plate compressors) were performed. Photographs of typical piston-type and swash plate compressors and their corresponding critical tribo-contacts are shown in Figure 3.1. To simulate the contact geometry in a wrist pin/ connecting rod interface of piston-type compressors, shown in Figure 3.1(a), the cylindrical pins were cut to length and oriented to create a line contact with a reciprocating disk coated with different polymeric coatings. The photograph and illustration in Figure 3.1(b) shows the contact configuration for

unidirectional tests, showing a crown shaped pin (which is an actual component used in swash plate compressors and referred to as shoe in this work) in contact with a rotating disk coated with different polymeric coatings, simulating a swash plate compressor.

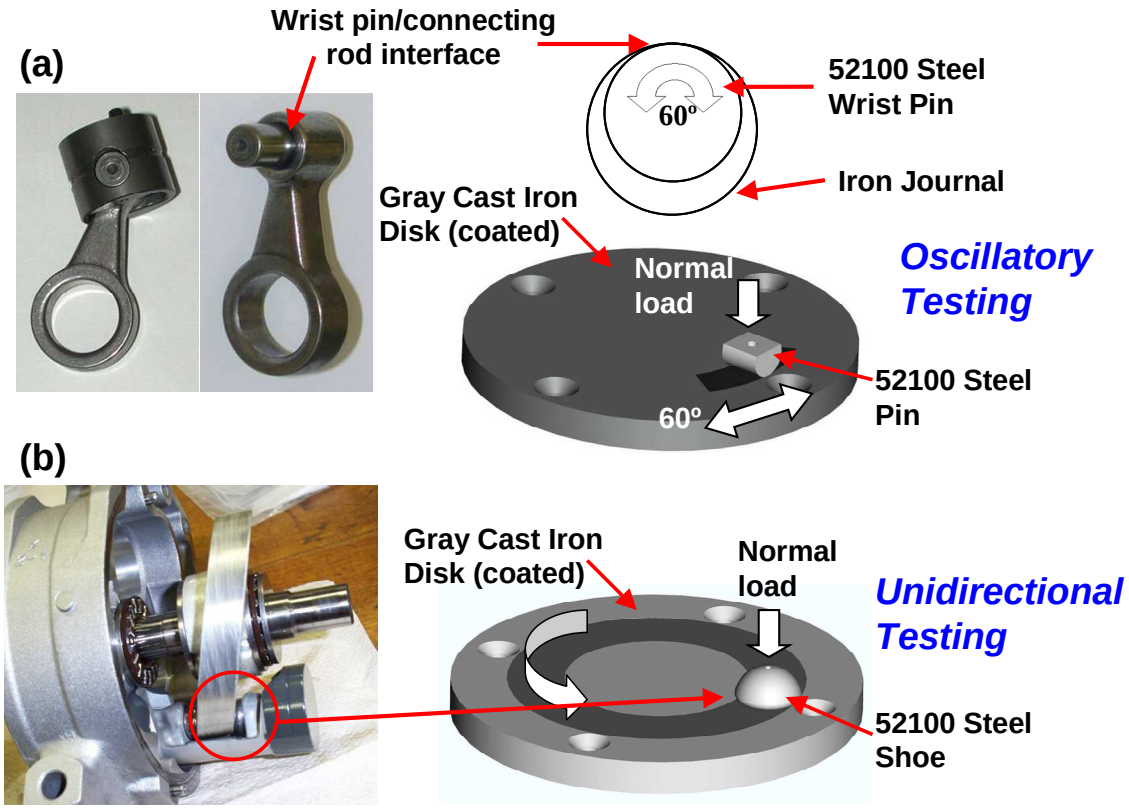

Figure 3.1 (a) Cylindrical self-aligned pin-on-disk test configuration for oscillatory testing simulating piston-type compressors and (b) crowned self-aligned pin (or shoe)-on-disk test configuration for unidirectional testing simulating swash plate compressors.

A specialized High Pressure Tribometer (HPT) was used to perform both types of experiments. The disk sample is fixed on the upper rotating spindle capable of unidirectional sliding speeds up to 2200 revolutions per minute (rpm) and reciprocating motion up to 4.85 Hz with variable oscillation amplitude. The temperature of the upper spindle and disk assembly can be regulated from -20°C to 120°C. The pin is placed on

the lower fixture whose vertical position is adjusted by a mechanical power screw mechanism, enabling a controlled normal load ranging from 45 N to 4450 N applied on the pin-on-disk interface. Also, this lower fixture is mounted on a 6-axis force transducer so that the forces in the x, y, and z linear directions can be measured *in-situ* to obtain the coefficient of friction (COF). Both the upper spindle and lower fixture holding the samples are located inside an environmentally controlled vacuum chamber of the HPT capable of pressure control from near near-zero up to 1.72 MPa (250 psi).

3.2.1 Samples

Gray cast iron (Dura-Bar® G2), a commonly used material in compressors with a bulk hardness of 2.2 GPa, was machined to 79 mm diameter and 8 mm thickness disks as shown in Figure 3.1. The disks had an initial (as machined) root-mean-square surface roughness (R_q) of 0.4 μm. After grit-blasting with aluminum oxide (which was performed before depositing the polymeric coatings to increase adhesion), R_q increased to 3.5 μm, which facilitated the deposition of polymeric coatings on the substrate surface. Seven different polymeric coatings, namely, PTFE/Pyrrolidone-1 (DuPont™ Teflon® 958-303), PTFE/Pyrrolidone-2 (DuPont™ Teflon® 958-414), Resin/PTFE/MoS_2 (Whitford Xylan® 1052), PEEK/PTFE (1704 PEEK/PTFE®), PEEK/Ceramic (1707 PEEK/Ceramic®), Fluorocarbon (Impreglon® 218), and PTFE/MoS_2 (Fluorolon® 325) were deposited on the grit-blasted substrates using a spray gun. The name of each coating already shows their base materials, but the entire compositions (including solvents) of these commercially available coatings are unknown due to the proprietary of the coating suppliers. In the case of DuPont™ coatings, they were dried for 5 min after

application, and then baked for 15 min at 343°C (650°F). These coatings can be cured at temperatures as low as 177°C (350°F) by extending the cure time, but the toughness and durability of the coating decreases as the cure temperature is reduced below 343°C. The entire deposition processes were performed by two authorized applicators, Orion Industries (for Teflon® and Xylan® coatings) and Southwest Impreglon (for PEEK, Impreglon® and Fluorolon® coatings), and further information on the application method for PTFE- and PEEK-based coatings can be found in Refs. Demas and Polycarpou (2008) and Escobar Nunez *et al.*, (2011), respectively.

Table 3.1 Mechanical properties of polymeric coatings, substrate, and pin used in this work.

	Samples	Hardness (GPa)	Roughness, R_q (μm)
Coating	PTFE/Pyrrolidone-1	0.38	2.28
	PTFE/Pyrrolidone-2	0.25	0.61
	Resin/PTFE/MoS_2	0.32	1.71
	PEEK/PTFE	0.37	1.00
	PEEK/Ceramic	0.24	0.92
	Fluorocarbon	0.25	1.53
	PTFE/MoS_2	0.24	1.14
Substrate	Dura-Bar® G2, Gray case iron	2.2	0.4
Pin	52100 Steel	11.7	0.035

The surface roughness of each coating was measured using a stylus profilometer (Tencor P-15™) and are summarized in Table 3.1 along with the coating's hardness values measured using a micro-Vickers tester. The average surface roughness values of the coatings were in the range from 1.2 μm to 3.3 μm. As expected, the hardness of the polymeric coatings was found to be lower than the substrate hardness. The thickness of

each coating was measured using cross section scanning electron microscopy (SEM); atypical such measurement is shown in Figure 3.2. For all polymeric coatings, their thickness values, measured over 200 μm length were not uniform, and in the range of 20 μm to 40 μm, which is much thicker than typical hard coatings such as diamond-like-carbon (DLC) and WC/C with a thickness of 2.5 μm (Solzak and Polycarpou, 2010).

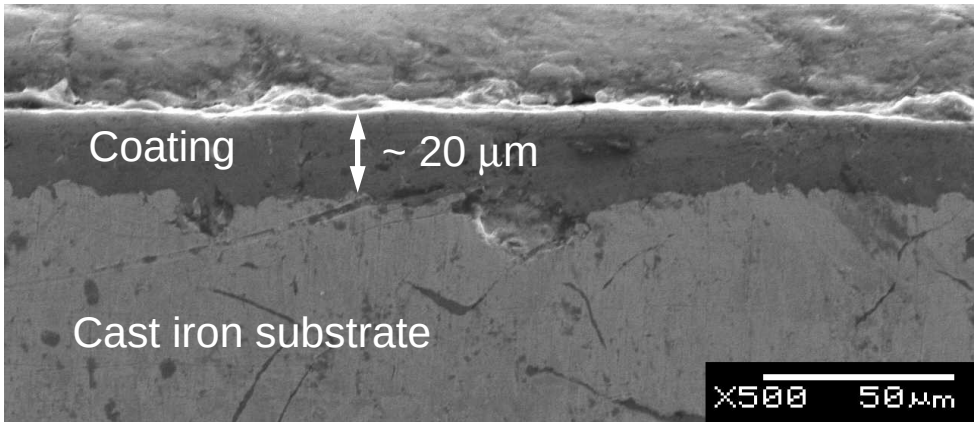

Figure 3.2 Representative cross-section SEM image showing the thickness of PTFE/Pyrrolidone-2 coating, on cast iron substrate.

The semi-cylindrical pins for the oscillatory experiments were made out of 52100 steel wrist pins, and were 8 mm in diameter and 8 mm long with a 1 mm diameter hole drilled up to 2 mm below the contact surface to accept a miniature thermocouple and measure the *in-situ* near contact temperature (NCT) during testing (Figure 3.1(a)). The crowned 52100 steel shoes for the unidirectional experiments were 9.6 mm in diameter, and also had a 1 mm diameter hole for thermocouple insertion.

3.2.2 Tribological testing conditions

Before testing, the non-coated pin samples were ultrasonically cleaned in acetone for 10 min, rinsed with 2-propanol, and dried with a warm air blower. The polymeric

coated disk samples were cleaned in 2-propanol and dried, but were not exposed to acetone.

For the oscillatory experiments simulating piston-type compressor operation (Figure 3.1(a)), a constant normal load of 445 N was applied on the stationary pin (corresponding to a nominal mean contact pressure of 450 MPa), representing aggressive compressor conditions. To enable run-in and avoid initial abrupt failures, the pin was gently brought into contact with the disk surface with a 44.5 N preload before test initiation. The coated disk was reciprocating at a frequency of 4.5 Hz with 60° amplitude (peak-to-peak) and an average wear track diameter of 47.6 mm producing an average linear velocity of 0.22 m/s. To examine the applicability of these coatings for use in oil-less compressors, tests were performed at 172 kPa (25 psi) R744 (CO_2) refrigerant environment with no lubricant. Also, all tests were performed at room temperature (21~23°C) conditions without any temperature feedback control on the HPT, thus allowing natural increase of the temperature on both pin and disk samples (with continuous sliding during testing). Two tests were performed for each condition for repeatability, and each test was run for 30 min, corresponding to a sliding distance of 396 m. Tests were stopped earlier when the friction coefficient and near contact temperature abruptly increased, indicating destruction of the coating and sudden catastrophic failure of the interface. Under oscillatory testing conditions, four of the coatings (PEEK/PTFE, PEEK/Ceramic, Fluorocarbon, PTFE/MoS_2) were tested in this work, as the other three coatings were tested under identical conditions in earlier work (Demas and Polycarpou, 2008) and were directly used in this work. For unidirectional testing, all seven coatings were tested.

For the swash plate compressor simulation, the unidirectional sliding tests were performed with a rotating speed of 1500 rpm and an average wear track diameter of 43.2 mm which corresponded to a linear speed of 3.75 m/s. Environmental conditions were the same as oscillatory testing (i.e., 445 N normal load, room temperature without any feedback control, 172 kPa of CO_2 refrigerant with no lubricant, and 30 min duration, corresponding to 6.75 km sliding distance). As the shoe is crowned the exact contact pressure is difficult to calculate and thus the contact load is used instead of the contact pressure. Similarly, two tests were performed for each condition, showing repeatable behavior. For the group of coatings which exhibited better tribological performance, additional unidirectional 3-hour long duration (durability) tests were performed to examine their long-term behavior, simulating compressor life tests (the 3 hour duration tests corresponded to 40.5 km sliding distance). Table 3.2 summarizes the experimental conditions for both oscillatory and unidirectional testing conditions.

Table 3.2 Summary of experimental conditions.

	Oscillatory	Unidirectional
Temperature (°C)	21 ~ 23	
Environment (Refrigerant)	25 psi of R744 (CO_2)	
Normal load (N)	445	
Contact geometry	Line contact	Crowned contact
Contact pressure (MPa)	450	-
Sliding speed (m/s)	0.22	3.75
Test duration	30 min	30 min, 3 hours

Using a stylus profilometer (Tencor P-15™), four different line scans were taken across the wear tracks generated on the disk surfaces after testing, and an average value

was recorded. From the line scan data, the exact wear volume loss of each coating could be precisely determined as described in Figure 3.3. Then, the normalized wear rate for each coating was calculated by dividing the wear volume by the normal load and the total sliding distance.

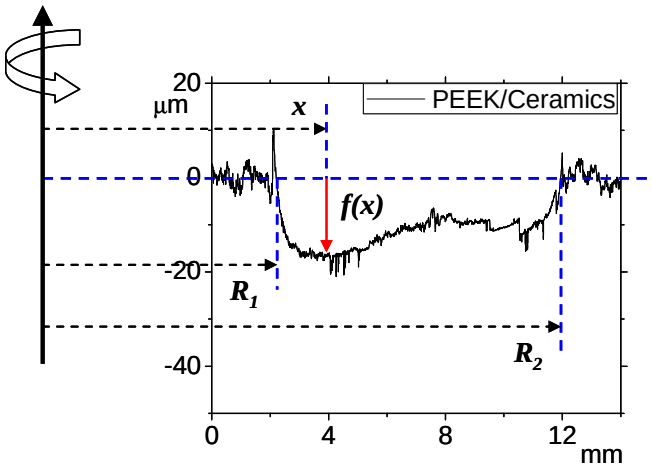

$$Wear\ Volume = L \cdot 2\pi \int_{R_1}^{R_2} xf(x)\,dx$$

L = 1 for unidirectional test,
1/3 for oscillatory test

Figure 3.3 Typical wear track showing the calculation of the wear volume.

3.3 Results and discussion

3.3.1 Oscillatory testing (piston-type compressors)

Representative friction coefficient and near contact temperature measurements of one of the polymeric coatings (PTFE/MoS_2) under dry-oscillatory conditions is shown in Figure 3.4. Two different tests are shown, exhibiting similar behavior, thus validating repeatability. The friction coefficient gradually increased for the first 10 min, and then slightly decreased, reaching a steady-state value at 15 min. This friction behavior was explained in Ref. Demas and Polycarpou (2008) by the third-body self-lubricating behavior of the generated wear debris particles. Initially during the running in period and as the coating is worn out, the friction coefficient increases because higher frictional

force is needed to generate more wear particles. At some point, the amount of wear debris generated is sufficient to act as a solid lubricant, thus preventing further wear of the coating, which results in steady-state behavior. This friction coefficient behavior was similar for all coatings, even though their absolute values were different (as it will be discussed later). In regards to the near contact temperature behavior, it quickly increased from room temperature (at the start of the test) to about 45°C during the first 1 min, and then followed the same trend as the friction coefficient.

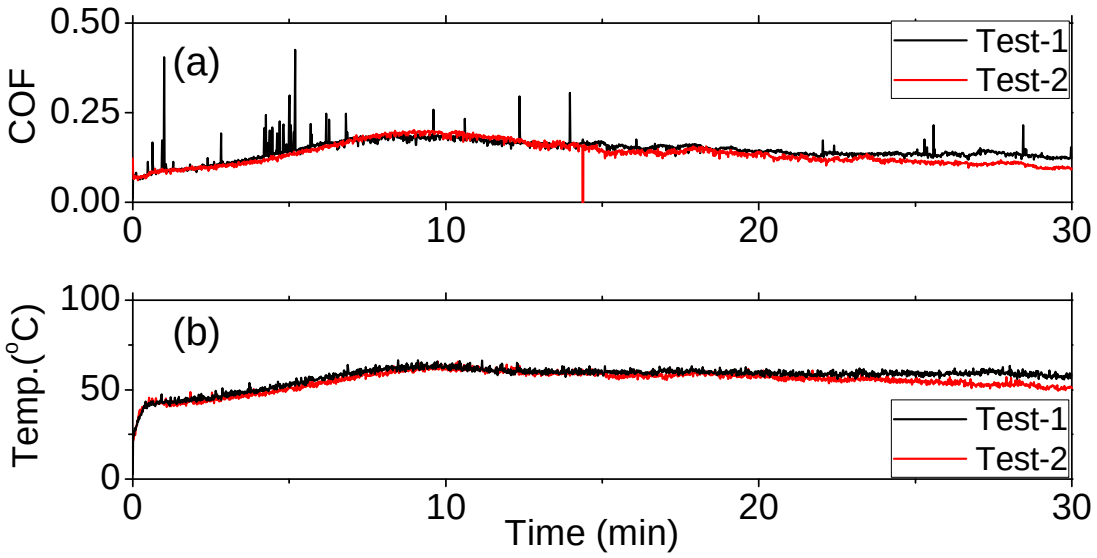

Figure 3.4 *In-situ* (a) friction coefficient and (b) near contact temperature of PTFE/MoS_2 coating during 30 min oscillatory testing. The sharp transients, especially in the friction data are electrical noise as the data is unfiltered.

Typical profilometric wear track measurements of the 4 coatings tested under dry-oscillatory conditions are shown in Figure 3.5. The wear track profiles of the other three coatings under the same testing conditions can be found in Ref. Demas and Polycarpou (2008). Due to relatively high contact pressure (450 MPa) in this condition, wear of the coatings was observed for all coatings. Among the 4 coatings shown in Figure 3.5,

PTFE/MoS_2 showed the highest wear resistance, with an average wear depth of 17 μm. PEEK-based coatings exhibited higher wear, around 40 μm, and in the case of PEEK/Ceramic coating, over 45 μm of wear, which corresponded to the total coating thickness. Nevertheless, none of these coatings exhibited catastrophic failure during the test duration, due to the lubricity effect of the wear debris trapped inside the wear tracks. The wear rate for each coating was calculated using the method discussed in Figure 3.3, and plotted on the *y*-axis along with the friction coefficient values on the *x*-axis, shown in Figure 3.6.

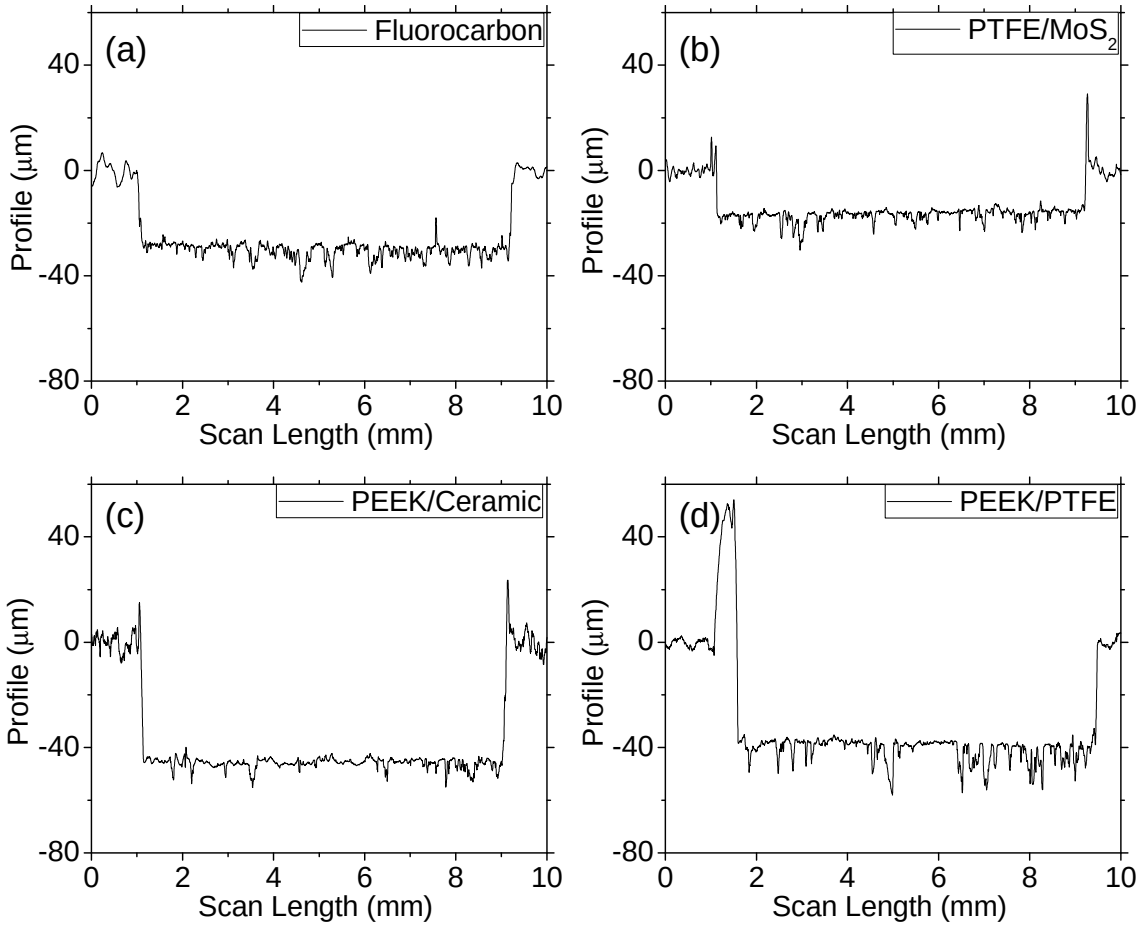

Figure 3.5 Typical profilometric wear track measurements of (a) Fluorocarbon, (b) PTFE/MoS_2, (c) PEEK/Ceramic, and (d) PEEK/PTFE coatings after 30 min oscillatory testing.

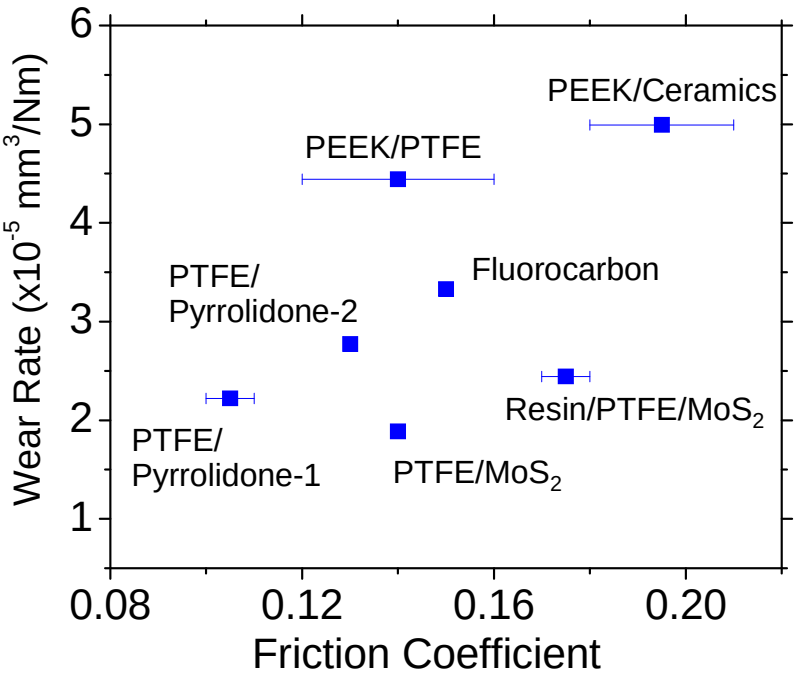

Figure 3.6 Friction coefficient (*x*-axis) vs. wear rate (*y*-axis) of seven polymeric coatings in CO_2 (22 °C and 25 psi) environment at 445 N normal load under dry-oscillatory conditions.

Referring to Figure 3.6, all coatings showed relatively low friction coefficient values in the range of 0.1 ~ 0.2 while their wear rate was of the order of 10^{-5} mm^3/N·m, which is higher than that of hard coatings such as DLC and CrN coatings (which is in the range of 10^{-8} ~ 10^{-9} mm^3/N·m (Holmberg and Matthews, 2009)). Note however that the wear rate values for the polymeric coatings represent upper bound estimates since the experiments can run much longer times without further wear, as shown later. The friction and wear behavior is affected by the additives in the polymeric coatings. Specifically, PTFE coatings blended with pyrrolidone showed the best friction performance with a friction coefficient of 0.1. Pyrrolidone, usually referred to as poly (vinyl pyrrolidone), has been investigated for medical applications such as articular cartilage replacement due to its excellent low frictional properties (Katta *et al.*, 2007). Coatings blended with MoS_2

(PTFE/MoS_2 and Resin/PTFE/MoS_2) exhibited higher wear resistance, as MoS_2 offers favorable surface properties due to its lamellar structure (which can sustain high normal loads and at the same time low shear strength between its planes, resulting in a lubricious low friction surface (Holmberg and Matthews, 2009)). The PEEK coating blended with ceramics exhibited the highest friction coefficient and wear rate among the seven coatings tested under dry-oscillatory conditions. Even though PEEK is usually known to be harder than PTFE, and thus expected to have better wear performance, this is not the case in our experiments, where polymeric coatings were tested (versus bulk). This performance variation of PTFE and PEEK polymers, depending on their form, either bulk or coating, is further discussed in conjunction to unidirectional testing results.

3.3.2 Unidirectional testing simulating swash plate compressors

3.3.2.1 Detailed experiments results

The aforementioned seven polymeric coatings are now evaluated using dry-unidirectional testing to better understand their behavior under simulated swash plate compressor conditions. Figure 3.7(a) and (b) show the *in-situ* measurements of the friction coefficient and near contact temperature, respectively. Lower friction coefficient values in the range of 0.04 ~ 0.1 were observed under unidirectional conditions, while their near contact temperature was 3 to 4 times higher compared to the oscillatory experiments (likely due to an order of magnitude higher sliding speed). The near contact temperature behavior for all the coatings was similar in that at the start of the tests, it was around 22 °C and reached 100 °C immediately after test initiation. After that, depending on the coating, it either remained steady under 150 °C or reached values up to 250 °C.

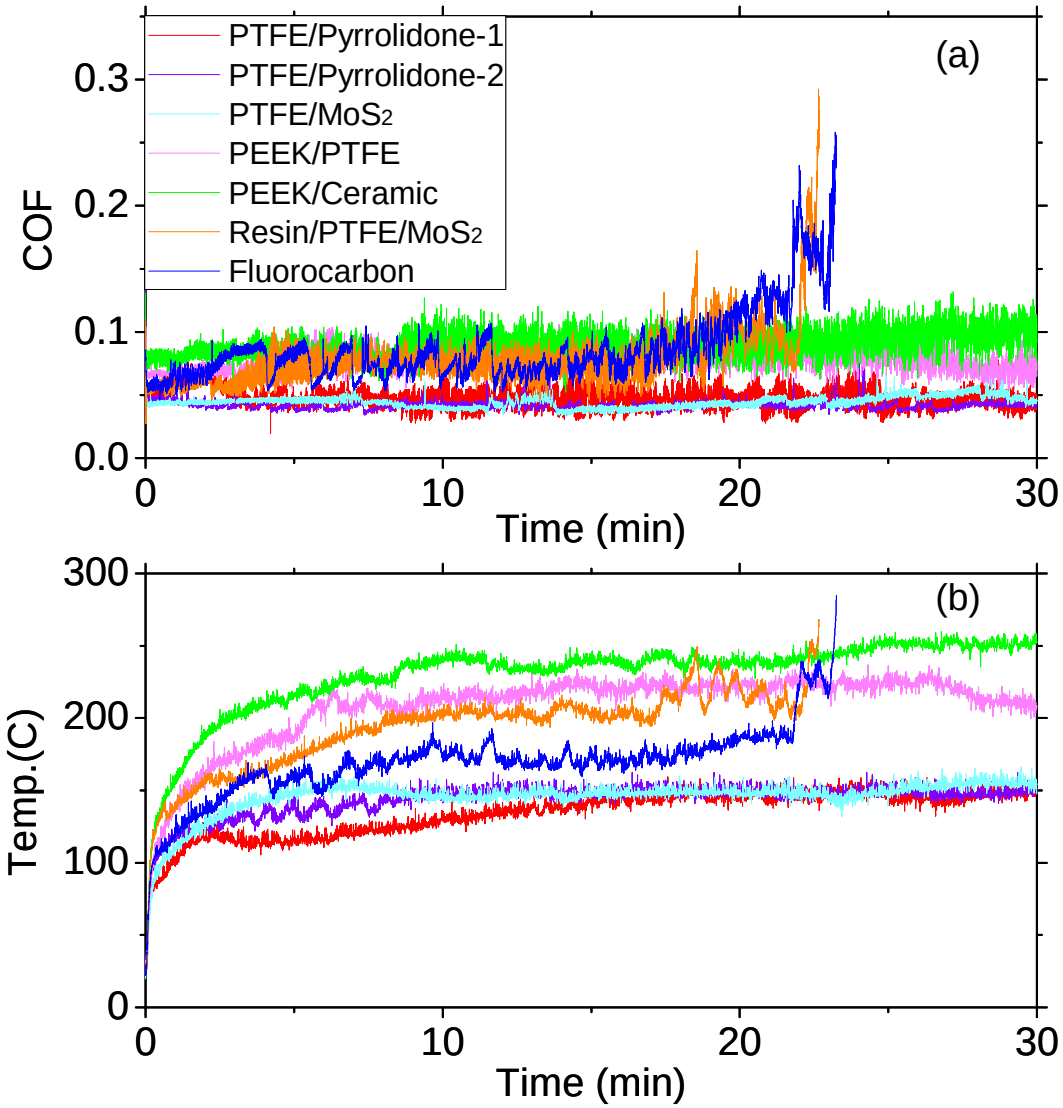

Figure 3.7 *In-situ* (a) friction coefficient (COF) and (b) near contact temperature (NCT) of seven polymeric coatings during 30 min unidirectional testing.

Based on the overall COF and NCT behaviors observed in Figure 3.7, coatings could be classified in three groups; 1) the best performing group (which includes PTFE/Pyrrolidone-1, PTFE/Pyrrolidone-2, and PTFE/MoS_2) showing the lowest COF around 0.04 ~ 0.05 and steady-state NCT of 150 °C, 2) the second group (PEEK/PTFE and PEEK/Ceramic) showing COF around 0.08 ~ 0.09 with 200 -250 °C NCT, and 3) the scuffed coating group (Resin/PTFE/MoS_2, Fluorocarbon) showing abrupt increase of

COF and NCT at around 23 min. Interestingly, this classification corresponded to the matrix the coating was made out of, in that PTFE-based coatings were the best performing group, PEEK-based coatings the second best group, and the others the worst performing group. It can be noticed from Figure 3.7(a) that the friction coefficient of PTFE-based coatings such as PTFE/Pyrrolidone-2 and PTFE/MoS_2 is not only low, but their values are also stable with very small deviations during the whole test, compared to fluctuating friction coefficient of PEEK-based coatings. This fluctuation of the COF is related to friction-induced wear mode, which is seen in the wear track profiles, shown next.

Figure 3.8 shows the wear track profiles of all seven polymeric coatings after 30 min testing under dry-unidirectional conditions. PEEK-based coatings that exhibited fluctuating friction coefficient also show material removal, due to friction-induced wear mode. On the other hand, PTFE-based coatings experienced only mild burnishing of less than 5 μm deep. Figure 3.8(a,b) and (c,d) show line scans of two different wear track locations for PTFE/Pyrrolidone-1 and PTFE/Pyrrolidone-2 coating, respectively. Both coatings exhibited similar mild wear behavior with an average wear depth of 2 ~ 4 μm, which was significantly lower compared to oscillatory testing results. The PTFE/MoS_2 coating showed slightly higher wear resistance with less than 2 μm of wear as seen in Figure 3.8(e). PEEK/PTFE was worn out completely, Figure 3.8(f), and its wear profile was the same as the crown shape of the counter-surface shoe. Despite this high wear, the PEEK-based coating survived the total 30 min testing due to the beneficial effect of the generated wear debris. The two scuffed coatings showed over 60 μm of sharp and deep wear scars, which penetrated through the coating and wear the cast iron substrate as well.

Note that these unidirectional test results could more clearly differentiate the wear performance between PTFE- and PEEK-based coatings, compared to the oscillatory experiments. This is attributed to an order of magnitude higher sliding distance with unidirectional testing.

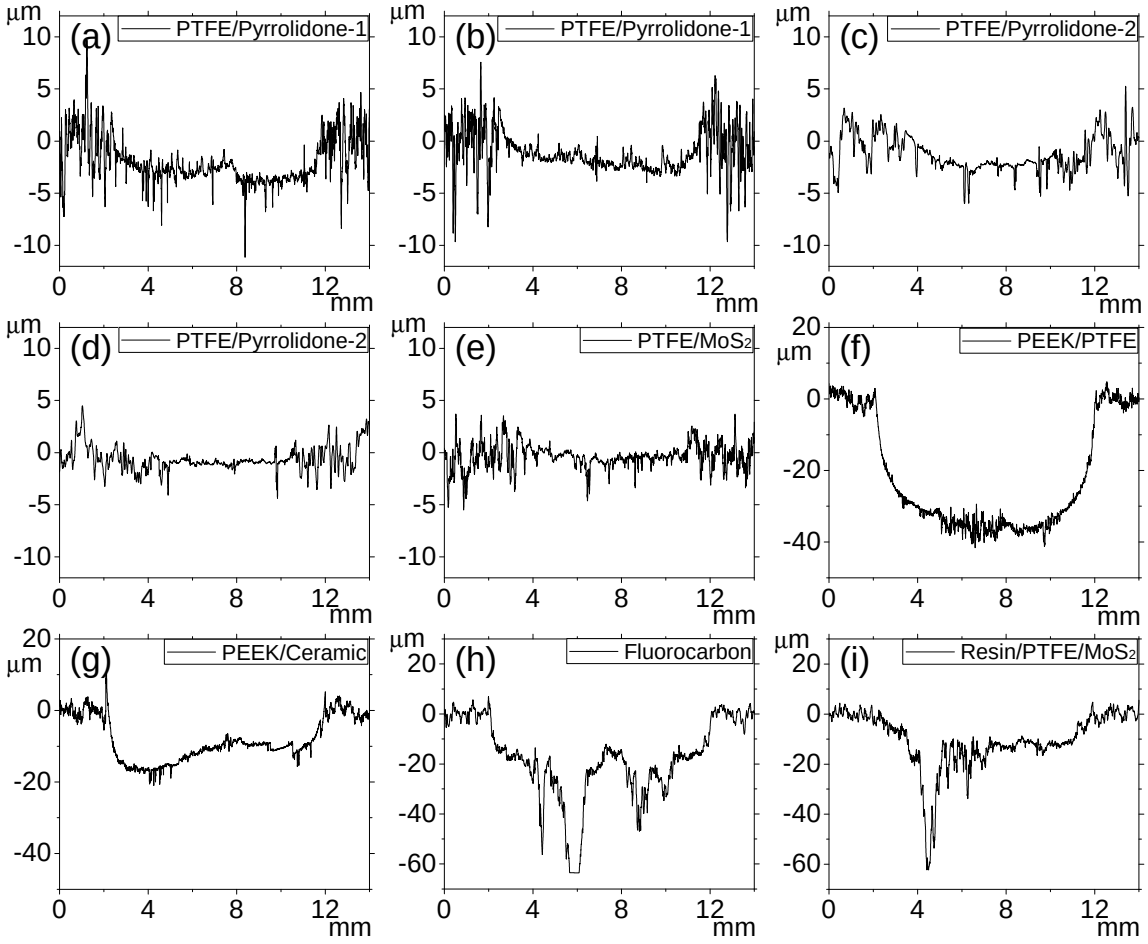

Figure 3.8 Profilometric wear track measurements of (a,b) PTFE/Pyrrolidone-1, (c,d) PTFE/Pyrrolidone-2, (e) PTFE/MoS_2, (f) PEEK/PTFE, (g) PEEK/Ceramic, (h) Fluorocarbon, and (i) Resin/PTFE/MoS_2 coatings after 30 min unidirectional testing.

In the case of the PTFE-based coatings shown in Figure 3.8(a) ~ (e), and which exhibited strong wear resistance, as the shoe was sliding on the coating surface,

smoothening of the wear track surfaces is clearly observable. Also, note that the mean plane of the smoothened wear track surface (from 4 to 10 mm scan length) is sometimes located slightly higher than the lowest point of the valleys in the original coating surfaces (both edges of wear profiles from 0 to 2 or from 12 to 14 mm scan length). This is attributed to the fact that the very fine PTFE-based wear debris (observed after testing) was filling the valleys and pits of the initial rough coating surfaces, and thus, solid polymer lubricant can stay continuously trapped inside the wear track, thus effectively lubricating the dry interface preventing catastrophic failure. None of these behaviors were observed in the other coatings, which alludes to the fact that this is a critical mechanism of polymeric coatings in determining their tribological performance. This "filling effect" of wear debris is also seen in the optical pictures in Figure 3.9, showing the wear tracks after unidirectional testing. The wear tracks of PTFE/Pyrrolidone-2 and PTFE/MoS_2 coatings are very glossy after sliding because the surface got smoothened due to the filling effect of the wear debris. On the contrary PEEK based coatings generated flake-like debris, and resulted in continuous coating material removal and thus higher wear rates. In the case of the scuffed coatings (Fluorocarbon and Resin/PTFE/MoS_2), complete penetration of the coatings was observed, thus exposing the cast iron substrate surface as seen in Figure 3.9(d). Because the counterpart (shoe) surface is extremely smooth (0.035 μm), the filling effect is not observable on the shoe surface, and in this case, usually very thin transfer film is supposed to be formed on it (Escobar Nunez *et al.*, 2011).

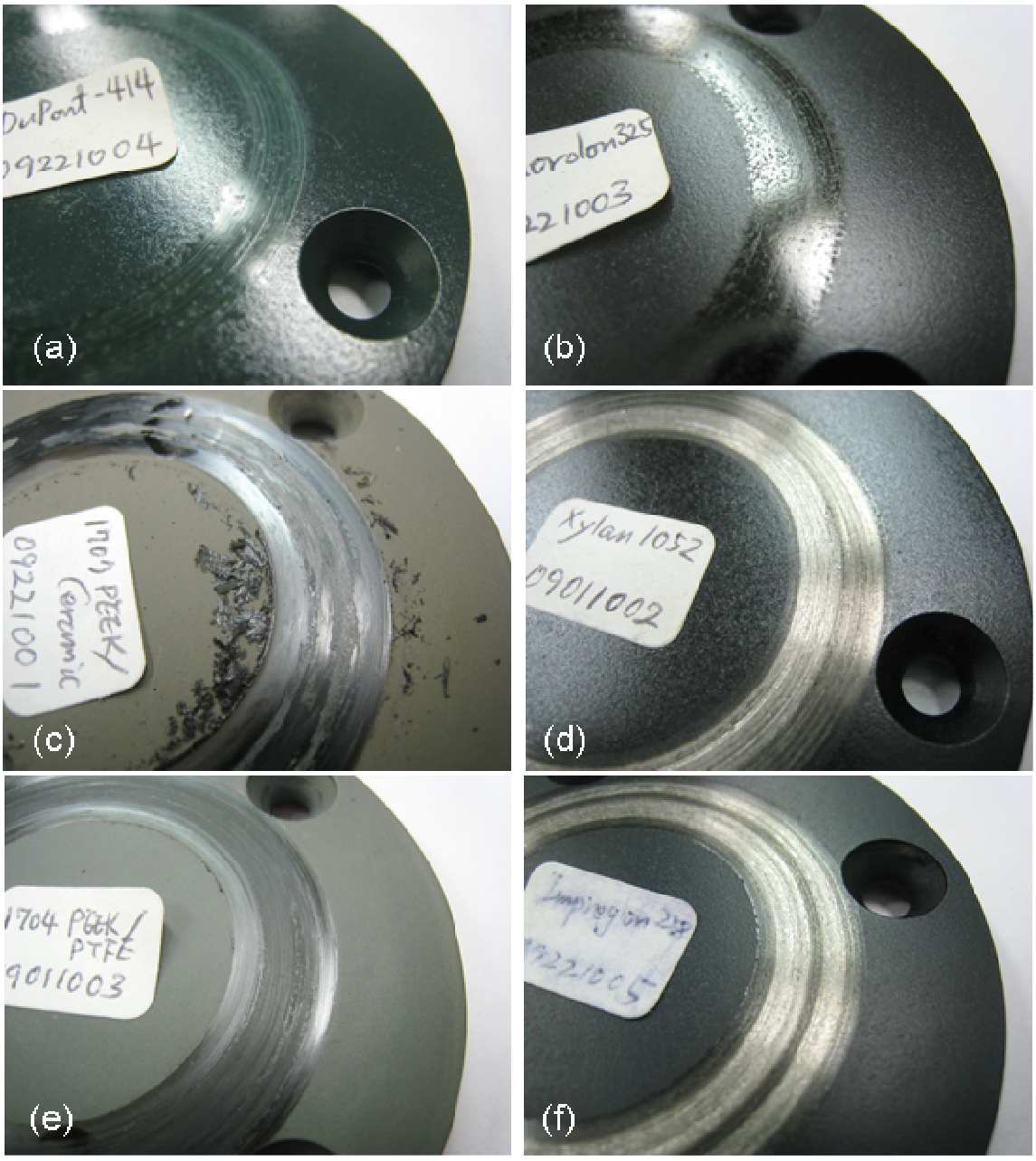

Figure 3.9 Optical images of the wear track surfaces after 30 min unidirectional testing; (a) PTFE/Pyrrolidone-2, (b) PTFE/MoS_2, (c) PEEK/Ceramic, (d) Resin/PTFE/MoS_2, (e) PEEK/PTFE, and (f) Fluorocarbon.

3.3.2.2 Oscillatory vs. unidirectional; coating vs. bulk and PTFE vs. PEEK

The wear rates for the unidirectional tests were also calculated and summarized in Table 3.3, along with average COF and NCT values during the steady-state period from

10 to 30 min. PTFE/Pyrrolidone-2 exhibited the lowest average COF value of 0.043, PTFE/MoS_2 the second lowest, and then PTFE/Pyrrolidone-1. However, their difference was very small with all three coatings being in the range of 0.043 ~ 0.047. These are significantly low friction coefficient values, bearing in mind that these are oil-less aggressive operating conditions. PTFE/MoS_2 coating showed the lowest wear rate with a value less than 10^{-7} mm^3/Nm. The friction coefficient for the PEEK-based coatings was almost twice as high compared to the PTFE-based coatings, and their wear rate was in the range of 6.73×10^{-6} ~ 1.63×10^{-5} mm^3/N·m (i.e., an order of magnitude higher than PTFE-based coatings).

Table 3.3 Average COF, NCT and wear rates of the polymeric coatings tested under dry-unidirectional conditions for 30 min.

	Polymeric Coatings	Ave. COF (Std.) (10 ~ 30 min)	Wear Rate (Std.) (mm^3/N·m)	NCT (Std.) (°C) (10 ~ 30 min)
Group 1	PTFE/Pyrrolidone-1	0.047 (0.007)	1.54E-6 (2.11E-7)	142.8 (5.9)
	PTFE/Pyrrolidone-2	0.043 (0.003)	1.23E-6 (2.97E-7)	148.6 (2.3)
	PTFE/MoS_2	0.044 (0.005)	3.76E-7 (8.64E-8)	148.7 (3.8)
Group 2	PEEK/PTFE	0.079 (0.008)	1.63E-5 (1.28E-6)	219.8 (5.2)
	PEEK/Ceramic	0.092 (0.010)	6.73E-6 (9.77E-7)	241.9 (6.5)
Group 3	Resin/PTFE/MoS_2	Scuffed	9.01E-6 (2.39E-7)	-
	Fluorocarbon	Scuffed	1.52E-5 (6.02E-7)	-

Figure 3.10 shows a direct comparison of both friction (linear scale) and wear (logarithmic scale) behavior of all coatings. From this comparison, it is clearly seen that the wear rates for all coatings tested under oscillatory conditions, are clustered in very

small range of $2\times10^{-5} \sim 5\times10^{-5}$ $mm^3/N\cdot m$, whereas, in the case of unidirectional testing conditions, the wear rate values vary in the range of 10^{-7} to 10^{-5} $mm^3/N\cdot m$. Also, in addition to the lower wear rates, the coatings tested under unidirectional conditions, exhibited lower friction coefficient values, compared to oscillatory testing conditions. It is cautioned against generalizing such finding, because the testing parameters (sliding speed, contact pressure and the shape of pin) were different for each testing condition, simulating specific type of compressor conditions. From Figure 3.10(a), PTFE/MoS_2 coating located in the lower left hand corner of the plot is the best performing coating for swash plate compressor simulation, whereas, for piston-type compressors, PTFE/Pyrrolidone-1 seems to be more favorable, as seen in Figure 3.10(b).

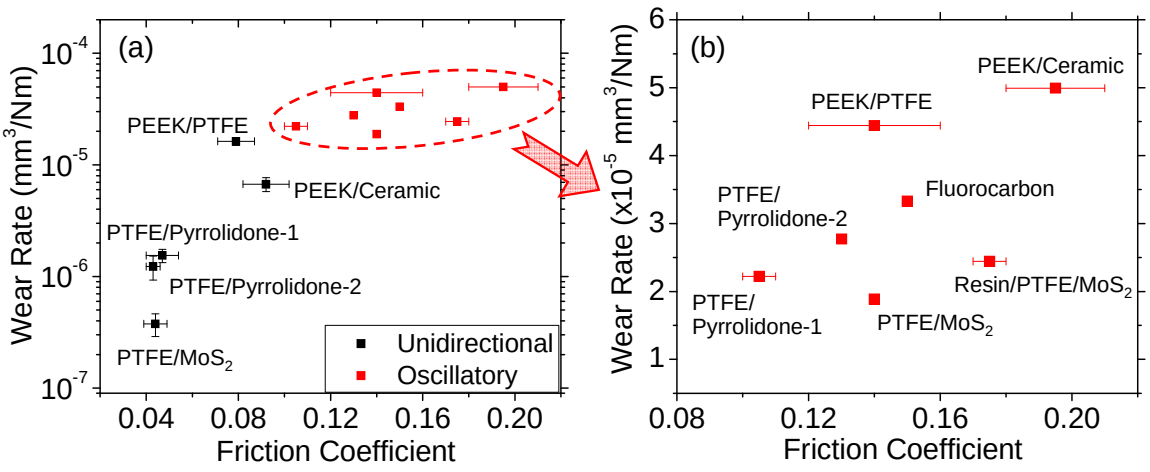

Figure 3.10 (a) Friction coefficient vs. wear rate of seven polymeric coatings under both unidirectional and oscillatory testing and (b) zoom-in of only oscillatory testing results.

A general finding from this work is that PTFE-based coatings exhibited better tribological performance than PEEK-based coatings, under both oscillatory and unidirectional conditions, and, interestingly, this was not the case for bulk polymers.

Cannaday and Polycarpou (2005), for example, demonstrated that bulk form of PEEK blended with graphite exhibited the lowest friction coefficient and wear rate compared to PTFE blended with graphite in both R-134A and ambient air environments (under unidirectional sliding conditions). Also, it was shown in Ref. Burris and Sawyer (2007) that bulk form of PEEK blended with PTFE exhibited lower wear rate than any other PTFE blends, such as PTFE/PEEK, PTFE/CNT and PTFE/Si_3N_4. These performance variations of PTFE and PEEK polymers depending on their form, either bulk or coating, could be attributed to the different wear mechanism for each case. For bulk materials, continuous scratching and peeling of polymers are the dominant wearing mechanism, and thus making harder materials tend to exhibit lower wear rate. This is why the harder PEEK blends usually perform better than PTFE blends when they are used in bulk form. In the case of coatings, wear debris comes to effectively serve as solid lubricant at some point due to usually very hard substrate material (cast iron in this work) which is not the case in bulk polymers where continuous material removal occurs. Therefore, the filling effect of the wear debris explained in Figure 3.8 becomes dominant in the wear behavior of polymeric coatings. In this case, the structure of the coating plays a key role in determining the formation of wear debris and the overall behavior of the coating. Originally, both PTFE and PEEK polymers are classified as crystalline thermoplastic along with the most widely used low density polyethylene (LDPE) (Brinson and Brinson, 2008). However, the sputtered PTFE films usually have an amorphous structure, resulting in very fine wear debris (Holmberg and Matthews, 2009) which is more favorable for effective lubrication. Obtaining an amorphous PEEK is almost impossible due to its high crystallizing speed and low thermal conductivity (Zhang et al., 2007).

SEM images of the worn surfaces for PEEK/PTFE and PTFE/Pyrrolidone-2 coatings could effectively show the above mentioned structural difference between two coatings as well as the insight of wear debris formation of each coating as seen in Figure 3.11. First, from Figure 3.11(a), it can be clearly seen that a big chunk of coating material was removed from the PEEK/PTFE coating surface by sliding, which explains the large size of wear debris for this coating. Also, the sub-surface area as marked in the figure showed the significantly porous structure of PEEK/PTFE coating. However, in the case of PTFE/Pyrrolidone-2 coating as seen in Figure 3.11(b), only mild plastic plowing was observed without any signs of severe material removal from the surface. Also, it seemed that fine powders were compressed together showing an extensively smooth top surface of PTFE/Pyrrolidone-2 coating, and thus resulting in its uniform microstructure. This is why the wear debris of PEEK-based coatings was larger and more flake-like as seen in Figure 3.9, and thus could not effectively fill the rough surfaces, resulting in higher friction coefficient and wear rate, compared to PTFE-based coatings. Thus, in the form of coatings, the wear performance of PTFE blends is improved and better, compared to the PEEK blends.

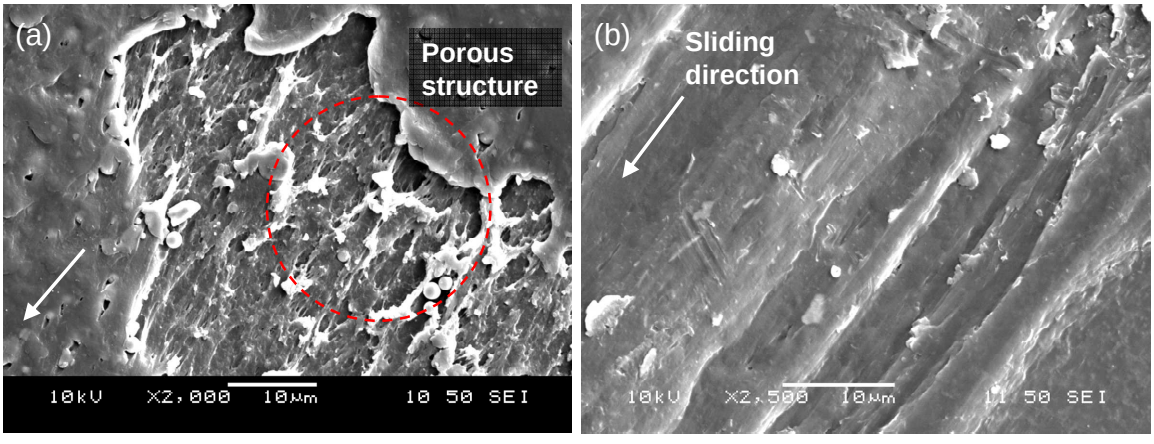

Figure 3.11 SEM images of the worn surfaces of (a) PEEK/PTFE coating and (b) PTFE/Pyrrolidone-2 coating after 30 min dry unidirectional sliding test.

3.3.2.3 Durability unidirectional testing

Since the 30 min tests (corresponding to 6.75 km sliding distance) might not be sufficiently long to validate the polymeric coating's reliability in compressor applications, and to also further substantiate the superiority of the PTFE-based coatings, 3 hour long duration unidirectional tests (corresponding to 40.5 km sliding distance) were performed for PTFE/Pyrrolidone-2, PTFE/MoS_2, and PEEK/PTFE coatings, and shown in Figure 3.12.

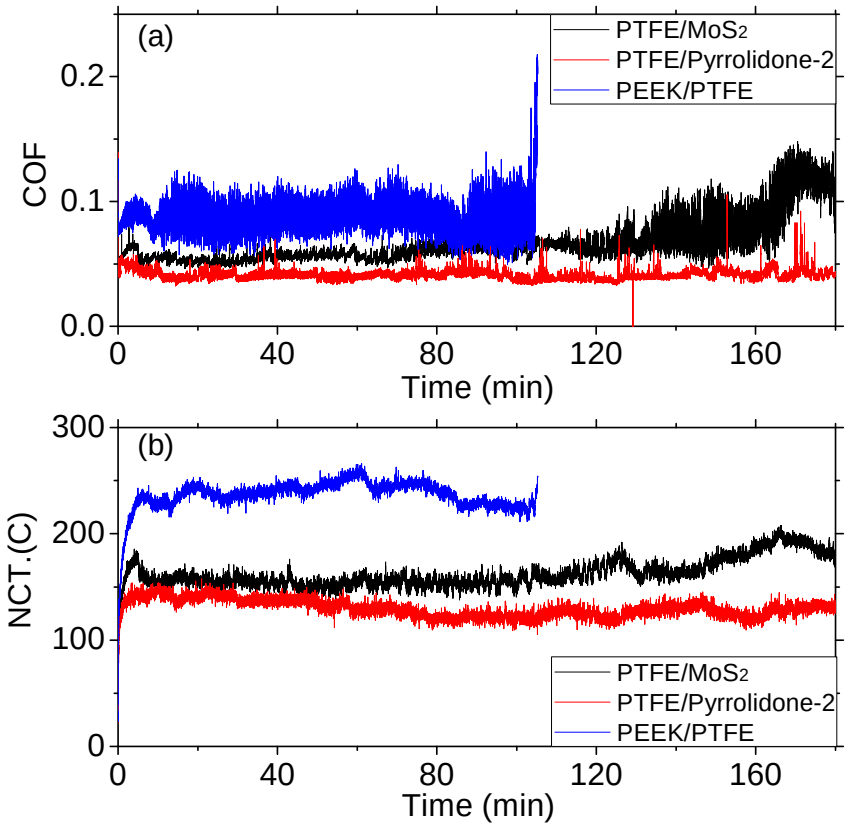

Figure 3.12 *In-situ* (a) friction coefficient and (b) near contact temperature of PTFE/MoS_2, PTFE/Pyrrolidone-2, and PEEK/PTFE coatings during 3 hour unidirectional testing.

Even though none of these coatings showed scuffing with the 30 min tests, PEEK/PTFE coating eventually scuffed after 105 min, with sharp increase of the friction coefficient as seen in Figure 3.12(a). Both PTFE-based coatings exhibited very stable

and lower friction coefficient than the PEEK-based coatings, however, the COF of PTFE/MoS_2 coating started to fluctuate after 2 hours and showed somewhat unstable behavior with increased values up to 0.13. Even though PTFE/MoS_2 coating didn't scuff until the end of the 3 hour testing, it would have eventually scuffed. This is because not only its COF became unstable, but its near contact temperature was also gradually increasing and reached 200 °C. The best performance was observed with PTFE/Pyrrolidone-2 coating with very stable friction coefficient, less than 0.05 during the whole test, and its NCT also being very stable and less than 150 °C, even after 3 hours.

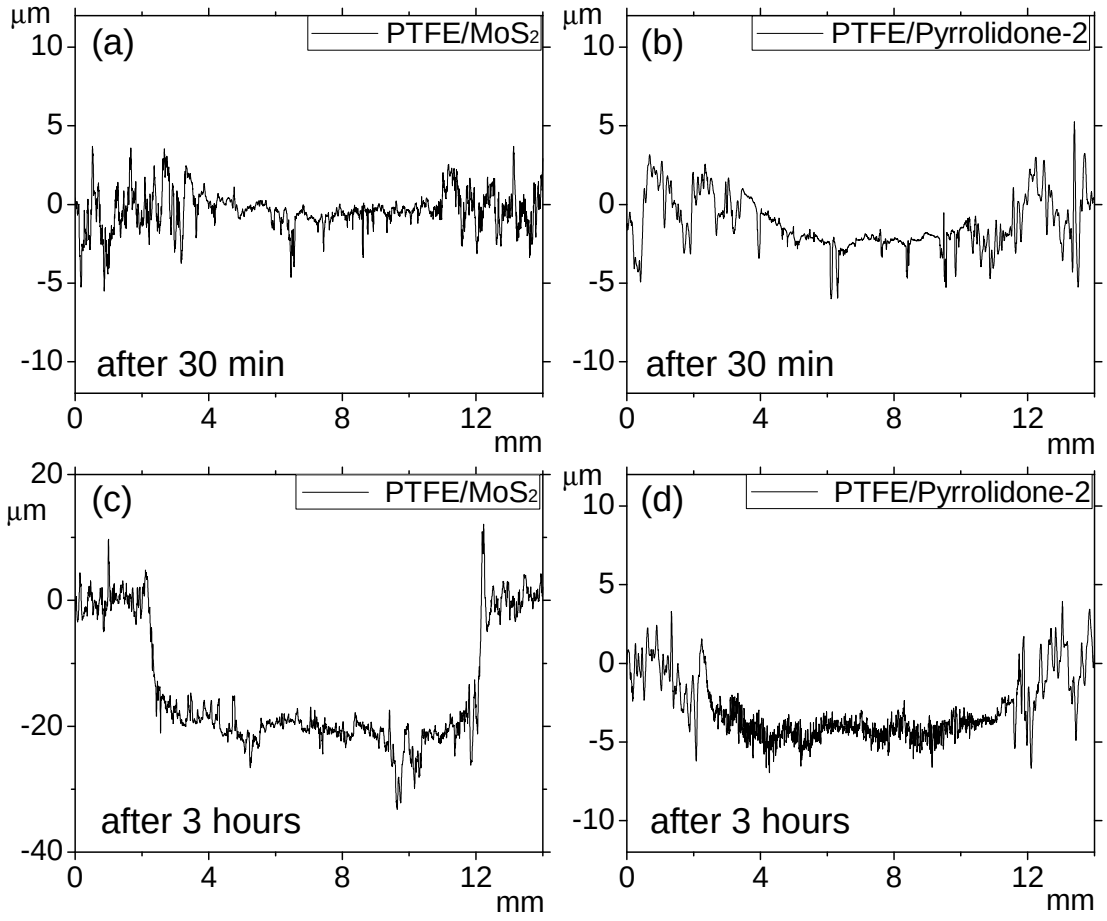

Figure 3.13 Profilometric wear track measurements of (a) PTFE/MoS_2 and (b) PTFE/Pyrrolidone-2 after 30 min, and (c) PTFE/MoS_2 and (d) PTFE/Pyrrolidone-2 after 3 hours under dry-unidirectional testing.

The wear track profiles of the two PTFE-based coatings after the durability 3 hour tests are shown in Figure 3.13(c,d) and compared with the 30 min test results, which are repeated in Figure 3.13(a,b). Both coatings exhibited only mild burnishing with less than 5 μm of wear depth after 30 min test. After the 3 hour tests, more material removal occurred with the PTFE/MoS_2 coating surface showing over 20 μm of wear depth, whereas, in the case of PTFE/Pyrrolidone-2 coating, surprisingly, still only 5 μm depth of material removal was observed. As discussed earlier, after 30 min testing, PTFE/MoS_2 coating seemed to perform the best under unidirectional sliding conditions. However, as shown after the 3 hour tests, PTFE/Pyrrolidone-2 coating had superior wear performance to the other coatings, relevant to compressor applications.

3.4 Conclusion

Different polymeric coatings based on PTFE, PEEK, fluorocarbon and resin were tested using a specialized tribometer under aggressive conditions simulating critical tribopairs of both piston-type (reciprocating motion) and swash plate (unidirectional motion) air-conditioning and refrigeration compressors. The following conclusions could be drawn:

(a) Higher friction coefficient values in the range of 0.1 ~ 0.2 and wear rate values of 10^{-5} $mm^3/N \cdot m$ were measured under oscillatory conditions. Better performance with lower friction coefficient values of 0.04 ~ 0.1 and wear rates of 10^{-7} $mm^3/N \cdot m$ were measured under unidirectional conditions. Under both operating conditions (but more so for unidirectional), polymeric coatings exhibited acceptable to superior tribological

performance, under aggressive oil-less compressor conditions, and thus are likely viable candidates for the next generation of oil-less compressors.

(b) PTFE-based coatings (PTFE/Pyrrolidone and PTFE/MoS_2) generally performed better than PEEK-based coatings (PEEK/PTFE and PEEK/Ceramic) under both piston-type (oscillatory motion) and swash plate (unidirectional motion) compressor conditions, which was not the case for bulk polymer blends (where typically PEEK composites filled with PTFE performed best).

(c) The effect of polymer coating wear debris, serving as a solid lubricant on the hard substrate surface, was shown to be more dominant in determining the overall wear behavior of polymeric coatings than the mechanical properties of the polymer coating itself. The structural changes in the PTFE coatings from semi-crystalline to amorphous caused by the coating process, resulted in very fine wear debris enhancing its lubricity. PEEK-based polymer coatings were still exhibiting crystalline structure after the coating process, due to its high crystallizing speed, thus resulting in large and flake-like wear debris.

(d) Durability or time-to-failure (3-hour duration) unidirectional testing corresponding to 40.5 km sliding distance showed superb friction and wear behavior of PTFE-based coatings, especially PTFE/Pyrrolidone-2, thus demonstrating its potential applicability for use in oil-less compressors.

CHAPTER 4: MECHANICAL/STRUCTURAL PROPERTY CHARACTERIZATION OF POLYMERIC COATINGS USING MICRO-INDENTATION

4.1 Introduction

In Chapter 3, the tribological performance of PTFE- and PEEK-based polymeric coatings were measured under compressor-specific operating conditions. In particular, PTFE-based coatings showed very good friction and wear behavior, under specific conditions, which included refrigerant environment typical to air-conditioning and refrigeration compressors. There is a need to identify simpler and more general characterization techniques to quantify the performance of such polymer surfaces than demanding tribological testing as in Chapter 3. One such technique is the measurement of the surface micromechanical properties of the polymer materials. However, the majority of such research has been done for bulk polymers (Klapperich *et al.*, 2001 and Briscoe *et al.*, 1998), with limited work on polymeric coatings (Strojny *et al.*, 1998, Xia *et al.*, 1998, Tayebi *et al.*, 2004, and Hay, 2009).

For bulk polymers, Klapperich *et al*. (2001) demonstrated that it was possible to distinguish between different polymers using the nanoindentation load-displacement data. Nanoindentation data on amorphous polymers such as poly (methyl methacrylate) (PMMA) and polycarbonates (PC) showed repeatability, and thus more uniform load-bearing properties, compared to semi-crystalline polymers such as low-density polyethylene (LDPE) and ultra-high-molecular-weight polyethylene (UHMWPE). Briscoe *et al*. (1998) also performed mechanical property measurements of bulk polymers using the nanoindentation technique. The softer nature of the UHMWPE system, which

is a semi-crystalline polymer, was compared to three amorphous polymers, PMMA, PC, and polystyrene (PS). These works showed that micromechanical properties of polymers were significantly affected by their microstructure.

In measuring the mechanical properties of coatings on a substrate, there is a complexity in obtaining coating properties that are not affected by the substrate properties (or to what extend they are affected). Strojny *et al*. (1998) and Xia *et al*. (1998) measured the properties of thin (less than 5 μm thick) PMMA and polyurethane-based coatings under controlled laboratory conditions, and showed the significant effect of substrate and surface topography on the measured modulus values. Tayebi *et al*. (2004) examined the substrate effects on the hardness of two coating/substrate systems, representative of a soft coating on a hard substrate (Au/Fused Quartz) and a hard coating on a soft substrate (SiO_2/Al), using both the nanoindentation and nanoscratch techniques. It was validated that at sufficiently shallow depths (which depend on the coating system as mentioned above and technique used), one can obtain "true coating" mechanical properties. Hay (2009) studied the substrate influence on the mechanical properties of three different kinds of dielectric films (5 GPa, 7 GPa, 15 GPa of modulus, respectively) on silicon wafers using instrumented indentation. It was observed that, at small contact depths, the error due to the substrate influence was small, but the uncertainty was greater due to "skin" effects such as surface roughness, tip variations, and stage vibrations. However, as indentation depth increased, the error due to substrate effects became dominant.

In this chapter, we report on the micromechanical properties of seven different PTFE- and PEEK-based polymeric coatings, with particular emphasis placed on the cast

iron substrate effects, and correlation with the polymer structure. Using a combination of large force range (~ 300 mN) and large displacement range (~ 7 μm) indentation, the complete coating response could be measured together with the effect of the hard substrate. The microstructural differences between the coatings were examined using scanning electron microscopy (SEM) and were used to explain differences in their micromechanical properties. The measured micromechanical properties, which could be readily obtained by performing simple laboratory indentation tests, were successfully correlated with compressor specific tribological experiments.

4.2 Experimental

4.2.1 Coatings

Figure 4.1 shows a representative coating and substrate sample used in this work which was already tribologically tested in Chapter 3 as well. Gray cast iron (Dura-Bar® G2) was chosen as a substrate material and machined to 79 mm diameter and 8 mm thickness disks, as can be seen in Figure 4.1(a). Seven different polymeric coatings, namely, PTFE/Pyrrolidone-1 (DuPont™ Teflon® 958-303), PTFE/Pyrrolidone-2 (DuPont™ Teflon® 958-414), Resin/PTFE/MoS_2 (Whitford Xylan® 1052), PEEK/PTFE (1704 PEEK/PTFE®), PEEK/Ceramic (1707 PEEK/Ceramic®), Fluorocarbon (Impreglon® 218), and PTFE/MoS_2 (Fluorolon® 325) were used in this chapter. Especially, pyrrolidone-based PTFE coatings (from DuPont™) have great toughness and abrasion resistance, thus exhibiting exceptional durability (Chapter 3). Coatings blended with MoS_2 can normally sustain high normal loads and may offer, at the same time, low shear strength due to lamellar structure of MoS_2, thus resulting in a lubricious low

friction surface. PEEK-based coatings were selected due to their better wear resistance than PTFE-based coatings which could be attributed to PEEK's stiff backbone chemical structure and high temperature stability (Escobar Nunez *et al.*, 2011).

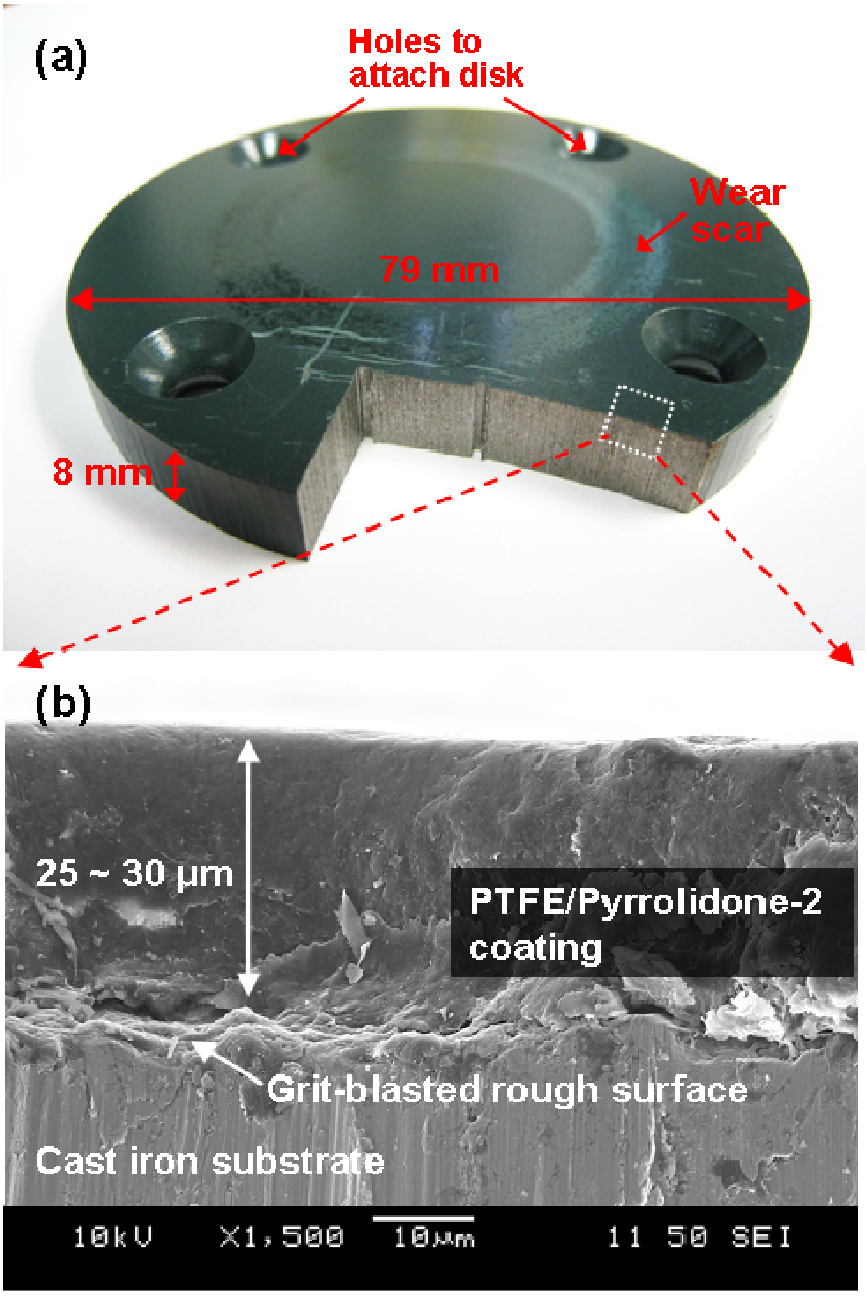

Figure 4.1 (a) PTFE/Pyrrolidone-2 (dark green color) coating on cast iron substrate (Dura-Bar® G2) and cut area for cross-section observation; (b) SEM image of coating cross-section showing the thickness of the coating and grit-blasted rough surface.

Figure 4.1(b) shows a representative cross-section of a coating system examined through SEM. The thickness of the PTFE/Pyrrolidone-2 coating shown in Figure 4.1(b) is 25 to 30 μm. The measured thicknesses of the other coatings were similar, in the range of 30 ± 10 μm, as summarized in Table 4.1 along with additional coating properties. These values are thicker than typical hard coatings, such as diamond-like-carbon (DLC) and WC/C (2.5 μm (Solzak and Polycarpou, 2010)). The roughness of each coating was measured using a stylus profilometer (Tencor P-15™) with 4 mm scan distance and 1 data/μm sampling rate. Figure 4.2 shows the representative surface profile (without any filtering) of each coating tested in this work. Root-mean-square (RMS) roughness values in Table 4.1 were calculated after band-pass filtering of these profiles with 2 μm short wavelength cutoff and 500 μm long wavelength cutoff. The average surface roughness values of the coatings were in the range of 0.6 μm to 2.3 μm, which was lower than the roughness after grit-blasting and before coating deposition, as expected. Interestingly, the coating roughness values vary significantly, likely due to the powder/particle size used in each coating.

Table 4.1 Physical properties of the polymeric coatings used in this work.

Coating	Curing Temp. (°C)	In-use Temp. (°C)	Color	Thickn-ess (μm)	RMS roughness [Std] (μm)
PTFE/Pyrrolidone-1	250 ~ 340	260	Matte black	26 ± 5	2.28 [0.09]
PTFE/Pyrrolidone-2	255	200	Dark green	23 ± 5	0.61 [0.08]
Resin/PTFE/MoS_2	220 ~ 345	260	Glossy black	20 ± 5	1.71 [0.07]
PTFE/MoS_2	316	260	Black	20 ± 5	1.14 [0.05]
Fluorocarbon	316	232	Navy black	25 ± 5	1.53 [0.15]
PEEK/PTFE	400	260	Dark gray	40 ± 5	1.00 [0.03]
PEEK/Ceramic	400	260	Beige-tan	38 ± 5	0.92 [0.05]

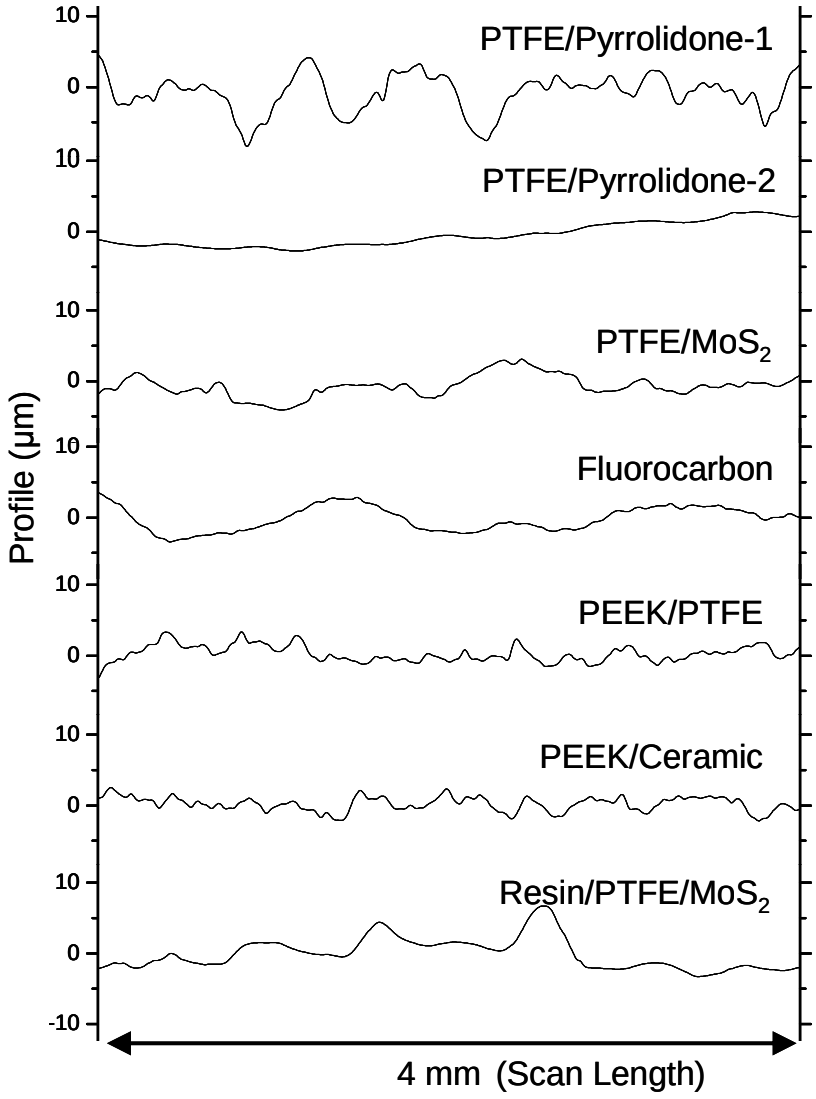

Figure 4.2 Surface roughness profiles of seven different polymeric coatings measured using a stylus profilometer (sampling rate is 1 data point/µm, no filtering).

4.2.2 High-load indentation and tip calibration

Micromechanical property measurements of polymeric coatings were performed using a TI-950 TriboIndenter™ equipped with a 3D OmniProbe™ (Hysitron, Inc.). This probe uses piezoresistive loading and capacitive sensing, enabling higher normal force indentations up to 2,687 mN, and a wide range of normal displacement sensing from 1

nm to 93.7 μm. This compares to a limited load (~ 12 mN) and displacement (~ 4.5 μm) ranges for conventional nanoindentation transducers, but consequently, its theoretical load (376 nN) and displacement resolutions (0.01 nm) are supposed to be lower than those of conventional transducer (1 nN and 0.006 nm). Additionally, its practical resolution values might be even lower due to vibration and thermal noise. Loading operates on the principle that when a voltage is applied to a pre-stressed piezoelectric material, it lengthens and pushes the indentation probe into the sample. The movement of the probe end-tip is carefully monitored and adjusted through a high-frequency digital feedback loop which collects information from the Z-axis load cell (load-controlled indentation). A Berkovich tip (three-sided pyramid) with a measured radius of curvature of 170 nm (Figure 4.3) was used in this work due to its suitability for bulk materials and relatively thick coatings.

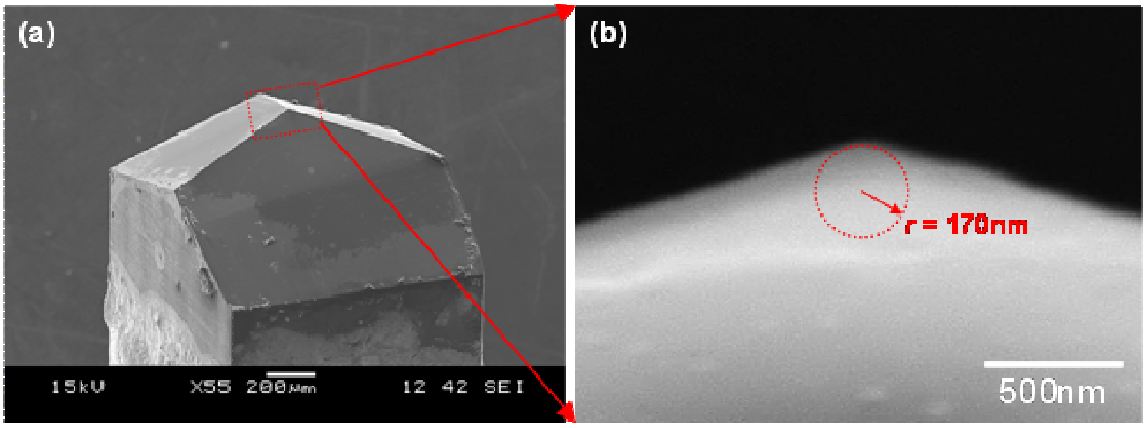

Figure 4.3 (a) SEM image of Berkovich tip used in the high-load indentation measurements and (b) zoom-in of tip end showing a nominal radius of curvature of about 170 nm.

A critical component of indentation measurements is the calibration of the tip, known as area function. It uses compliance method, also known as the Oliver-Pharr

method (Oliver and Pharr, 1992), where the mechanical properties are calculated based on the contact area of the probe tip to the sample, under a certain load. Since indentation measurements give us only contact depth information, the tip area function correlating the contact area and the contact depth needs to be determined/ known for the tip used in the measurements. Note that contact depth h_c is defined as the vertical distance along which contact is made by the tip during loading, and is less than the maximum penetration depth (h_{max}) due to the elastic property of the indented surface (Oliver and Pharr, 1992). If the tip was manufactured to be perfect without any defects (which is not the case), the area function will be simply the geometrical shape function of a pre-specified tip such as,

$$A_c(h_c) = 24.5\, h_c^2 \tag{4.1}$$

in the case of the Berkovich tip. However, due to tip imperfections, the area function usually takes the following polynomial form.

$$A_c(h_c) = C_0 h_c^2 + C_1 h_c + C_2 h_c^{1/2} + C_3 h_c^{1/4} + C_4 h_c^{1/8} + \cdots . \tag{4.2}$$

To determine the coefficients of the above equation, indentations at varying penetration depths (corresponding to similar depth range as the desired measurements) are performed on a standard material. Then, since the modulus of the standard material is known, the contact area corresponding to each contact depth (A_c, h_c) can be calculated and plotted as in Figure 4.4, and finally, the coefficients are determined by polynomial curve-fitting.

Two important elements that affect the tip calibration and thus the material property values are 1) the choice of the standard sample and 2) the contact depth range of calibration. In this study, a modified bismaleimide polymer (manufactured by BASF Corp) (Chasiotis *et al.*, 2005) with a reduced modulus value of 5.0 GPa was used as the

calibration standard, as its value is similar to the polymeric coatings to be tested in this work. Note that we did not use the widely used fused Quartz standard because its reduced modulus is significantly higher than our interest, namely 69.6 GPa. Calibration was performed with 22 varying loads from 1 mN to 800 mN (under the exact same loading conditions as the measurements detailed later) resulting in 0.5 to 6.5 μm of contact depths (Figure 4.4) which were of similar range to those of the actual measurements. Once the tip is completely calibrated with the coefficients seen in Figure 4.4, this tip area function is directly used for the calculation of the mechanical properties during the indentation measurements. The detailed calculation process using the compliance method which involves the determination of the elastic modulus and hardness exclusively from the initial unloading portion of the load-displacement curve can be found in the literatures (Oliver and Pharr, 1992 and Hay and Pharr, 2000).

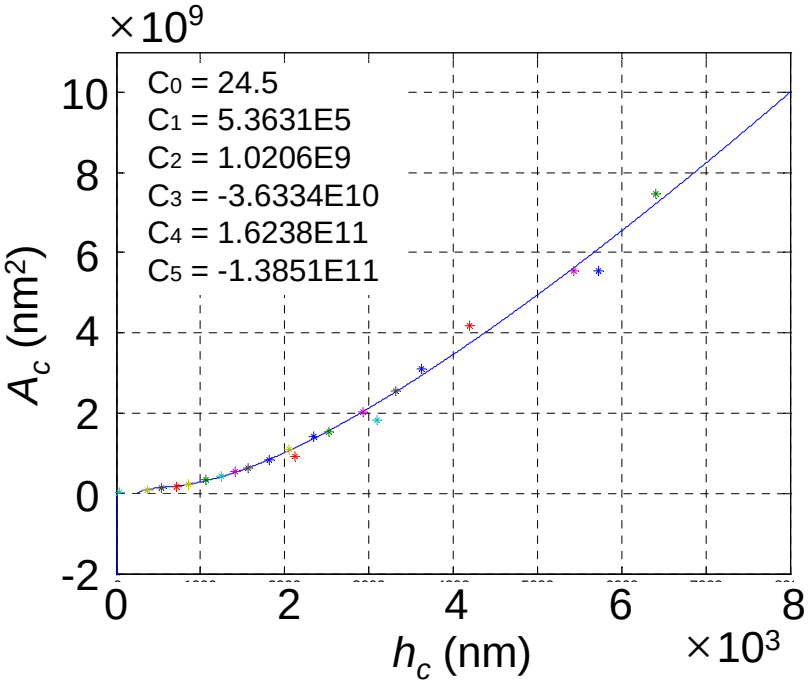

Figure 4.4 Polynomial curve-fitting of measured contact area versus contact depth to determine the coefficients of tip area function.

4.2.3 Measurement details

A typical indentation experiment on a polymeric material involves engaging the probe tip to the sample surface under a light load (2 μN), indenting to a pre-specified maximum load at a constant loading rate (10 mN/s), holding at the peak load (5 sec in this case) to reduce creep effects (Briscoe *et al.*, 1998), and then withdrawing the tip at the same rate as during loading (-10 mN/s). This is called trapezoidal loading profile, compared to the most commonly used triangular profile which does not have a hold-time at the peak load. The initial set of indentations were performed on PTFE/Pyrrolidone-2 coatings using both trapezoidal and triangular loading profiles with a maximum load of 70 mN to examine possible creep behavior. Also, for the triangular loading, three different loading/unloading rates (2, 10 and 30 mN/s) were explored to investigate their effect on the slope of the initial part of the unloading curve (and thus the calculated property values). As for the main indentation measurements on the 7 different polymeric coatings for extracting their mechanical properties, a trapezoidal loading profile at a constant loading/unloading rate of ±10 mN/s was used for about 10 varying maximum loads between 5 to 400 mN (which correspond within the calibration range). For each maximum load, six indentations were repeated at different areas (resulting in approximately 60 indentations for each coating sample), thus resulting in 420 indentations in total. Although this method of using single loading/unloading indentations is time consuming, compared to the partial unloading method, it is preferred for precise examination of polymer material properties. Also, in this work, single

indentations showed valuable phenomena for each coating, which correlated their structural properties with their tribological behavior.

4.3 Results and discussion

4.3.1 High-load indentation

4.3.1.1 Creep behavior

First, the general behavior of the polymeric coatings under high load indentation is discussed before we present the measurements of the specific coating's mechanical properties. Figure 4.5(a) shows a representative load-displacement curve obtained from a single indentation on PTFE/Pyrrolidone-1 with 20 mN maximum load. Figure 4.5(b) shows the in-situ time varying load and displacement of the probe tip-end. It can be seen that the indenting process was load controlled and its profile was trapezoidal with 5 sec of hold time at the peak load.

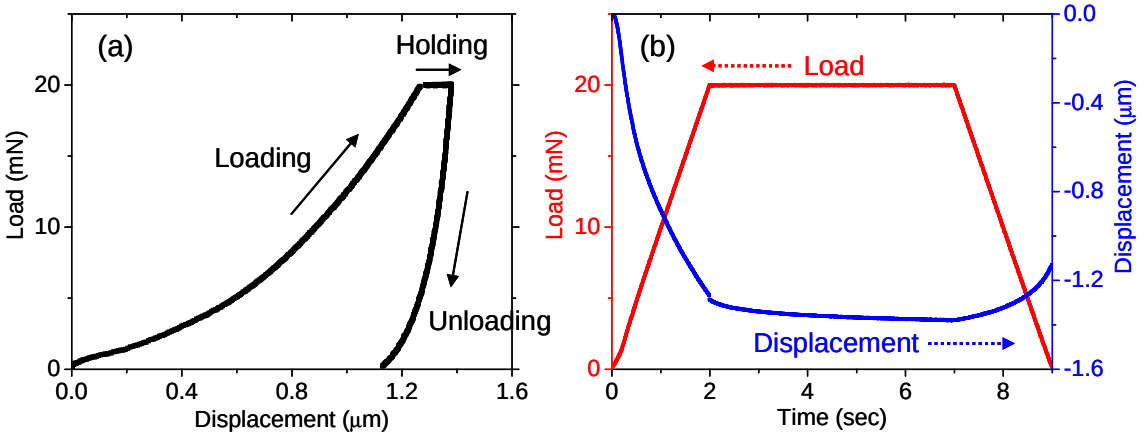

Figure 4.5 (a) Representative load-displacement curve obtained from a single indentation on PTFE/Pyrrolidone-1, (b) corresponding in-situ load and displacement plots versus time.

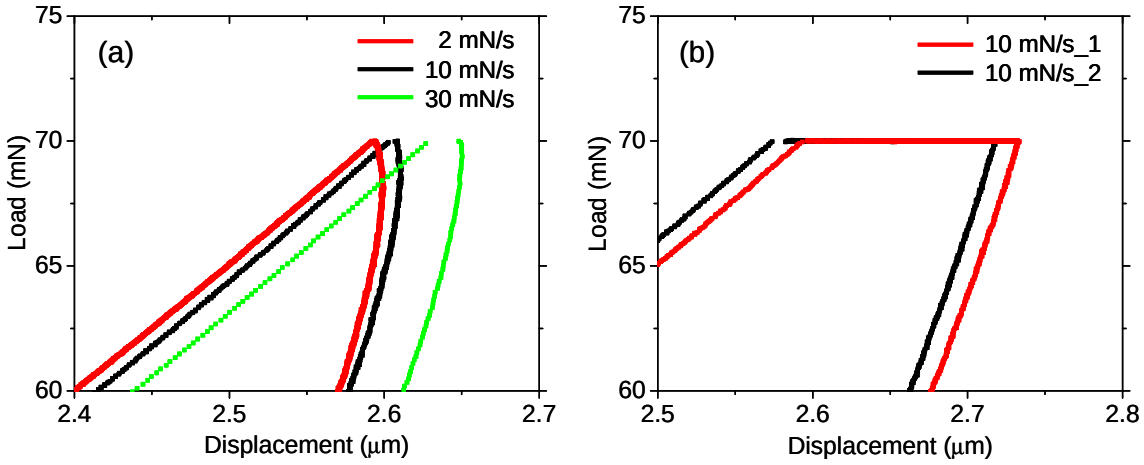

Figure 4.6 Load-displacement curves of PTFE/Pyrrodilne-2 obtained using (a) triangular loading profile with three different loading rates, (b) trapezoidal loading profile with a fixed loading rate of 10 mN/s.

Figure 4.6(a) depicts the load-displacement curves on PTFE/Pyrrolidone-2 using triangular loading (70 mN maximum load and three different loading rates of 2, 10 and 30 mN/s). Coating creep behavior is readily seen in these measurements, since while the load started to decrease after its maximum value the displacement was still increasing by a small amount until it finally started to decrease. This behavior is observed for all three loading rates, but most pronounced with the slowest rate of 2 mN/s. Consequently, the calculation of the mechanical properties, which involves the initial portion of the unloading curve, will be affected by this time-dependant deformation. To eliminate the presence of the creep effect, we hold the indenter tip at the maximum load for sufficient time for the material to reach a mechanical equilibrium before the unloading segment begins, as seen in Figure 4.6(b). It was found that 5 sec hold at the maximum load eliminated the creep effect. It should be noted that the gap on the plots, especially in the case of 30 mN/s (green curve) in Figure 4.6(a) was caused by a significantly high loading rate. In such cases, due to the inertial effects of the tip itself, there is a small gap (jump)

on the plot where the data cannot be detected. Examining the 10 mN/s shows a smaller gap compared to the 30 mN/s, while the 2 mN/s loading rate does not show any gap. The modulus and hardness values calculated from both triangular and trapezoidal loading profiles were compared in Table 4.2. It was observed that the higher loading rate in the triangular loading case had little creep effect, and resulted in similar property values from indentations using the trapezoidal loading profile. It should be noted, however, that the difference was not significant, as the case observed with conventional (lower load nanoindentation). This is likely due to the fact that the measurements were performed over a larger range of a couple of micrometers, and not in the sub-micron range as with conventional nanoindentation.

Table 4.2 Comparison of mechanical properties of PTFE/Pyrrolidone-2.

Loading profile	Loading rate (mN/s)	E_r [std] (GPa)	H [Std] (MPa)
Triangular	2	3.79 [0.08]	51.1 [1.8]
	10	3.73 [0.10]	52.4 [1.4]
	30	3.61 [0.08]	49.8 [2.2]
Trapezoidal	10	3.61 [0.14]	50.2 [2.7]

4.3.1.2 Substrate effect

Although partial unloading tests offer an easy and quick method for obtaining large amounts of indentation data (at different contact depths), there are known limitations, especially for polymeric materials. Specifically, the test time is relatively long, which exacerbates the creep behavior. In this section, the modulus and hardness values

extracted from both partial-unloading and multiple single-loading tests are compared in Figure 4.7. Figure 4.7(a) shows the load-displacement curves of multiple single-loading indentation experiments on PTFE/Pyrrolidone-2 with varying maximum loads from 30 mN to 200 mN. In the figure, only two indentations for each maximum load were plotted for better observation (instead of the total six measurements that were performed for each maximum load). Figure 4.7(b) shows the load-displacement curve of one cycle partial-unloading indentation on the same coating surface (note that only one cycle profile out of five actual measurements was included in Figure 4.7(b) for clarity). The main difference between these two tests is that for the single-loading case, each loading-unloading cycle was performed at a different location of the coating surface, whereas, for the partial-unloading case, all the successive loading-unloading measurements were performed at the same location, thus resulting in only one indentation impression on the surface, compared to many impressions in the single-loading case. The extracted reduced modulus values calculated from both methods were plotted in Figure 4.7(c), and the hardness values in Figure 4.7(d). Compared to the *in-situ* load-displacement plots (raw data) that are plotted versus displacement in Figure 4.7(a) and 4.7(b), the reduced modulus and hardness values are plotted with respect to the contact depth (h_c) of which property values are extracted as a function. In the single-loading case, the six modulus values calculated under the same maximum load were averaged, showing the standard deviation of the contact depth and modulus values in the x- and y-axes, respectively. In the partial-unloading case, all the values from the five cycles of partial-unloading were plotted without any averaging (as indicated by the five different colors for the partial-unloading data in Figure 4.7(c) and 4.7(d)). Although it was observed that partial-

unloading resulted in slightly higher values, which becomes clearer as the contact depth increases, their differences were not significant. This is because only at higher contact depths the accumulated error by plastic deformation with successive indentation at the same location takes effect. The comparison of hardness values from both indentation methods also showed very similar trends with even less differences in Figure 4.7(d). Therefore, in this work, both indentation methods were used; specifically, single-loading indentations were used for direct comparison of the different coatings, and partial-unloading for examining the substrate effect on the measurement properties.

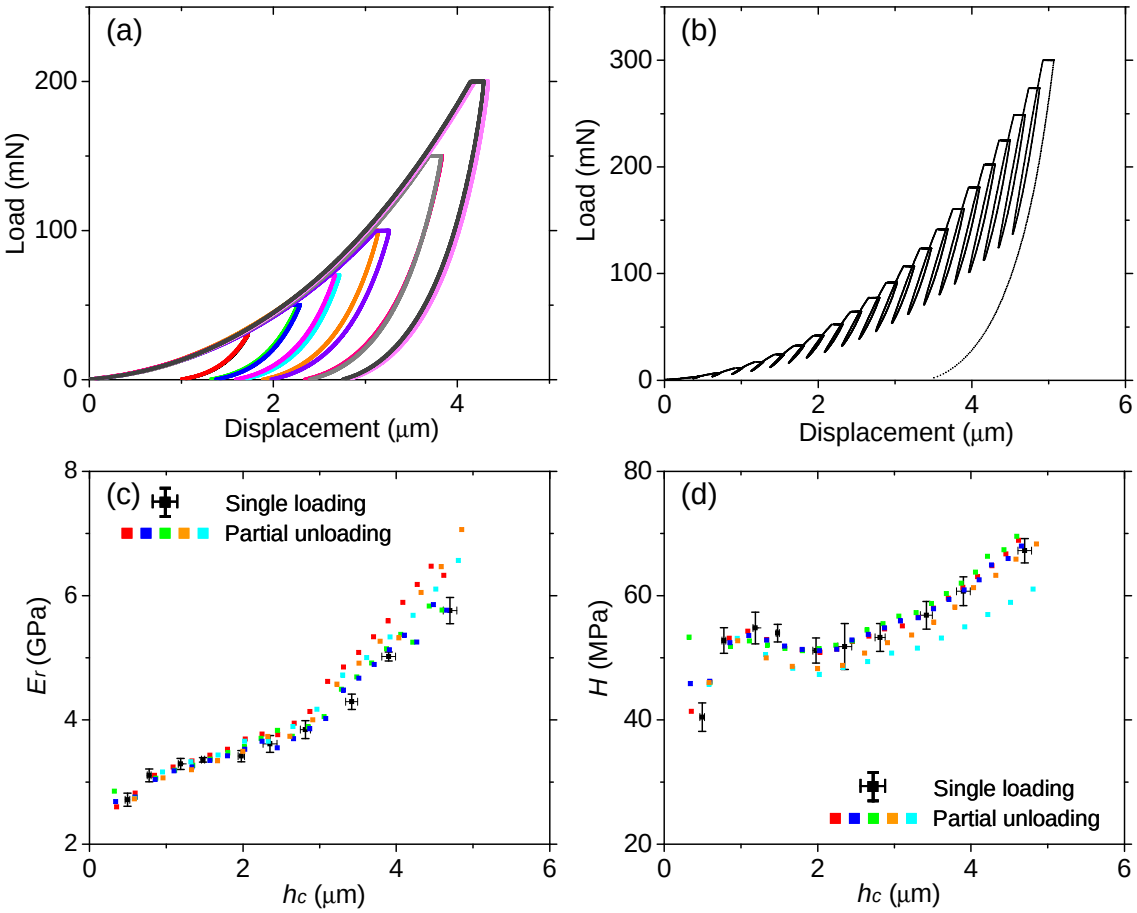

Figure 4.7 Load-displacement curves of PTFE/Pyrrolidone-2 coating obtained from (a) multiple single-loadings with 6 varying maximum loads (shown are two indentations for each maximum load) and (b) one cycle of partial unloading with 300 mN maximum load. (c) reduced modulus and (d) hardness values.

Relatively high load (up to 600 mN resulting in more than 6 μm contact depth) indentations using partial-unloading profiles were performed on two different coatings, Resin/PTFE/MoS_2 and PTFE/Pyrrolidone-2, as seen in Figure 4.8. These experiments were able to extract the mechanical properties of the coating, and clearly observe the overall behavior of the substrate-coating system. The elastic modulus and hardness values are shown in Figure 4.8(a) and 4.8(b), respectively. Both figures show higher mechanical property values for Resin/PTFE/MoS_2 compared to PTFE/Pyrrolidone-2, through the whole depth range. Of particular interest is to obtain the coating properties decoupled from the substrate effect. The elastic modulus of Resin/PTFE/MoS_2 initially showed an increasing trend up to 1 μm contact depth, then exhibited a small plateau region from 1 μm to 1.5 μm, and then started to increase again with increasing contact depth, as seen in Figure 4.8(a).

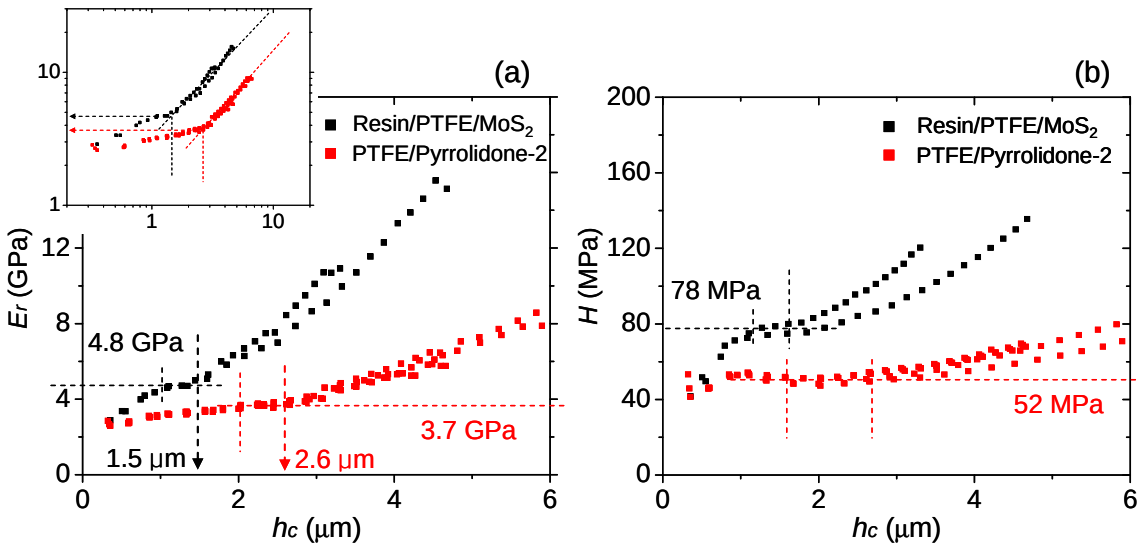

Figure 4.8 (a) Elastic modulus (inset shows the same plot in log-log scale), (b) hardness values calculated from partial-unloading indentations for Resin/PTFE/MoS_2 and PTFE/Pyrrolidone-2 coatings. Indicated plateau regions show the polymeric coating properties without substrate effects.

PTFE/Pyrrolidone-2 showed similar reduced modulus trends with a constant value region of 3.7 GPa from 2 μm to 2.6 μm contact depth. This trend is observed in the hardness measurements as well for both coatings, as seen in Figure 4.8(b). The slight increase in modulus and hardness at shallow contact depths is likely an artifact resulting from surface roughness, tip variation, and stage vibration (Hay, 2009), which are significant at shallow depths. Note that according to the ISO 14577, to avoid the influence of surface roughness on the extracted thin film properties, the surface roughness of the tested sample should be lower than 5 % of the indentation depth at which results are required. However, from past experience we have found that even in the presence of higher roughness since the indenter tip geometry is typically small and the slopes of the roughness are large, reliable measurements could be performed beyond the 5 % (Pergande *et al.*, 2004). Clearly having such soft coatings on a much harder substrate (cast iron) results in substrate effects at contact depths as low as 10 % of the coating thickness. This is because the plastic zone induced by the indenter propagates deeper into the coating, and at some critical contact depth (where the plateau region ends), the plastic zone reaches the coating/substrate interface (Ohmura *et al.*, 2001). The critical contact depths, where substrate effects become significant are 2.6 μm for PTFE/Pyrrolidone-2 and 1.5 μm for Resin/PTFE/MoS_2, which are clearly observed in the log-log inset in Figure 4.8(a). These critical contact depths correspond to 11 % and 8 % of their coating thickness, respectively, and are lower than what was reported by Tayebi *et al.* (2004) in the case of a thin (less than 1 μm) gold film on a hard substrate. They showed that substrate effects were seen when the contact depth was 20 % of the coating thickness. In the present study that uses softer polymeric coatings, the substrate

influences the results at lower contact depths. The tested polymeric coatings in this work also showed very small range of plateau regions corresponding to actual coating's properties as seen in Figure 4.8. Therefore, the best choice for obtaining the coating properties (that are both surface roughness- and substrate-independent) is at the critical contact depth where the substrate effect starts because the surface uncertainties mainly caused by surface roughness effect decrease with increasing contact depth. Knowing the critical contact depth (which is found to be 8-11 % for the polymeric coatings deposited on a hard substrate system), then the exact coating thickness can also be obtained without the need to measure it via cross section SEM. However, to precisely estimate the coating thickness, the critical contact depth and the precise geometry of the probe tip are needed to calculate the exact size of the plastic zone (Mata *et al.*, 2006).

4.3.2 Mechanical properties

In this section, the full-unloading method (multiple single-loadings) was used to perform indentation measurements on seven different coating samples to compare their micromechanical properties. Moreover, these readily obtained micromechanical properties were correlated with the coating's structural properties and tribological performance. For each coating, a trapezoidal loading profile at a constant loading/unloading rate of ±10mN/s was used for nine to eleven varying maximum loads between 5 mN to 400 mN. For each maximum load, six indentations were repeated on different areas that were 150 μm apart from each other, as seen in Figure 4.9. The group of these six indentations was at least 2 mm apart from the other group of six indentations performed under a different maximum load. As can be seen in Figure 4.9, the condition

of the top surface was different for each coating. PTFE/Pyrrolidone-1 had a rough surface, compared to a very smooth and flat surface of PTFE/Pyrrolidone-2 coating. For such rough surfaces, conventional small load nanoindentation technique is unable to produce meaningful results.

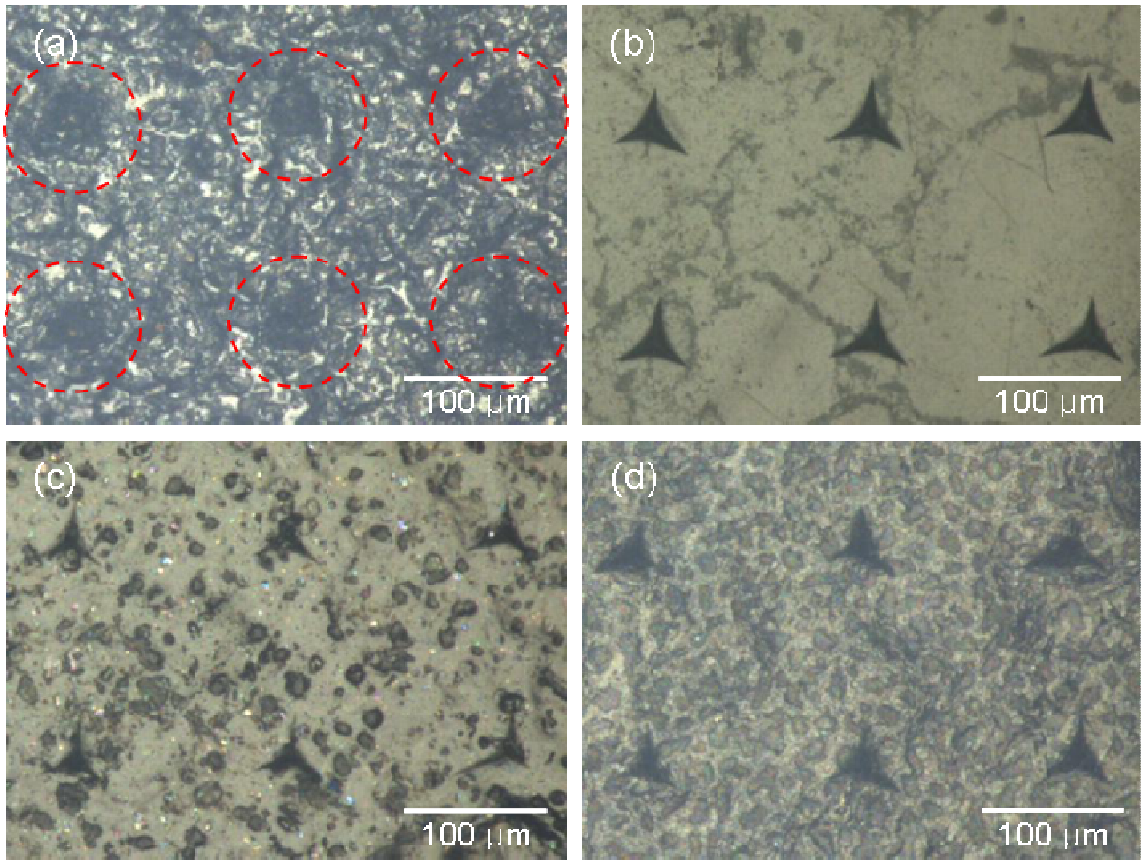

Figure 4.9 Residual images after nanoindentation experiments using 300 mN maximum load: (a) PTFE/Pyrrolidone-1, (b) PTFE/Pyrrolidone-2, (c) PTFE/MoS_2, and (d) Fluorocarbon coatings. Indentations were performed 150 µm apart from each other.

4.3.2.1 Correlation with microstructure

Analysis was performed on two representative PTFE- (PTFE/Pyrrolidone-2) and PEEK-based (PEEK/PTFE) coatings to examine the main differences in their micromechanical properties and correlation with their microstructure, as well as

correlation with their tribological performance (section 4.3.3). Figure 4.10(a) and 4.10(b) show the load-displacement curves of PTFE/Pyrrolidone-2 and PEEK/PTFE coatings, respectively. The elastic modulus and hardness values determined from these curves (six measurements for each maximum load instead of the two shown in the figure) are plotted in Figure 4.10(c) and 4.10(d), respectively. Clear differences on load-displacement curves between the two coatings could be observed; PTFE/Pyrrolidone-2 in Figure 4.10(a) exhibited repeatable load-displacement behavior, namely, the two curves at the same maximum load showed exactly the same path. Also, note that the loading curves in this case are almost identical, for all peak load experiments. Considering that each indentation was performed at a different area of the coating surface, this repeatability implies very uniform structure and mechanical properties over the whole coating surface area. At the same time, the smoothly increasing loading curve shows their structural uniformity through the coating thickness. These characteristics explain the small x- and y-axis error bars of the elastic modulus and hardness of PTFE/Pyrrodlidone-2 coating, as seen in Figure 4.10(c) and 4.10(d). Thus, PTFE/Pyrrolidone-2 coating can be thought to have amorphous-like microstructure.

In the case of PEEK/PTFE coating, the load-displacement curves showed completely different paths for all indentations, and the slopes of the loading curves differ significantly. This implies that the mechanical properties of PEEK/PTFE coating differ from location-to-location on the surface, which can also be seen by the large error bars of elastic modulus and hardness of PEEK/PTFE coating in Figure 4.10(c) and 4.10(d). Also, examining the loading curve, its slope is not smoothly increasing, but changing at some penetration depth, which means its microstructure is not uniform through the coating

thickness. As the tip is penetrating the coating, it finds a nonhomogeneous material, with different mechanical properties (either amorphous or crystalline), showing the semi-crystalline microstructure of PEEK/PTFE coatings.

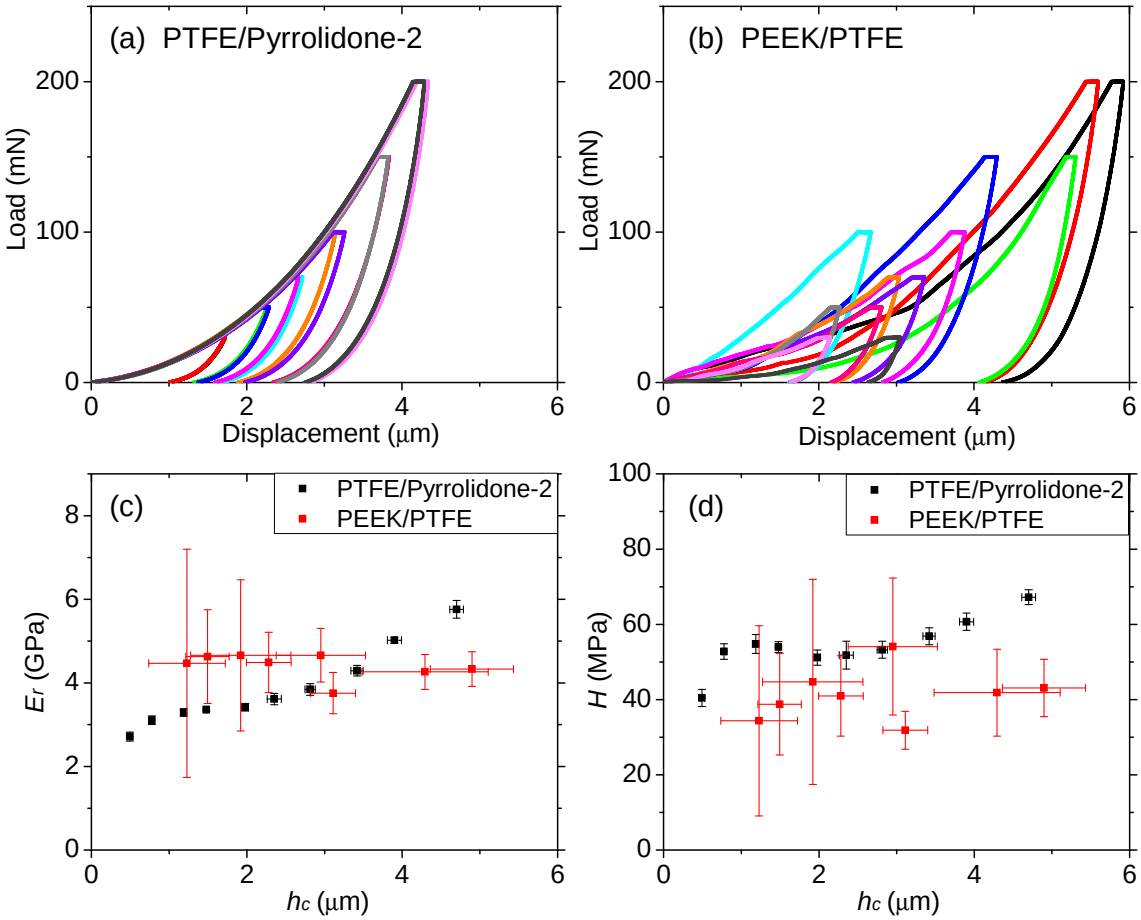

Figure 4.10 Load-displacement curves of (a) PTFE/Pyrrolidone-2 and (b) PEEK/PTFE coatings showing their load-bearing properties. Extracted (c) reduced modulus and (d) hardness values.

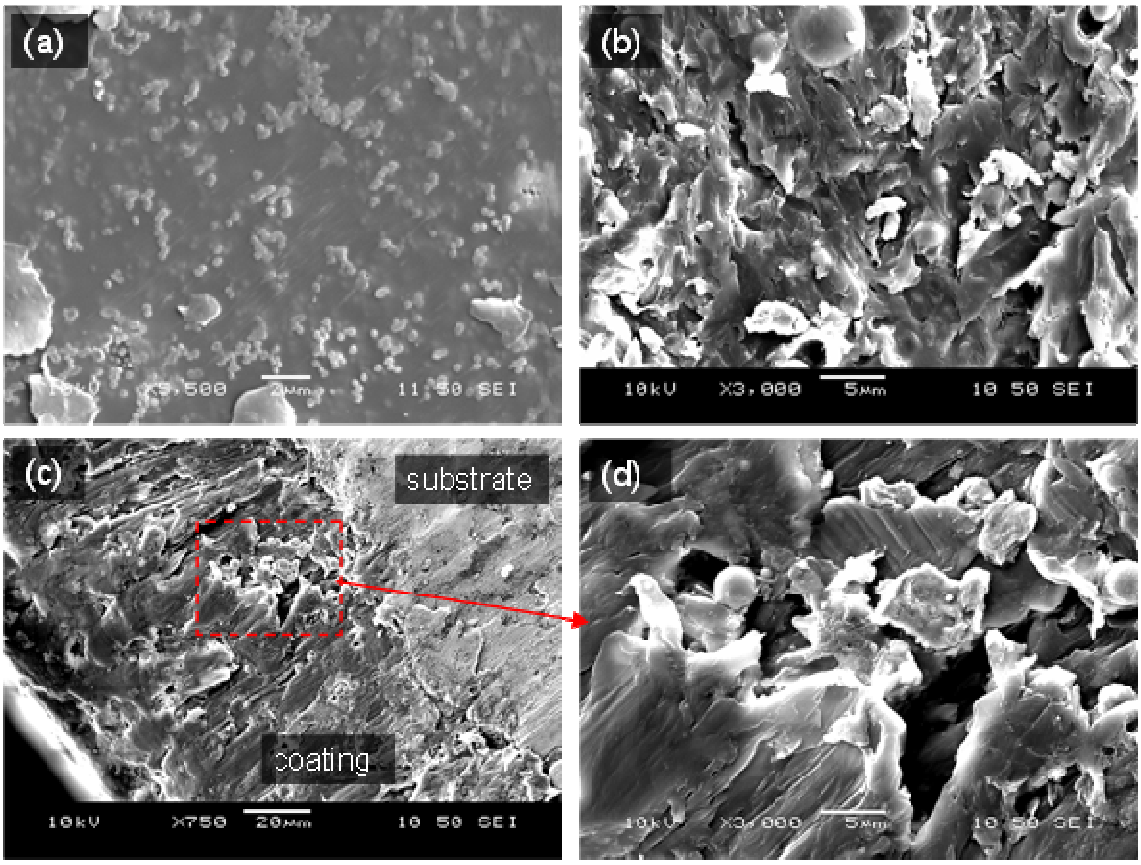

Figure 4.11 SEM top view surface images of (a) PTFE/Pyrrolidone-2 and (b) PEEK/PTFE coatings. (c) SEM cross section image of PEEK/PTFE coating and (d) zoom-in of (c) showing large flake-like particles.

These structure-induced differences in mechanical properties for the two coatings could be seen by the SEM images in Figure 4.11. In the case of PTFE/Pyrrolidone-2 coating, Figure 4.11(a), we cannot see any crystal or grain structures even under higher magnification. It seems that fine powders were compressed together showing a very smooth top surface of PTFE/Pyrrolidone-2. However, the PEEK/PTFE coating surface, Figure 4.11(b), shows very non-uniform surface which consists of large size of particles, thus resulting in porous structure. The sub surface structure could also be observed from the cross section images in Figure 4.11(c) and 4.11(d) for PEEK/PTFE coating (refer to Figure 4.1(b) for cross section image of PTFE/Pyrrolidone-2 coating). They show flake-

like particles, and thus semi-crystalline structure of PEEK/PTFE coating, whereas an amorphous structure of PTFE/Pyrrolidone-2 coating. Therefore, in the case of PEEK/PTFE, depending on where the probe tip indents, either crystal particle or porous area is pushed by the tip, and thus different mechanical properties are measured. However, PTFE/Pyrrolidone-2 results in very constant mechanical properties regardless of the indentation area and the penetration depth. Such uniform and consistent micromechanical properties are expected to also have superior tribological performance (section 4.3.3).

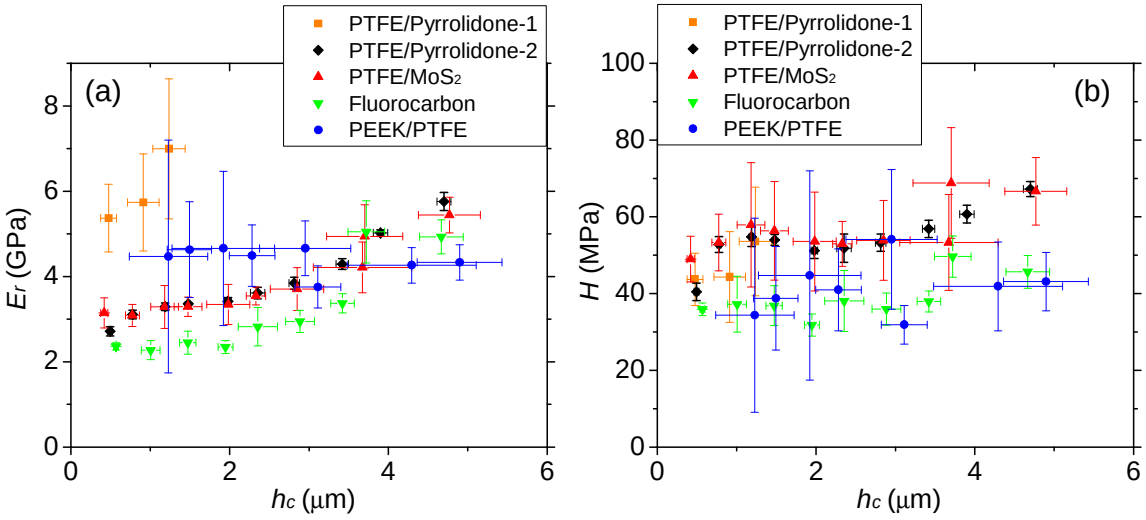

Figure 4.12 Extracted (a) elastic modulus and (b) hardness values with respect to contact depth.

4.3.2.2 Elastic modulus and hardness

Figure 4.12 shows the elastic modulus and hardness values of 5 different coatings as a function of contact depth. Each data point shows an averaged elastic modulus (y-axis) and contact depth (x-axis) along with their standard deviations (error bars in both axes) from six indentation measurements at a given maximum load. In all cases except

PEEK/PTFE, the elastic modulus exhibits constant values at lower contact depths around 1.5 to 2 μm, and then increases with increasing contact depth due to the substrate effect as discussed in section 4.3.1.2. In the case of PEEK/PTFE coating, due to its porous structure, the elastic modulus is rarely affected by the substrate, thus resulting in constant values with increasing contact depth. Interestingly, it can be observed that the elastic modulus of PTFE/Pyrrolidone-1 coating is significantly higher than that of other coatings as seen in Figure 4.12(a) (note that values at higher than 1 μm contact depths were not included in the figure due to excessive pile-up during indentation, and thus inaccurate values). Note that excessive pile-up phenomenon was only observed with PTFE/Pyrrolidone-1 as seen in Figure 4.13. The underestimated contact area due to the pile-up effects was clearly observed for PTFE/Pyrrolidone-1 coating in Figure 4.13(a), compared to other coatings with no pile-up, for example, PTFE/Pyrrolidone-2 shown in Figure 4.13(b). Usually, for polymer materials, a blunt tip with around 20 μm nominal radius is recommended to simply compress the material under the tip to avoid any plastic deformation. However, when sharp indenters like the Berkovich are employed, indentation becomes both elastic and plastic, thus resulting in such plastic deformation as pile-up or sink-in. In the case of pile-up where material plastically uplifts around the contact impression, the actual contact area is larger than that predicted by the area function discussed in section 4.2.2. Therefore, both elastic modulus and hardness values are overestimated as can be seen in Figure 4.12 for PTFE/Pyrrolidone-1 (Hay, 2000 and Bolshakov and Pharr, 1998). Finite element simulations for conical indenters (Bolshakov and Pharr, 1998) have shown that the ratio of final indentation depth, h_f (the depth of the indentation impression after unloading) to the depth of the indentation at peak load, h_{max}

can be used as an indication of when pile-up is an important factor. Pile-up is significant only when $h_f/h_{max} > 0.7$ and the material does not appreciably work harden. For such materials, failure to account for the pile-up can lead to an underestimation of the contact area deduced from indentation load-displacement data by as much as 60%, thus resulting in an overestimation of the hardness and elastic modulus. When $h_f/h_{max} < 0.7$, or in all materials that moderately work harden, pile-up is not a significant factor, and the Oliver–Pharr model can be expected to give reasonable results. In this work in all coatings, except PTFE/Pyrrolidone-1, the latter is the case and thus pile up effects can be safely ignored.

From Figure 4.12, the elastic modulus and hardness values of each coating could be obtained and summarized in Figure 4.14. These data are average values from the plateau region at the lower contact depth, to obtain substrate-independent properties. It was observed that PEEK-based coatings exhibited higher elastic modulus than PTFE-based coatings, with the hardness values showing the opposite trend.

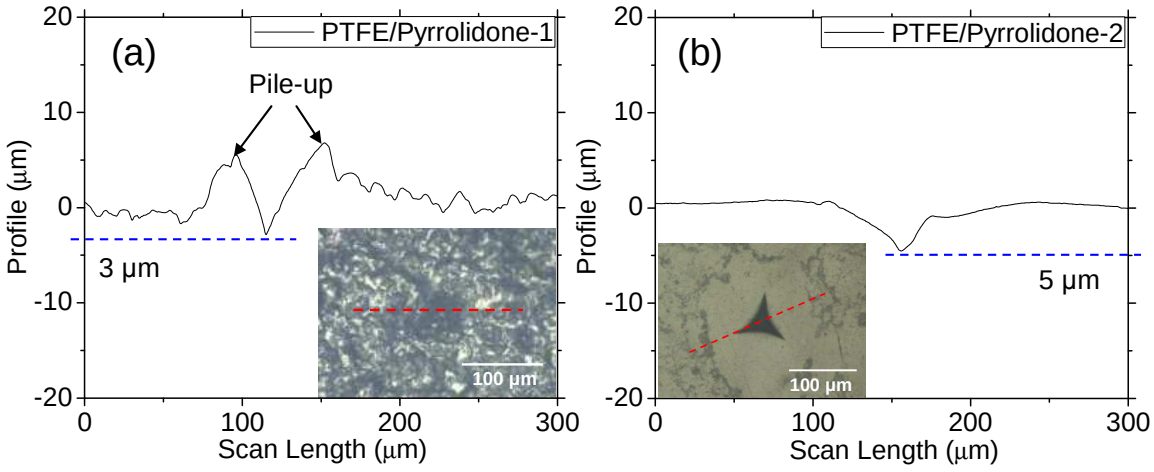

Figure 4.13 Cross-section line profile of indentation residual impressions: (a) PTFE/Pyrrolidone-1 and (b) PTFE/Pyrrolidone-2 coatings.

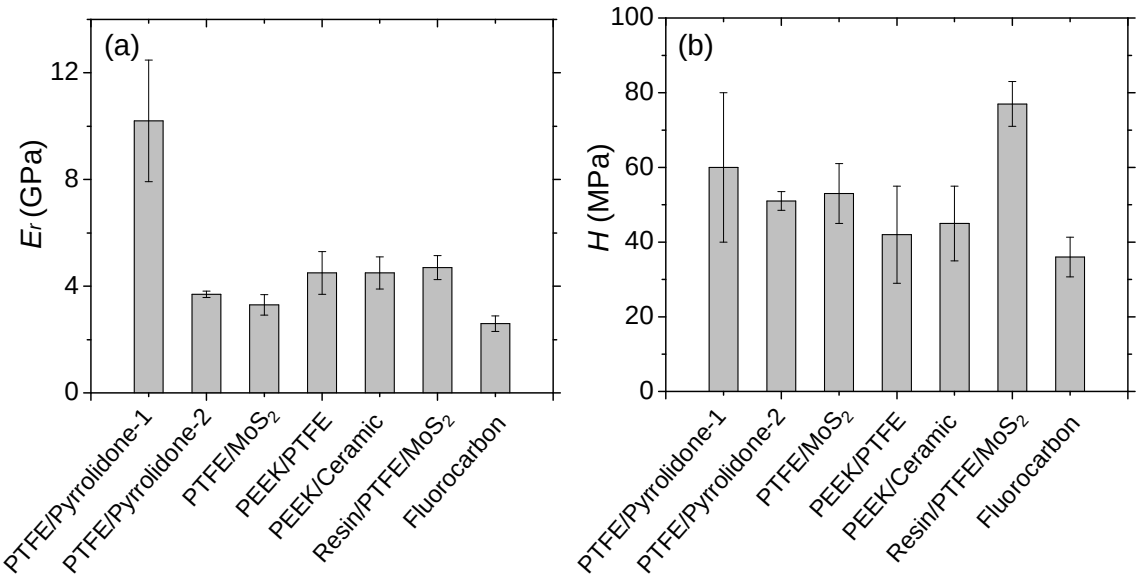

Figure 4.14 Substrate-independent (a) elastic modulus and (b) hardness of 7 different polymeric coatings.

4.3.3 Correlation with tribological performance

The indentation results and structural properties of the two representative PTFE- and PEEK-based coatings were directly correlated with their tribological performance that was already reported in Chpater 3. The friction and wear behavior of the same coatings were measured under oil-less air-conditioning and refrigeration (ACR) compressor conditions, specifically, using a steel pin on coated disks under unidirectional sliding (3.75 m/s), room temperature, 25 psi of CO_2 environment, 445 N normal load and no liquid lubricant present. PTFE/Pyrrolidone-2 showed the lowest and most stable friction coefficient of 0.043 (Std.= 0.003) for the whole duration of 30 min sliding, whereas the PEEK/PTFE coating showed significantly fluctuating friction coefficient with an average value of 0.079 (Std.= 0.008). Also, the PEEK/PTFE coating showed an order of magnitude higher wear rate than the PTFE/Pyrrolidone-2 coating.

When a coating has uniform mechanical properties over the whole surface area as PTFE/Pyrrolidone-2, it exhibits very consistent load-bearing properties through the whole coating surface as the sliding tests proceed, thus resulting in stable friction behavior. Also, due to its uniform (amorphous) microstructure through the thickness, it can maintain its consistent frictional performance in spite of removal of coating material (wear) with sliding; consequently assuring long-term reliability of PTFE/Pyrrolidone-2 coating (survived over 40 km sliding distance test in section 3.3.2.3). However, the significantly varying (inconsistent) mechanical properties of PEEK/PTFE coating (over its surface and also through its thickness) resulted in inconsistent load-bearing properties as the pin is sliding over the coating surface, thus exhibiting fluctuations in friction coefficient and consequently higher wear. Therefore, it can be thought that the repeatability of the load-displacement curves during the indentation measurements (Figure 4.10(a) and 4.10(b)) could be directly related to their tribological performance.

Similarly, this correlation can also be seen from the mechanical property plots in Figure 4.14. What appears to be more important than the averaged property values in Figure 4.14 is the relative length of the error bars for each coating (variability). The length of error bars of each coating caused by inconsistent mechanical properties is directly related to their frictional behavior under sliding tests. The most stable friction coefficient of PTFE/Pyrrolidone-2 coating corresponded to the shortest error bars in the mechanical properties in Figure 4.14, and the second most stable friction coefficient of PTFE/MoS_2 also agreed with its mechanical property results. The most fluctuating friction coefficient with PEEK/PTFE coating showed the largest error bars in their mechanical property plots. As already discussed above, this is because coatings with

uniform microstructure, which in turn have uniform mechanical properties through the coating thickness and over the surface area have a more stable frictional behavior. The significantly large error bars of PTFE/Pyrrolidone-1 coating are attributed to the complicated effect of pile-up rather than the coating structure. Therefore, based on this correlation, simple mechanical property measurements using the indentation technique provide information about the expected tribological behavior of polymeric coatings.

4.4 Conclusion

The micromechanical properties of different polymeric coatings were measured using instrumented high-load indentation. The differences in mechanical properties between the coatings could be explained by the coatings microstructure, which also correlated very well with their tribological performance. Based on the indentation and SEM results, the following conclusions could be drawn:

(a) Procedures were established for high-load instrumented indentation on polymeric coatings, considering loading profiles and loading rates as well as their effect on the measured micromechanical properties. Using a trapezoidal profile with 10 mN/s loading rate ensured elimination of creep effects. Single loading-unloading indentation versus partial-unloading multiple indentations is preferred, even though the extracted coating properties were very similar.

(b) Using high-load indentations over the thickness of the coating, it was found that at lower contact depths (indenting few percent of the coating thickness) inconsistent elastic modulus and hardness values were measured due to surface “skin” effects. After that, there was a small plateau region up to a critical contact depth, which was

found to be about 10 % of the coating thickness, where substrate effects become evident. This plateau region gives the "true" micromechanical properties of the coatings.

(c) One of the PTFE- and one of the PEEK-based coatings were further examined after nanoindentation using SEM, and it was found that the PTFE coating exhibited very repeatable load-displacement behavior and extracted micromechanical properties, indicating a uniform and amorphous microstructure. The PEEK coating's load-displacement behavior was quite variable and unpredictable, which was attributed to its semi-crystalline porous microstructure. The consistent behavior of the PTFE coating was correlated with its superior tribological behavior.

(d) The measured micromechanical properties of the various polymeric coatings tested showed that PEEK-based coatings exhibited higher elastic modulus than PTFE-based coatings, while their hardness values showed the opposite trend. Their tribological performance, however, is not as much directly related to their micromechanical properties, but rather to the coating structural uniformity, as evident form the instrumented load/unload curves and manifested in their consistent (in the case of PTFE coatings) versus variable (in the case of PEEK coatings) micromechanical properties.

CHAPTER 5: HIGH TEMPERATURE BEHAVIOR AND VISCO-ELASTIC BEHAVIOR OF POLYMERIC COATINGS

5.1 Introduction

In the arena of high performance tribo-materials, blended polymers have been increasingly used for bearing and sliding parts in various industrial applications. With the development of functional additives and blending processing technologies, both the frictional and wear properties of polymer composites could be further improved, which was impossible with unblended polymer materials (Cannaday and Polycarpou, 2005). Additionally, by coating light-weight substrates with polymer composite materials such as polytetrafluoroethylene (PTFE)- and polyetheretherketone (PEEK)-based polymers with excellent lubricity and wear resistance, both economical (light weight machines, and thus more fuel efficient) and ecological (less lubricant) advances could be achieved in industrial equipment such as air-conditioning and refrigeration compressors. Due to higher performance requirements of current and future equipment, it is expected that tribopairs will experience higher sliding speeds, normal loads, and thus operating temperatures. With known limitations of polymeric materials, especially low glass transition temperatures, it is important to investigate the temperature limit of these coatings.

It is well known that increasing temperatures can lead to significant changes in polymer properties such as viscoelasticity and modulus (Brinson and Brinson, 2008), and accordingly, the tribological behavior of polymer surface can also be affected by the change in the operating temperature. Zhang *et al.* (2006) investigated the effect of changing sliding velocity and normal load on the frictional behavior of PEEK/SiC-

composite coatings, and found that the behavior was determined by the interfacial contact temperature of the sliding parts, which was induced by the coupling effect of both sliding velocity and normal load. Therefore, the decrease in shear strength of the coating caused by increasing contact temperature could explain the reduction of friction coefficient with increasing sliding velocity. Also, they showed that the frictional behavior of polymer surfaces was significantly changed especially in the vicinity of its glass transition temperature (T_g).

Chang *et al.* (2007) and Zhang *et al.* (2008) measured the frictional force changes of polymer composites with increasing temperature. They showed that the frictional force was determined by the product of adhesion (depending on the real contact area) on the interfacial zone and the shearing strength of the subsurface zone of the polymers (both of which were determined by the interfacial contact temperature between the two sliding surfaces). Hanchi and Eiss (1997) discussed the frictional behavior of PEEK-based composite surfaces in terms of the impact of temperature on the worn surface morphology and recovery property. Specifically, they characterized the recovery property of polymer surfaces at elevated temperatures, and showed that surfaces with higher recovery exhibited lower friction coefficient. Therefore, in this work, the elastic recovery property of polymeric coatings is further investigated quantitatively using an instrumented scratch test. Scratch testing is commonly used to examine not only the mechanical properties and damage mechanism of thin films, but also the elastic-plastic properties of polymer surfaces (Lin *et al.*, 2000). Using a '3-step measurement method' (pre-scan, actual in-situ scratch and post-scan) (Lin *et al.*, 2000), elastic, plastic, and thus recovery rate of polymer surfaces can be quantitatively measured.

The tribological performance of PTFE- and PEEK-based polymeric coatings was investigated under room temperature environmental conditions in Chapter 3. PTFE-based coatings showed exceptional friction behavior with acceptable wear resistance, and PEEK-based coatings exhibited promising tribological performance as a solid lubricant, thus necessitating further investigation of these coatings under aggressive higher temperature conditions. In this work, PTFE- and PEEK-based polymeric coatings were tribologically tested under elevated temperature conditions to examine their high temperature tribology along with their performance limits. Also, scratch measurements were performed on polymeric coating surfaces to measure their elastic recovery properties, and to correlate them with their frictional behaviors.

5.2 Experimental

5.2.1 Samples

Three of the seven coatings listed in Table 4.1, namely, PTFE/Pyrrolidone-1 (DuPont™ Teflon® 958-303), PTFE/Pyrrolidone-2 (DuPont™ Teflon® 958-414), PEEK/PTFE (1704 PEEK/PTFE®) were used in this chapter. Additionally, two different Aromatic Thermosetting Polyesters (ATSP)-based coatings, 1 % ATSP/PTFE (where there is 1 % of PTFE in ATSP without any additional materials) and 5 % ATSP/MoS_2 (i.e., 5 % MoS_2 in ATSP), were prepared by ATSP Innovations LLC (ATSP Innovations). The same substrate material, gray cast iron, was used for these coatings as well, but these coating materials were differently deposited on the substrate using a solution cast method. For all polymeric coatings, their thickness values, measured over 200 μm areas were relatively uniform, and in the range of 25 μm to 35 μm, which is much thicker than

typical hard coatings such as diamond-like-carbon (DLC) and WC/C with a thickness of 2.5 μm (Solzak and Polycarpou, 2010). The RMS roughness of each coating was measured using a stylus profilometer (Tencor P-15™) and found to be in the range of 0.61~2.28 μm.

5.2.2 Tribological testing

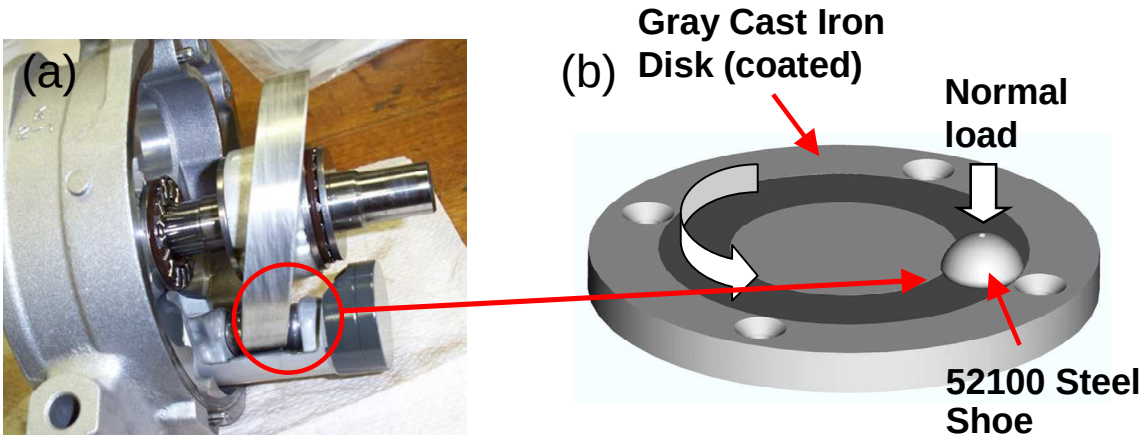

Figure 5.1 (a) Photograph of a cut-away automotive swash-plate compressor, (b) schematic of a crowned self-aligned pin (known as shoe)-on-disk test configuration for unidirectional testing simulating a swash plate compressor.

Unidirectional sliding tests were performed on PTFE- and PEEK-based polymeric coatings at controlled elevated environment temperatures up to 110°C (machine chamber setting in closed loop). Note that the interface temperature is likely higher than the chamber temperature setting. Figure 5.1(a) shows a photograph of a typical swash-plate compressor showing the rotating swash-plate making contact with several crowned pins that drive the pistons. Figure 5.1(b) shows the contact configuration for unidirectional testing, showing a crown shaped pin (which is an actual component used in swash plate compressors and referred to as shoe in this work) in contact with a rotating disk coated

with different polymeric coatings. The shoe is made out of 52100 steel, and is 9.6 mm in diameter with a 1 mm diameter hole drilled up to 2 mm below the contact surface (on the back side) to accept a miniature thermocouple and measure the *in-situ* near contact temperature (NCT) during testing. The RMS roughness and hardness of the shoe surface was measured and found to be 0.03 ~ 0.04 μm and 11 ~ 12.5 GPa, respectively. These values are significantly smoother and harder than the polymeric coated disk surfaces. Three different chamber temperatures, room (23°C), 75°C and 110°C were used, where a recirculating heat transfer fluid was used to achieve these temperatures in the tribochamber. Note that the measured NCT is typically higher than the set chamber temperature due to frictional heating.

Table 5.1 summarizes the experimental conditions for unidirectional sliding tests. Before each test, the non-coated pin samples were ultrasonically cleaned in acetone for 10 min, rinsed with 2-propanol, and finally dried with a warm air blower. The polymeric coated disk samples were cleaned in 2-propanol and were not exposed to acetone. A specialized High-Pressure- Tribometer (HPT) enabling high temperature testing up to 120°C was used for the tribological testing in this work (detailed explanation of the HPT can be found in chapter 3 and the cited references).

Table 5.1 Summary of experimental conditions

	Testing conditions
Machine setting temperature (°C)	23, 75 and 110
Environment (refrigerant)	R744 (CO_2) at 25 psi
Normal load (N)	445
Contact geometry	Complex, primarily nominally flat
Nominal contact pressure (MPa)	30
Sliding speed (m/s)	3.75
Test duration (mins)	30, 60

5.2.3 Scratch measurements

The PTFE/Pyrrolidone-2, PEEK/PTFE and the two ATSP-based coatings that were used for the tribological tests were also subjected to microscratch testing using a TI-950 TriboIndenter^{TM} (Hysitron, Inc.) equipped with a 3D OmniProbe^{TM} (Hysitron, Inc.). These tests were performed in order to quantitatively characterize the elastic recovery behavior of polymer surfaces which was though to be closely correlated to their frictional performances. The utilized machine uses piezoresistive loading and capacitive sensing and is capable of higher load instrumented scratch experiments, with a maximum lateral force of 5 N and a maximum normal force of 2.7 N. The maximum range of lateral and normal displacements is 150 mm and 100 μm, respectively.

Figure 5.2 depicts typical ramp-loading scratch experiments that were used for characterizing the coating's. Pre- and post-scratch scans of the surface topography were also performed due to the viscoelastic behavior and the relatively high hardness of the coatings. Therefore, each scratch experiment consists of three steps: (1) a pre-scratch scan to measure the topography of the original surface to be scratched, (2) an actual ramp loading scratch, and (3) a post-scratch scan to measure the residual deformation of the scratched surface. All three steps were performed at the exact same location. At the beginning and end of each step, a pre- and a post-profile scan, which is about 12 % of the scratch length, is performed to correct the alignment of the data, as shown in Figure 5.2(a). After the completion of a scratch test, the scratch profile (red line) and the residual profile (green line) are normalized based on the reference original surface (black line) to precisely quantify the true depth of scratch as well as the elastic and plastic

deformations of each coating surface, as seen in Figure 5.2(b). Along with the displacement plots, the *in-situ* lateral and normal forces are recorded, thus resulting in the *in-situ* friction coefficient of the scratched surface.

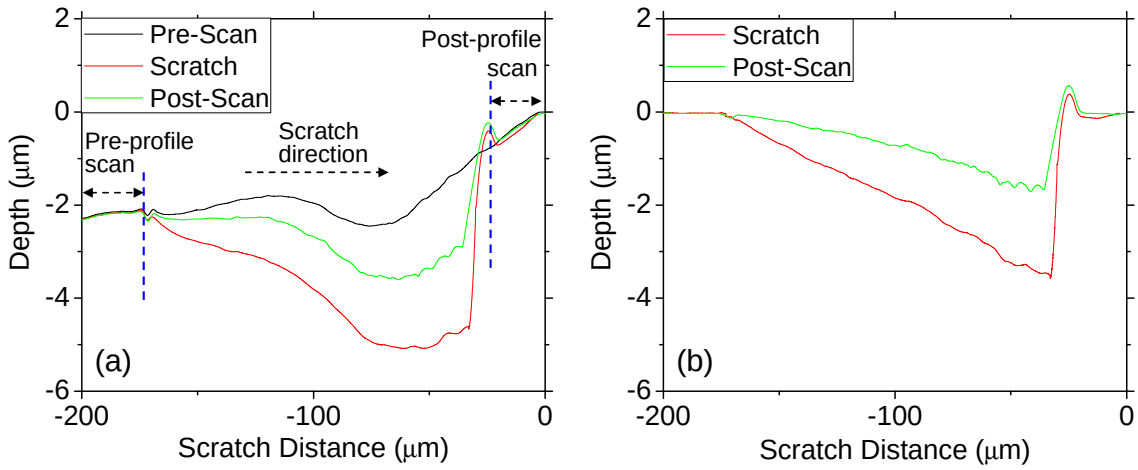

Figure 5.2 Representative ramp-loading microscratch curves showing (a) low load pre-scratch scan (black), in-situ scratch displacement (red), and low load post-scratch scan (green); (b) normalized scratch and post-scratch scans.

When performing scratch testing, it is critical that the test parameters of scratch velocity and loading rate are kept consistent throughout the samples being compared. For all samples in this work, the scratch velocity and the loading rate were kept constant at 7.5 μm/s and 1 mN/s, respectively. A constant normal load of 200 μN was applied for both the pre- and post-scratch scans. Each sample was scratched 4 times for each maximum load (three different maximum loads of 10, 20, and 30 mN, thus resulting in 12 scratches for each sample) to ensure repeatability and establish the scatter in the results. The tip used for the scratch tests was a 60° conical tip with a tip radius of 4.3 μm as seen in Figure 5.3.

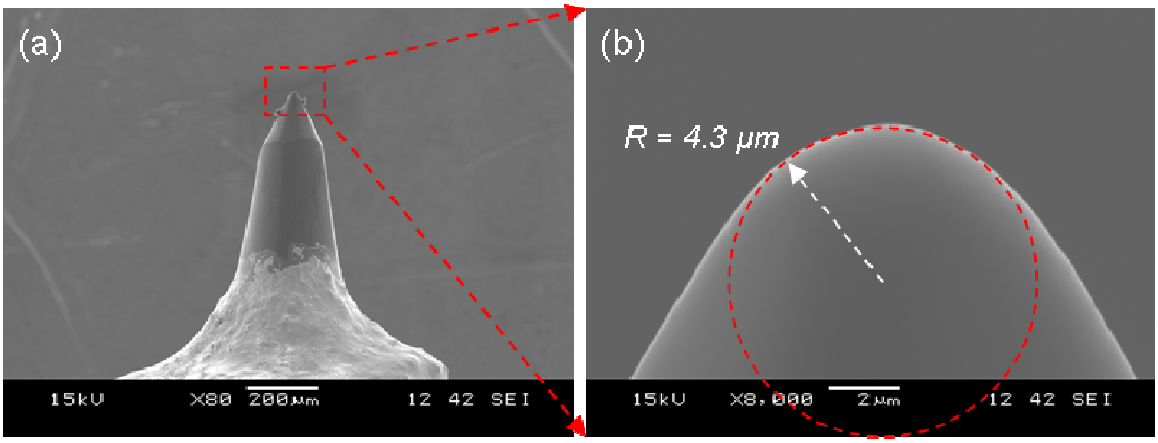

Figure 5.3 (a) Scanning electron microscopy (SEM) image of conical tip used for scratch testing in this work, (b) zoomed in image showing the tip radius.

5.3 Results and discussion

5.3.1 Tribology of polymeric coatings at elevated temperatures

5.3.1.1 Elevated temperature tribological testing

Figure 5.4(a) and 5.4(b) show the in-situ friction coefficient and NCT, respectively, with respect to the duration of the test under unidirectional sliding for three different polymeric coatings tested under room temperature conditions. As shown, all three coatings survived the duration of the 30 min tests, showing acceptable frictional behavior with average friction coefficient values (taken from 10-30 min) of 0.079 (and a standard deviation, std of 0.008) for PEEK/PTFE, 0.047 (std 0.007) for PTFE/Pyrrolidone-1, and 0.043 (std 0.003) for PTFE/Pyrrolidone-2. As already pointed out, even though the environmental (machine) temperature was set to 23°C, the NCT (which is close to the actual interfacial temperature) is significantly higher due to friction-induced heating. The NCT clearly differentiated PTFE- and PEEK-based coatings as seen in Figure 5.4(b). Both PTFE/Pyrrolidone-1 and PTFE/Pyrrolidone-2 coatings had similar NCT between 100°C and 150°C (gradually increased to a maximum

of 150°C). In the case of PEEK/PTFE coating, the NCT reached 200°C after 6 min and stayed at around 220°C through the test duration. This can be attributed to the fact that PEEK-based coatings have low thermal conductivity due to their porous and semi-crystalline structure compared to the amorphous structure of PTFE-based coatings (Chapter 4), as well as to the fact the COF was higher (and thus more heat generated). Note that similar behavior is seen with longer duration (60 min) tests under the same conditions in Chapter 3.

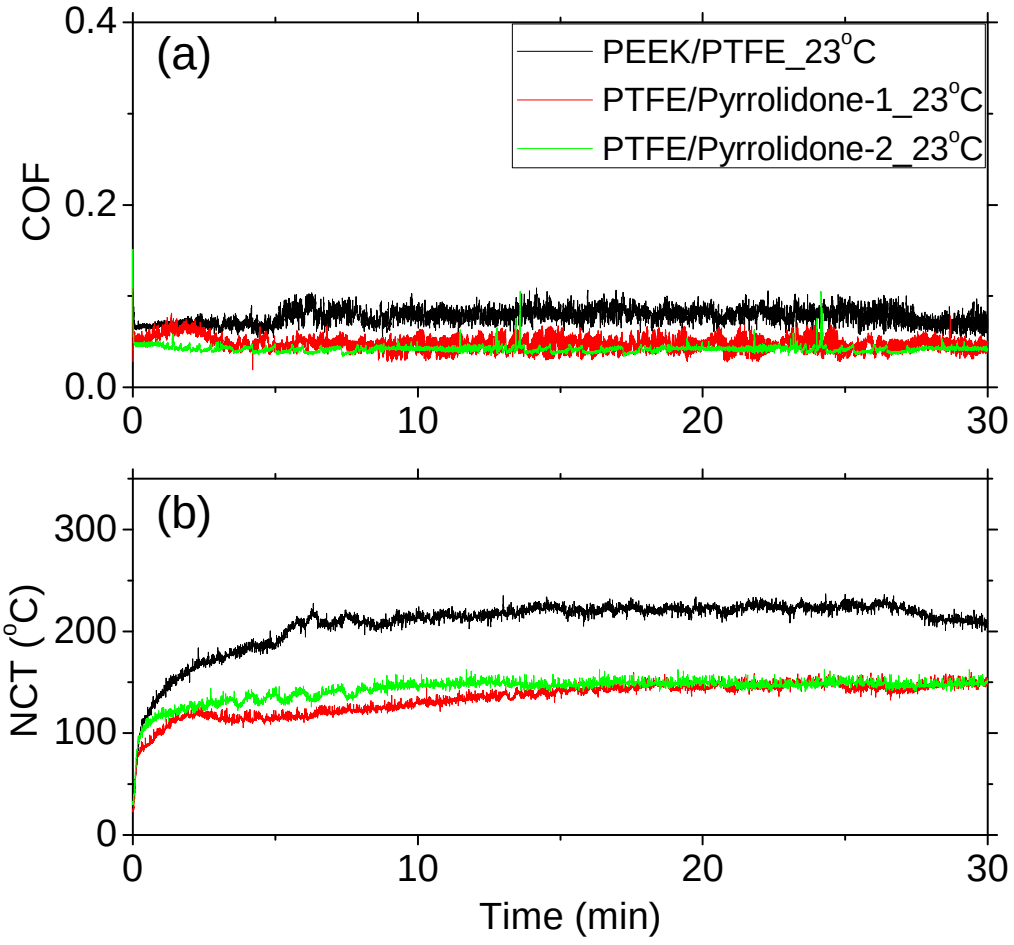

Figure 5.4 *In-situ* (a) friction coefficient and (b) near contact temperature (NCT) of PEEK/PTFE (black), PTFE/Pyrroliodne-1 (red), and PTFE/Pyrrolidone-2 (green) coatings during 30 min dry unidirectional sliding tests under room temperature (23°C) condition.

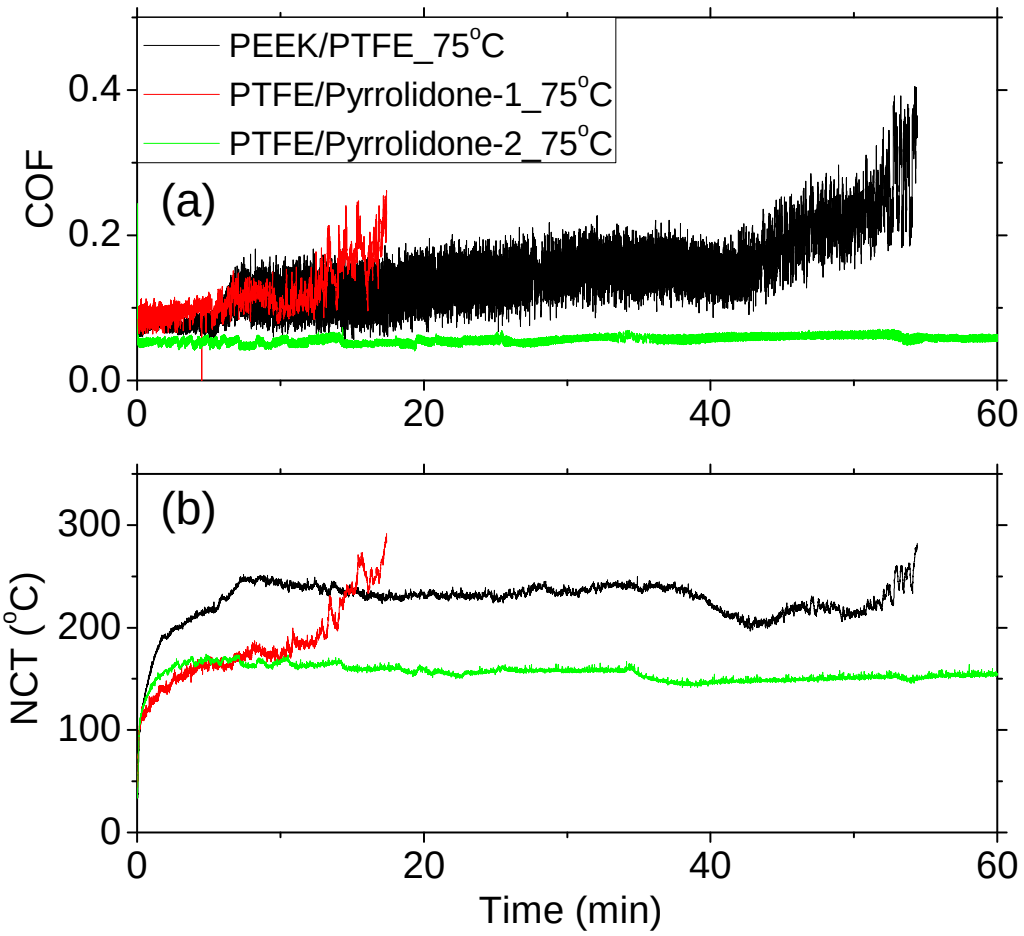

Figure 5.5 *In-situ* (a) friction coefficient and (b) NCT of PEEK/PTFE (black), PTFE/Pyrroliodne-1 (red), and PTFE/Pyrrolidone-2 (green) coatings during 60 min dry unidirectional sliding tests at 75°C.

Figure 5.5 shows the frictional behavior of the coatings under higher temperature testing of 75°C and up to 60 min duration. PTFE/Pyrrolidone-2 was the only coating which survived the whole test duration under this condition, while all three coatings survived the room temperature testing, Figure 5.4. Under this temperature, it could be clearly observed from Figure 5.5(b) that the NCT for each coating was higher than that under room temperature testing. Due to its low thermal conductivity, the NCT of PEEK/PTFE coating reached almost 250°C after 8 min testing, which is known as its limit for in-use temperature (Escobar Nunez *et al.*, 2011). This resulted in severe friction

coefficient fluctuation with an average value gradually increasing up to 0.2. This coating was eventually completely penetrated and lost its functionality after around 54 min with an abrupt increase in its COF and NCT. In the case of PTFE/Pyrrolidone-1 coating, its COF was around 0.1 from the beginning of the test with its NCT over 150°C. Consequently, the higher frictional force generates more heat which is being dissipated into the contact interface of the coating thus resulting in a continuous increase of the NCT. Therefore, the PTFE/Pyrrolidone-1 coating failed after 17 min with a sharp increase of both COF and NCT, thus showing relatively weaker thermal performance than any other coatings tested. In the case of PTFE/Pyrrolidone-2 coating, even though it survived the whole duration of the test, its COF and NCT were slightly higher than those at room temperature.

For the PTFE/Pyrrolidone-2, which showed the best performance under 75°C, another test under even higher temperature of 110°C was performed to further investigate the frictional behavior and temperature limit, shown in Figure 5.6. This will answer two questions arising from the previous two sets of tests at 23°C (Figure 5.4) and 75°C (Figure 5.5); 1) why is the friction behavior of polymeric coatings deteriorating with increasing NCT, and 2) why PEEK/PTFE coating performed worse than PTFE/Pyrrolidone-2 coating under both temperature conditions. Referring to Figure 5.6, clearly this coating survived the 1-hour test duration even at 110°C, with a NCT slightly over 170°C and stable frictional behavior. Interestingly, the highest temperature condition showed the lowest COF through the whole duration of the test. The 75°C tests showed the highest COF, with the 23°C in-between. This frictional behavior is in

agreement with earlier studies of polymer materials at elevated temperatures (Hanchi and Eiss, 1997, Zhang *et al.*, 2008, and Lu and Friedrich, 1995).

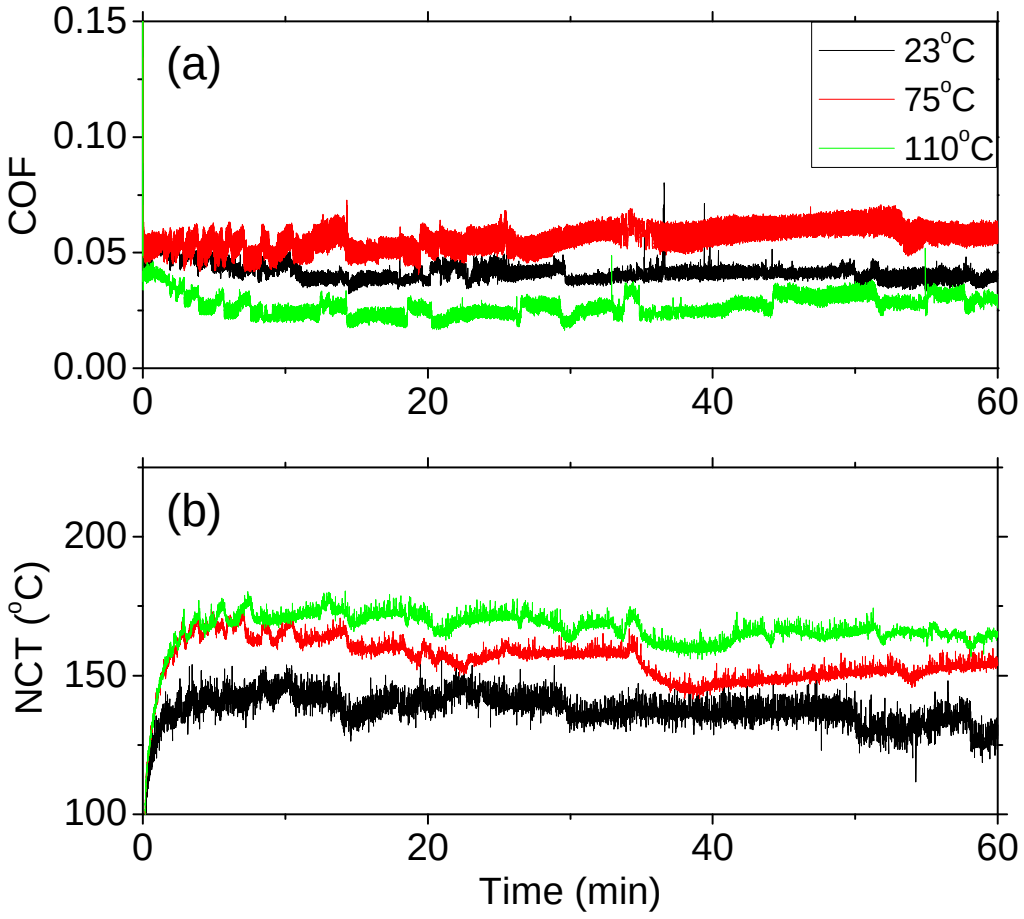

Figure 5.6 *In-situ* (a) friction coefficient and (b) NCT of PTFE/Pyrrolidone-2 coating during 60 min dry unidirectional sliding test under three different temperatures.

5.3.1.2 Friction mechanism of polymer surfaces at elevated temperatures

To better understand this behavior, we need to understand how the frictional force is determined for sliding wear of a polymer surface against a metallic counterpart. The surface layer of the polymer involved in the frictional process can be classified into two zones: the interfacial zone with a depth of about 100 nm and the subsurface zone

corresponding to the depth of the coating thickness (Zhang *et al.*, 2008). The frictional force resulting from the adhesion equals the product of the "real contact area" of the interfacial zone (with the counterpart) and the "shear stress" of the subsurface zone (Chang *et al.*, 2007). The real contact area between two counterparts is directly related to the viscoelastic property of the interfacial zone, which is eventually determined by the interfacial temperature (NCT).

Usually the decreased elastic modulus (more plastic) of a polymer surface at higher temperatures, results in an increase in the real contact area, thus inducing more adhesion (mainly Van der Waals and hydrogen bonding for most polymers). However, at the same time, the shearing strength of the subsurface zone is also determined by its viscoelastic property, and softened polymers (less viscous) at high temperatures are supposed to have lower shearing strength. Therefore, increased NCT, results in two contrary effects on the COF; the increased real contact area and the decreased shear strength. Depending on which effect is more dominant, the final value of the COF can be either increased or decreased with elevated temperature. Therefore, it can be concluded that the overall friction behavior of a polymer surface is determined by the viscoelastic property of the polymer, which directly depends on the NCT.

There are five regions of viscoelastic behavior of polymers with increasing temperature. These are glassy, transition, rubbery, rubbery flow, and liquid flow regions, depending on the value of relaxation modulus (Brinson and Brinson, 2008). Among them, the transition region near the glass transition temperature (T_g) is known as the critical point determining the overall tribological behavior of a polymer surface. This is because in this region the viscoelastic property of polymers changes significantly. With

increasing temperature up to T_g, polymer surfaces become more plastic with a decline in their elastic property caused by thermally activated molecular relaxation, which results in increased real contact area and thus higher adhesion at the interface (Hanchi and Eiss, 1997 and Zhang *et al.*, 2008).

However, despite the thermal relaxation of polymer materials, the molecular mobility is still limited below T_g, and thus there's only a small decrease in their shearing strength. Therefore, with increasing temperature up to T_g, the increased real contact area and adhesion in the interfacial zone is dominant, compared to the reduced shearing strength in the subsurface zone, thus resulting in an increase in the COF. However, once the NCT exceeds T_g, the polymer enters a rubbery state due to the complete scission of molecular chains, thus resulting in rapid and abrupt decline of polymer viscosity and shearing strength. Under this higher temperature condition ($> T_g$), the adhesion of the interfacial zone doesn't play a significant role in the frictional behavior of the polymer surface, and it is dominated by the rapidly reduced shearing strength of the subsurface zone. Therefore, once the NCT exceeds T_g, the COF decreases with increasing temperature, which was clearly observed in the present work, Figure 5.6, in agreement with Refs. Hanchi and Eiss (1997), Zhang *et al.* (2006), Zhang et al. (2008), and Lu and Friedrich (1995).

In summary, with increasing NCT by whatever reasons (increased sliding speed, normal load or setting temperature), a polymer surface becomes more plastic and in the vicinity of T_g results in the highest COF. Under this condition, more plastic deformation and plowing are observed on the worn surfaces (Hanchi and Eiss, 1997 and Zhang *et al.*, 2008). Then, as the NCT exceeds T_g, the COF starts to decrease due to the rapid decline

of viscosity and shearing strength of the polymer (Zhang *et al.*, 2006). This is why the frictional behavior of PTFE/Pyrrolidone-2 coating with elevated temperature was as shown in Figure 5.6. Figure 5.7 summarizes the average friction coefficient vs. NCT of PTFE/Pyrrolidone-2 coating from the in-situ results of Figure 5.6. First, the COF increased with increasing NCT and showed the highest COF value (0.057) at a NCT of 155°C. This temperature, 155°C is considered as the actual T_g of PTFE/Pyrrolidone-2 polymers and slightly higher than that of pure PTFE (130°C) due to its additives (Araki, 1965). Then, as the NCT increased further, the COF decreased to 0.026 due to the change of the state of the polymer.

In the case of PEEK/PTFE coating, it didn't show such frictional behavior with increasing temperature and failed at 75°C due to its semi-crystalline microstructure (Chapter 4). Usually, amorphous structured polymers present more viscoelastic features with clear T_g, with the transition region suppressed in crystalline materials, thus there is no abrupt drop of the modulus (shearing strength). In this case, their viscoelastic property is more affected by melting temperature (T_m) rather than T_g, and thus their plasticity continuously increases up to T_m. That's why the COF of PEEK/PTFE coating was relatively high and being fully plastic at over 200°C NCT (Figure 5.4), and eventually failed at higher NCT conditions as seen in Figure 5.5.

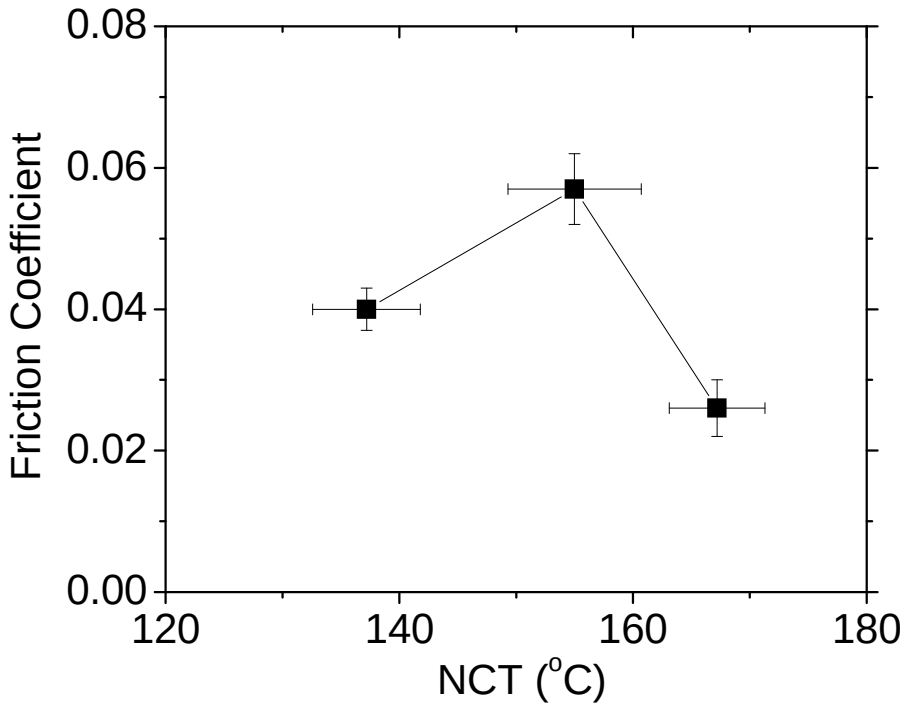

Setting Temp. (°C)	NCT (°C) (10 ~ 60 min)	COF (10 ~ 60 min)
23 °C	137.2 (4.6)	0.040 (0.003)
75 °C	155.0 (5.7)	0.057 (0.005)
110 °C	167.2 (4.1)	0.026 (0.004)

Figure 5.7 Average friction coefficient versus NCT of PTFE/Pyrrolidone-2 coating tested under dry unidirectional sliding conditions at room and elevated temperatures. Error bars in the figure and parentheses in the table designate ± 1 standard deviation.

5.3.1.3 Elastic recovery of polymer surfaces

Hanchi and Eiss (1997) studied the relationship between elastic recovery and frictional behavior of polymer surfaces at elevated NCT, showing that surfaces with higher recovery exhibited lower COF. This is because a more elastic surface with a higher recovery property has lower real contact area, and thus lower adhesion compared to the plastic surface with plastic deformation/ plowing and material removal. Therefore, this elastic recovery property can explain the frictional behavior of polymers with

increasing temperature, and also could potentially explain as to why PTFE/Pyrrolidone-2 exhibited better frictional behavior than PEEK/PTFE coatings. The clear difference of elastic recovery (plasticity) between PTFE/Pyrrolidone-2 and PEEK/PTFE coatings can be qualitatively seen from their worn surfaces examined by SEM, as seen in Figure 5.8. Figure 5.8(a) and 5.8(b) depict the worn surface of PEEK/PTFE coating tested at 23°C, showing "regular" material stacks perpendicular to the direction of sliding caused by adhesion-induced plastic deformation (stick-slip of shoe). Also, from Figure 5.8(b), it can be observed that the coating material is removed as a big chunk from the surface. Therefore, relatively high friction coefficient along with higher friction-induced heating of PEEK/PTFE coating is ascribable to these severe plastic deformation and material removal caused by its significantly plastic surface. In the case of PTFE/Pyrroildone-2, even though some plastic plowing was observed from the worn surface tested at 23°C (Figure 5.8(c) and 5.8(d)), it was not as severe as PEEK/PTFE coating due to PTFE/Pyrrolidone-2 coating's relatively elastic surface, thus resulting in relatively low COF. In the next section, the elastic recovery property of these coatings is quantitatively examined using scratch tests and correlated with their frictional behavior.

From the elevated temperature tribotesting, it was shown that the overall frictional behavior of polymer surfaces was determined by their viscoelastic properties, which also changes with their NCT. The more elastic is the polymer surface (with higher recovery) the lower is the COF because a plastic surface has a higher real contact area, thus resulting in higher adhesion and adhesion-induced plastic deformation/plowing leading to higher frictional force.

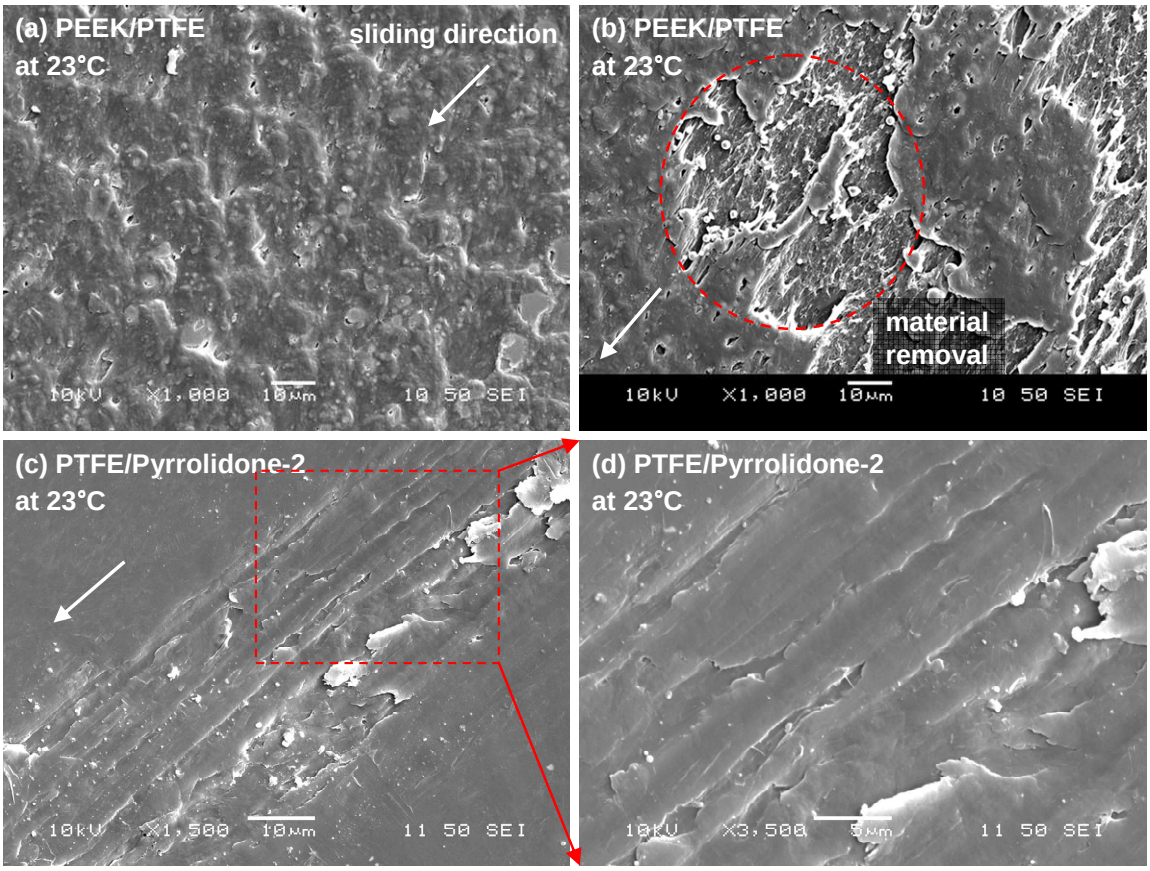

Figure 5.8 SEM images of the worn surfaces of (a), (b) PEEK/PTFE coating; (c) PTFE/Pyrrolidone-2 coating; (d) zoomed in image of worn track from (c), after 30 min dry unidirectional sliding at 23°C.

5.3.2 Quantitative recovery property characterized by scratch measurements

PTFE-, PEEK-, and ATSP-based polymeric coatings were subjected to microscratch testing to investigate their viscoelastic (recovery) properties and to correlate these results with their tribological behavior. Figure 5.9(a,c,e) and Figure 5.9(b,d,f) show representative microscratch results obtained with ramp loading up to 10mN for PTFE/Pyrrolidone-2 and PEEK/PTFE coatings, respectively. As described in section 5.2.3, the in-situ scratch profiles were normalized using the pre-scan to correct for the surface topography. Shown in the Figure 5.9(c) and 5.9(d) are the in-situ deformations

with red color (that includes both elastic and plastic deformation) as well as the post scan with green color that shows the permanent (or plastic) deformation only (the difference being the elastic recovery). In the case of PEEK/PTFE, most deformation was plastic as seen in Figure 5.9(d). Also, compared to the smooth scratch curves of PTFE/Pyrrolidone-2, Figure 5.9(c), PEEK/PTFE showed significant fluctuations. This can be attributed to both its rougher surface, and also to its non-uniform (semi-crystalline) structure which was also examined in Chapter 4. Along with the scratch curves, the *in-situ* friction coefficient corresponding to the scratch curve (red) was also measured as seen in Figure 5.9(e) and 5.9(f). Relatively stable COF was observed for PTFE/Pyrrolidone-2 coating, while PEEK/PTFE coating showed some fluctuation due to its rough surface as well as its semi-crystalline microstructure.

Figure 5.10(a,c,e) and Figure 5.10(b,d,f) show the microscratch results obtained with ramp loading up to 20 mN for 1% ATSP/PTFE and 5% ATSP/MoS_2 coatings, respectively. Compared to PTFE- and PEEK-based coatings, these coatings showed relatively smoother scratch curves and thus stable friction coefficient during the scratch. Also, it was observed that most of deformation was elastic for ATSP-based coatings showing significant amount of recovery of deformed surfaces.

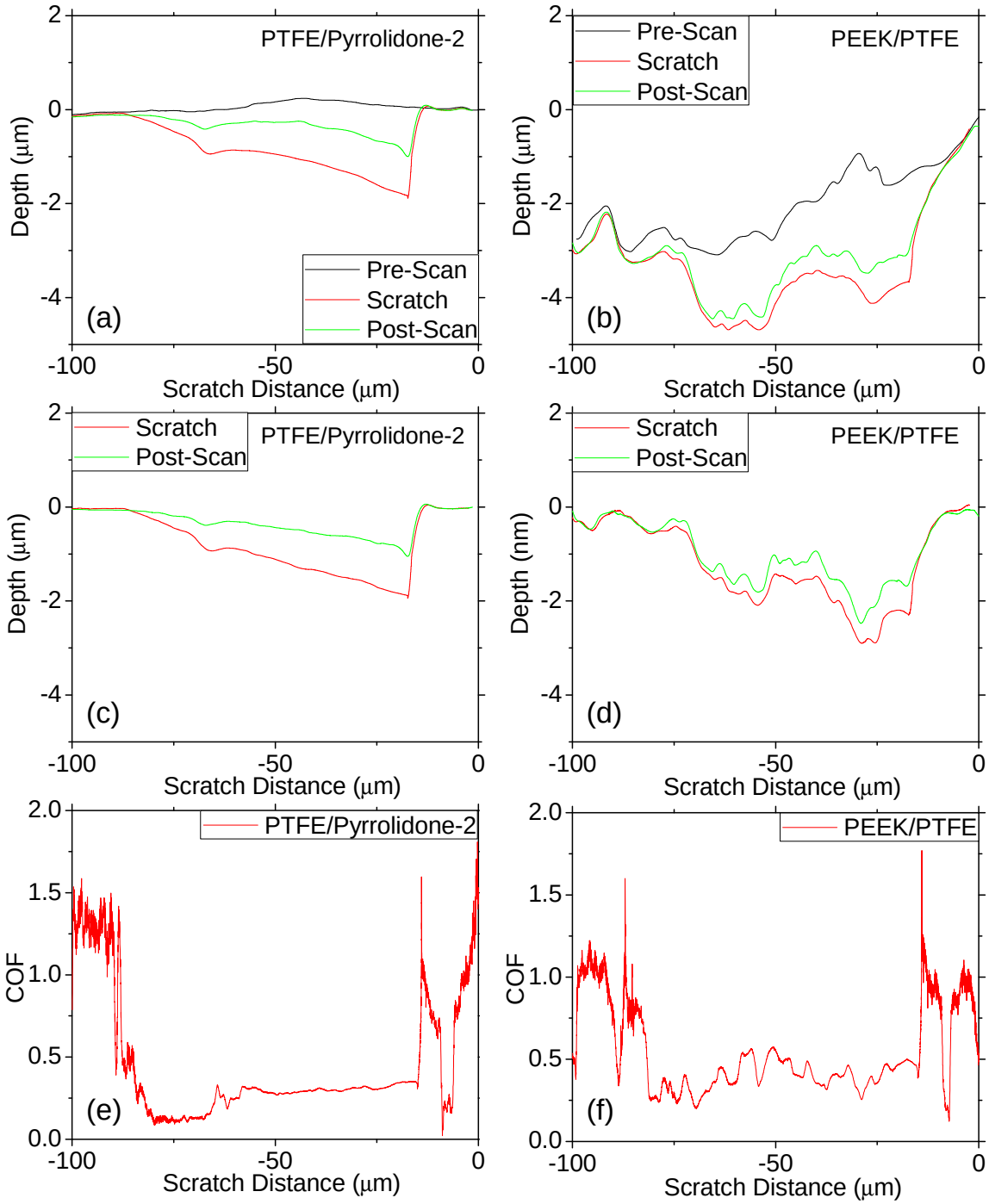

Figure 5.9 Microscratch curves from ramp-loading up to 10 mN for (a) PTFE/Pyrrolidone-2 ((c) after normalization), and (b) PEEK/PTFE ((d) after normalization). *In-situ* friction coefficient of (e) PTFE/Pyrrolidone-2 and (f) PEEK/PTFE coatings monitored during the actual scratch cycle.

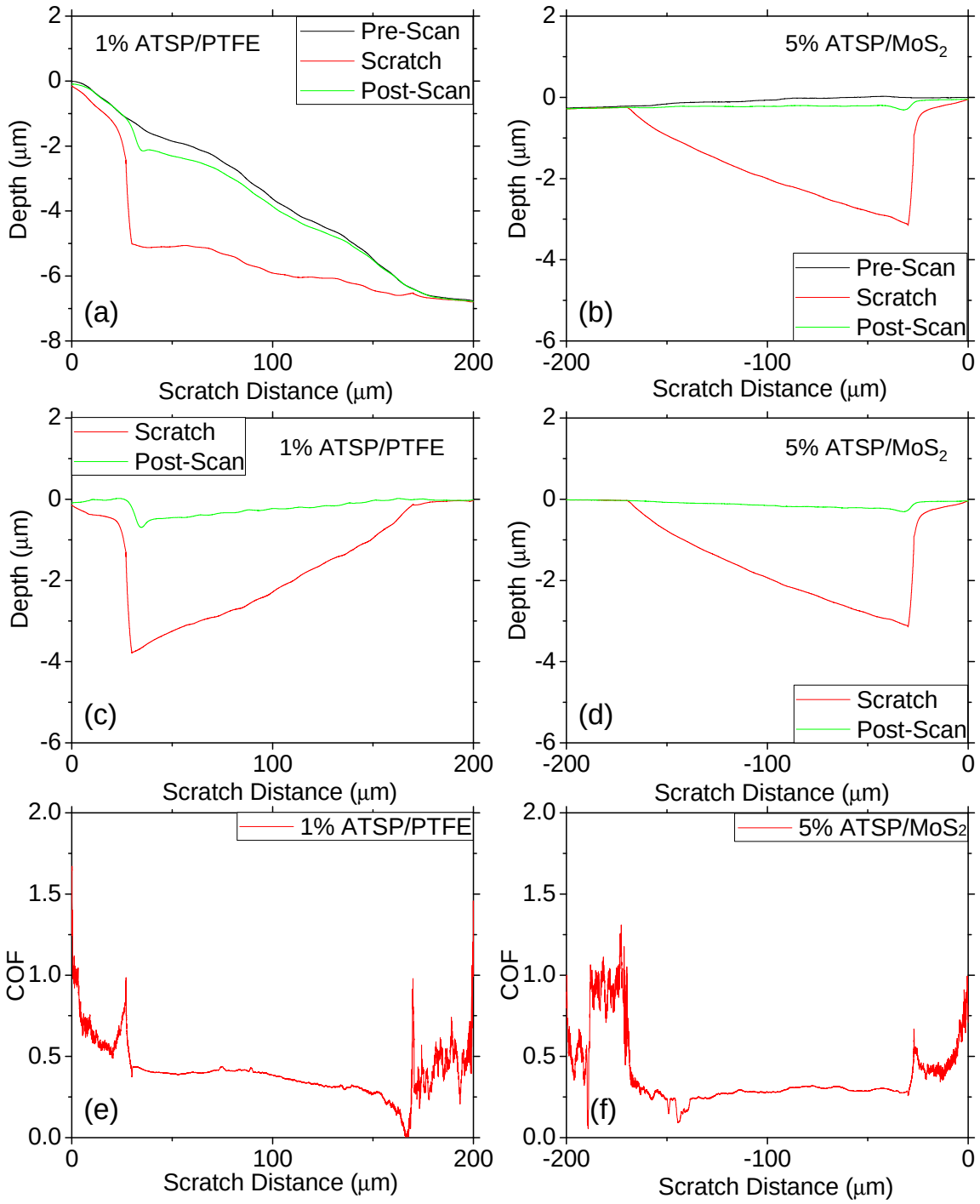

Figure 5.10 Microscratch curves from ramp-loading up to 10 mN for (a) 1% ATSP/PTFE ((c) after normalization), and (b) 5% ATSP/MoS_2 ((d) after normalization). *In-situ* friction coefficient of (e) 1% ATSP/PTFE and (f) 5% ATSP/MoS_2 coatings monitored during the actual scratch cycle.

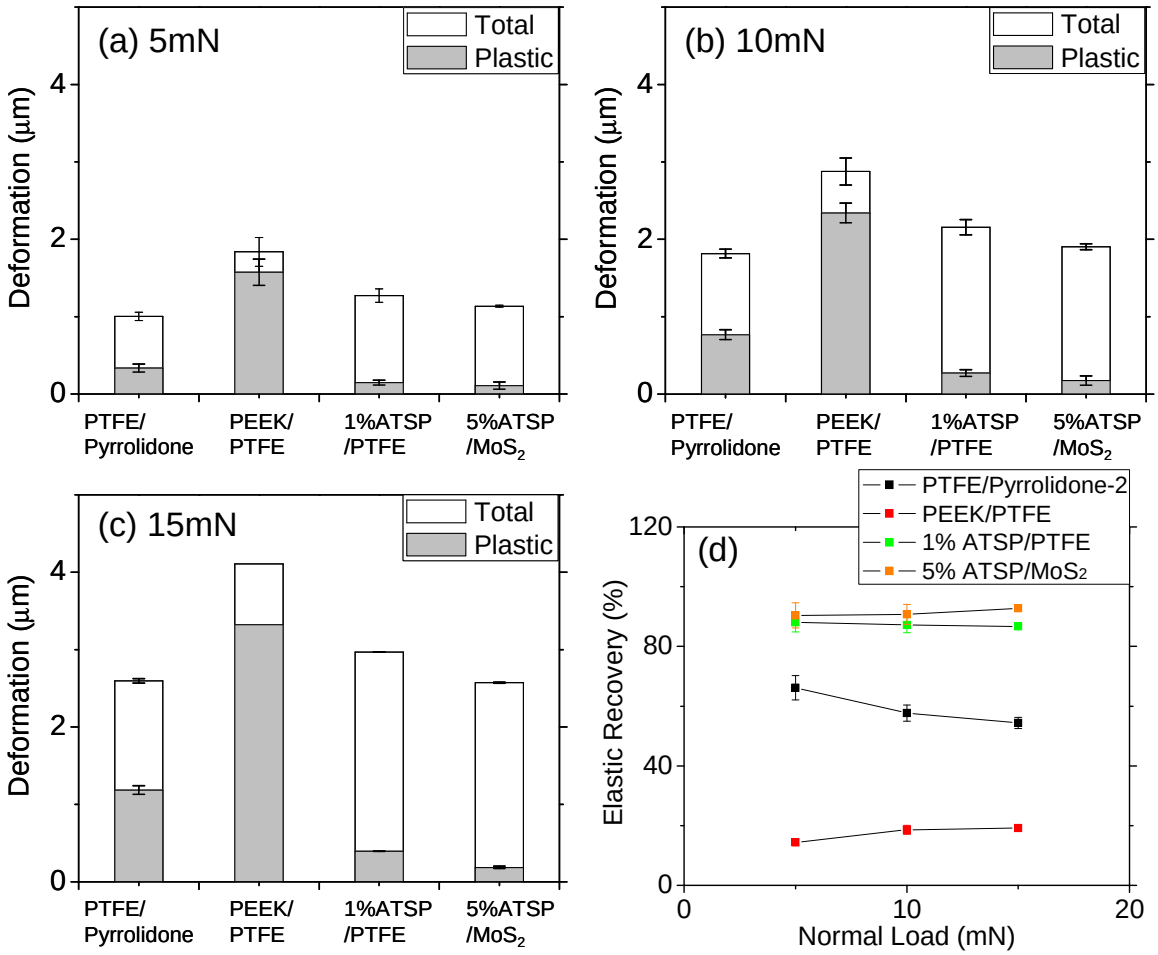

Figure 5.11 Total (penetration depth) and plastic (permanent) deformation of four different polymeric coating surfaces at (a) 5mN, (b) 10mN, and (c) 15mN normal load; (d) elastic recovery of coatings with respect to normal loads.

Based on the scratch curves observed in Figure 5.9 and Figure 5.10, the precise amount of total and plastic (permanent) deformation for each coating at different normal loads could be calculated as seen in Figure 5.11(a) (5mN), 5.11(b) (10mN), and 5.11(c) (15mN). As for the total deformation (penetration depth), PEEK/PTFE coating showed the highest values under all three loading conditions showing its relatively softer surface property than any of other coating surfaces. The remaining three coatings showed similar total deformations. However, the more important aspect in comparing the recovery

property of each surface is the percent elastic recovery (%). It is calculated as the ratio of the "elastic deformation (difference between total and plastic deformation)" to the "total deformation," and plotted with varying normal loads as seen in Figure 5.11(d). PEEK/PTFE coating showed the lowest recovery with less than 20 %, while PTFE/Pyrrolidone-2 exhibited about three times higher recovery than PEEK/PTFE coating for all three normal load conditions.

This finding proves our previous discussion and expectation that polymer surfaces with higher elastic recovery would have better frictional behavior due to their lower real contact area, and thus lower adhesion (Hanchi and Eiss, 1997). Interestingly, both ATSP-based coatings exhibited significantly higher recovery rates around 90% (the 5% ATSP/MoS_2 coating showed slightly higher recovery than the 1% ATSP/PTFE coating). Even though, unfortunately, these two ATSP-based coatings were not tribologically tested using HPT, their frictional behavior could be directly compared with other PTFE- and PEEK-based coatings as shown in Figure 5.12. This plot was constructed based on the *in-situ* COF recording during the scratch measurements which was already described in Figures 5.9(e), 5.9(f), 5.10(e), and 5.10(f).

In agreement with the recovery property of each coating as discussed above, the COF of 5% ATSP/MoS_2 coating which had the highest recovery exhibited the lowest COF values for all increasing normal load conditions. Then, PTFE/Pyrrolidone-2 and 1% ATSP/PTFE coatings showed similar COF with increasing normal loads. As already observed from HPT testing, PEEK/PTFE coating showed the highest COF values in this comparison as well due to its significantly plastic surface property. Therefore, from the scratch testing of different polymeric coating surfaces, it could be observed once again

that the surface with higher elastic recovery property had better frictional behavior than surfaces with highly plastic property such as PEEK/PTFE coating.

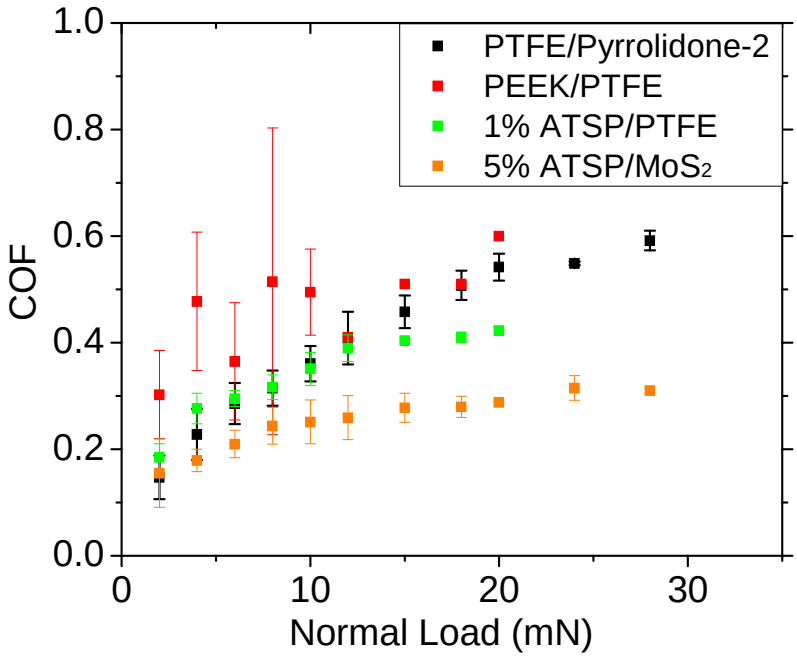

Figure 5.12 *In-situ* friction coefficient vs. normal loads of 4 different polymeric coating surfaces measured during actual scratch cycle.

5.4 Conclusion

PTFE- and PEEK-based polymeric coatings were tribologically tested using a specialized tribometer under unidirectional sliding conditions with elevated temperatures simulating the aggressive ACR compressor operations. Also, these polymeric coating surfaces were subjected to scratch testing to investigate their viscoelastic (recovery) properties and to correlate them with their frictional behaviors from the tribometer testing, and the following conclusions could be drawn:

(a) Among various PTFE- and PEEK-based coatings, PTFE/Pyrrolidone-2 was the only coating which survived the whole duration of 60 min testing under 75°C setting

temperature condition. The other coating surfaces were severely scuffed with very sharp and abrupt increase in their COF and NCT values, even though all of these coatings already exhibited promising tribological behaviors with COF less than 0.1 under room temperature setting condition. Then, PTFE/Pyrrolidone-2 coating was tested under even higher temperature (110 °C), and it showed the lowest COF value so far.

(b) From the frictional behavior of PTFE/Pyrrolidone-2 coating at elevated temperatures, it was observed that COF of amorphous structured polymer surface increased with increasing near contact temperatures, showing maximum COF value at its NCT in the vicinity of its glass transition temperature. This is because, with increasing NCT, the polymer surface becomes more plastic resulting in higher real contact area, and thus higher adhesion on the interfacial zone. Then, as the NCT exceeds the T_g, the COF decreases due to the rapid decline of viscosity and shearing strength on the subsurface zone of polymer caused by the complete scission of molecular chains at a temperature higher than T_g. Therefore, it can be summarized that the overall frictional behavior of polymer coatings is determined by the viscoelastic property of polymers which directly depends on its near contact temperature.

(c) In order to verify that the polymer surfaces with higher recovery usually had lower COF, the elastic recovery of PTFE-, PEEK-, and ATSP-based polymeric coating surfaces was examined using basic room temperature scratch testing. As expected, the PTFE/Pyrrolidone-2 coating surface exhibited three times higher elastic recovery (60 %) than PEEK/PTFE coating surface (20 %). Also, ATSP-based coating surfaces

showed the highest recovery of around 90 % with the lowest COF values observed directly from the *in-situ* COF measurements during the scratching process.

CHAPTER 6: FRETTING EXPERIMENTS AND TRANSFER FILM EFFECTS OF POLYMERIC COATINGS

6.1 Introduction

The sliding contact of polymers in the form of coatings against metallic counterfaces is becoming increasingly common in industrial applications due to improved coating processes on light weight substrates as well as favorable tribological behavior of polymeric coatings under moderate to severe contact conditions. A type of motion encountered in industrial bearing contact applications is reciprocating motion with extremely small amplitude of few mm to sub-mm, which is usually referred to as fretting motion or dithering motion. Of particular interest in this work is the tribological performance of polymeric coating contact surfaces in air-conditioning and refrigeration compressors experiencing such motion, e.g., in a scroll compressor.

The tribological behavior of advanced blended bulk polymers has been extensively studied, and their superior tribological performance is usually attributed to their unique property of effective transfer film formation on the counterface during dry sliding (Burris *et al.*, 2008, Wang and Yan, 2006, Wang and Yan, 2007, Lu and Friedrich, 1995, Bahadur and Schwartz, 2008, Bahadur and Sunkara, 2005, and Bahadur, 2000). Specifically, Burris *et al.* (2008) and Wang and Yan (2006) showed that the retention of protective transfer films strongly adhered to the counterface is primarily responsible for the improvements in wear resistance. Studies about the effects of fillers on the tribological behavior of polymer composites also show that improved wear performance is related to how well the fillers improved the ability of composites to form transfer films (Wang and Yan, 2006, Bahadur, 2000, and Friedrich *et al.*, 2005). The mechanism of

transfer film development by abrasion of the softer polymeric material by the harder counter-surface metal asperities has been studied under somewhat idealistic conditions of low load, slow unidirectional sliding speed and smooth interfaces.

The mechanism and effectiveness of transfer film formation for polymeric coatings (versus bulk) has not been investigated and such mechanism may or may not be the same as for bulk materials. The nature of the coatings is such that effective transfer film formation is critical since penetrating the thin polymeric coating will likely result in catastrophic failure as one would expose metal-to-metal contact (unless some sort of protective layer is formed). This is typically not the case for bulk polymers since there is an abundance of polymer material to replenish any worn transfer films. Note that the use of polymeric coatings versus bulk polymers in bearing applications in machinery can resolve issues associated with bulk polymers such as long-term stability and reduced cost.

Tribological studies of high bearing blended polymers in the form of coatings are scarce, compared to bulk polymers. Tribological studies of polymeric coatings have been already reported in Chapter 3 under specific refrigerant environments, simulating air-conditioning and refrigeration compressor surfaces. These studies focused on unidirectional high speed sliding applications (e.g., as encountered in swash-plate automotive air-conditioning compressors) and large oscillatory motion simulating the wrist-pin/bushing contact in reciprocating compressors. From these studies, it was shown that PTFE-based (vs PEEK-based) polymeric coatings exhibited superior tribological performance. In this chapter, two representative PTFE- and PEEK-based polymeric coatings were tribologically tested under both unlubricated (dry) and liquid lubricated fretting test conditions under aggressive normal loads to examine their scuffing resistance

limits. The mechanism of transfer film formation and their role on the sliding wear were studied using Scanning Electron Microscopy (SEM) and profilometric roughness measurements.

6.2 Experimental

6.2.1 Coating systems

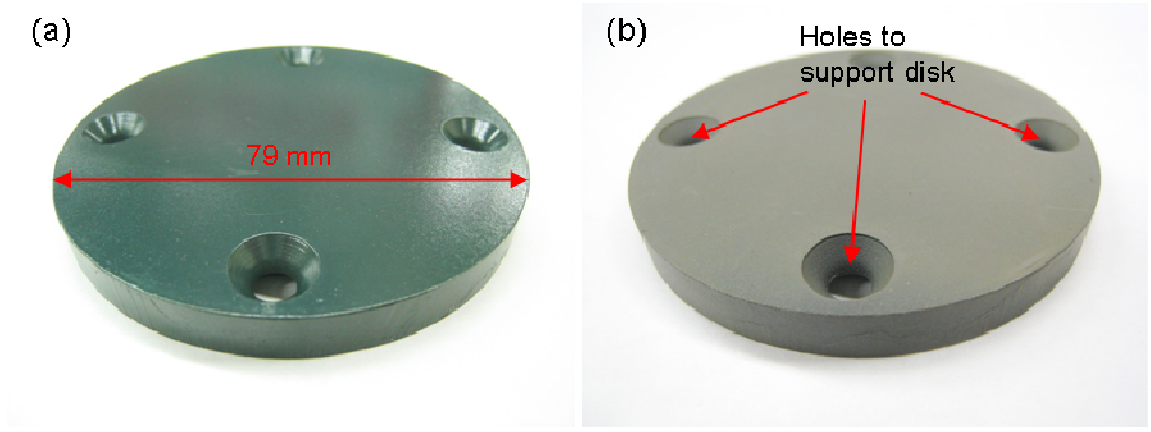

Figure 6.1 Photographs of coated disk samples: (a) PTFE/Pyrrolidone, (b) PEEK/PTFE.

Two of the seven coatings listed in Table 4.1, namely, PTFE/Pyrrolidone (DuPont™ Teflon® 958-414) and PEEK/PTFE (1704 PEEK/PTFE®) were used in this chapter. Photographs of those coatings are depicted in Figure 6.1 and the physical properties of the coatings are given in Table 6.1. PTFE/ Pyrrolidone coating showed a glossy and dark-green colored surface, while PEEK/PTFE has a dark gray colored and matte finish.

The surface roughness (R_q) of the two coatings was measured using a stylus profilometer (Tencor P-15™) and summarized in Table 6.1. The PEEK/PTFE coating surface shows higher roughness (1.00 μm) than the PTFE/Pyrrolidone coating (0.61 μm),

which can be attributed to the coating powder/particle size used. The thickness of the two coatings was measured using cross section SEM, and found to be 23 ± 5 μm and 40 ± 5 μm, respectively, for PTFE/ Pyrrolidone and PEEK/PTFE coatings.

Table 6.1 Physical properties of the polymeric coatings used in this work.

	PTFE/Pyrrolidone	PEEK/PTFE
Color	Dark green	Dark gray
Thickness (μm)	23 ± 5	40 ± 5
R_q (Std.) (μm)	0.61 (0.08)	1.00 (0.03)
Elastic modulus (Std.) (GPa)	3.7 (0.1)	4.5 (0.8)
Hardness (Std.) (MPa)	51 (3)	42 (13)

6.2.2 Tribological testing conditions

A high pressure tribometer (HPT) enabling the application of a precisely controlled (closed loop) normal load and the measurement of *in-situ* friction coefficient on the pin-on-disk (coated) contact interface was used for the fretting experiments. The pin is placed on the lower stationary holder which is directly mounted on a force transducer sensing both normal force and friction force, thus obtaining the friction coefficient. The coated disk is securely attached on the upper oscillating spindle, enabling fretting-type of motion at the interface. Further details of the HPT can be found in Escobar Nunez *et al.* (2011) and Demas and Polycarpou (2008).

The pins were also made out of the same gray cast iron as the substrates, and machined as seen in Figure 6.2. In addition to the "standard" cylindrical pin having 6.3 mm diameter (of contact area), a reduced diameter (3.2 mm) pin was also used to achieve

higher contact pressure testing. The roughness of the pin surfaces was 0.3 μm – 0.4 μm (smoother than the polymeric coating surfaces).

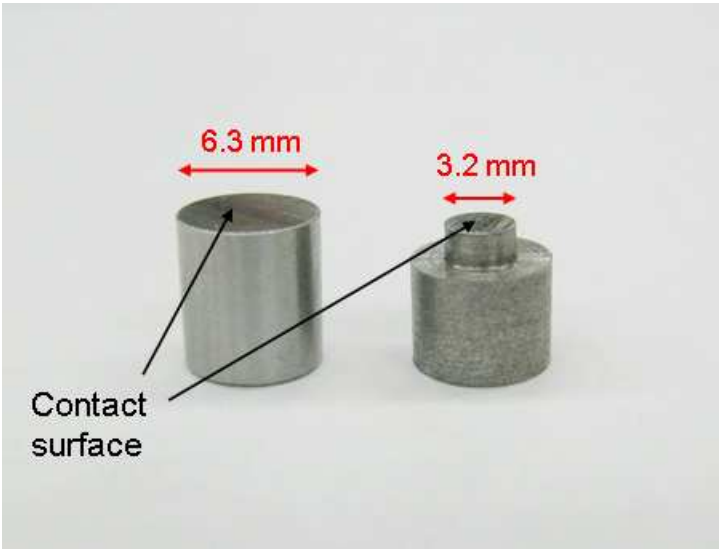

Figure 6.2 Photographs of the cylindrical pins. The 6.3 mm diameter contact surface is considered as "standard" size and the reduced diameter (3.2 mm) pin enables higher contact pressures.

Fretting motion with 3 mm translation amplitude and 4.4 Hz reciprocating frequency was imposed on the pin-on-disk interface, thus resulting in an average linear sliding speed of 26.4 mm/s. The applied normal load started from 133 N (30 lb), and progressively increased by 133 N every 2 min, up to 1334 N (300 lb) (20 min testing) to examine the scuffing resistance of the coatings. Assuming a nominally flat pin surface under the initial 133 N normal load, the corresponding contact pressures are 4.28 MPa and 16.58 MPa for the regular pin and the reduced diameter pin, respectively. Testing was performed under conditions simulating a compressor environment, namely, inside an environmentally controlled chamber filled with 40 psi of R-134A refrigerant at room temperature. Table 6.2 summarizes the experimental conditions used in this work.

Additionally, liquid lubricated testing was performed under exactly the same testing conditions to investigate the interaction between lubricant and the polymeric coatings under fretting conditions (the need for such testing is that even though polymeric coatings are envisioned to replace liquid lubricants in the future, it is likely that there will be a transitional phase where the polymeric coatings will be used together with existing liquid lubricants). For the lubricated tests, a commercially available polyolester (POE)-based lubricant (RL32-3MAF) that was currently used in existing air-conditioning and refrigeration compressors was used. This lubricant has a viscosity of 31.2 cSt at 40 °C and 5.8 cSt at 100 °C, and its viscosity index (VI) is 125.

Before each test, the non-coated pin samples were ultrasonically cleaned in acetone for 10 min, rinsed with 2-propanol, and dried with a warm air blower. The polymeric coated disk samples were cleaned in 2-propanol and were not exposed to acetone.

Table 6.2 Summary of experimental conditions

	Testing conditions
Temperature (°C)	23 (room temperature)
Environment (refrigerant)	R-134A at 40 psi
Reciprocating frequency (Hz)	4.4
Reciprocating amplitude (mm)	3
Average linear sliding speed (mm/s)	26.4
Contact geometry	Nominally flat surface contact
Normal load (N)	133 - 1334
Nominal contact pressure (MPa)	4.28 – 42.8 (6.3mm pin), 16.58 – 165.8 (3.2 mm pin)
Test duration (min)	20 (up to failure)

6.3 Results and discussion

6.3.1 Fretting experiments

6.3.1.1 Unlubricated scuffing experiments

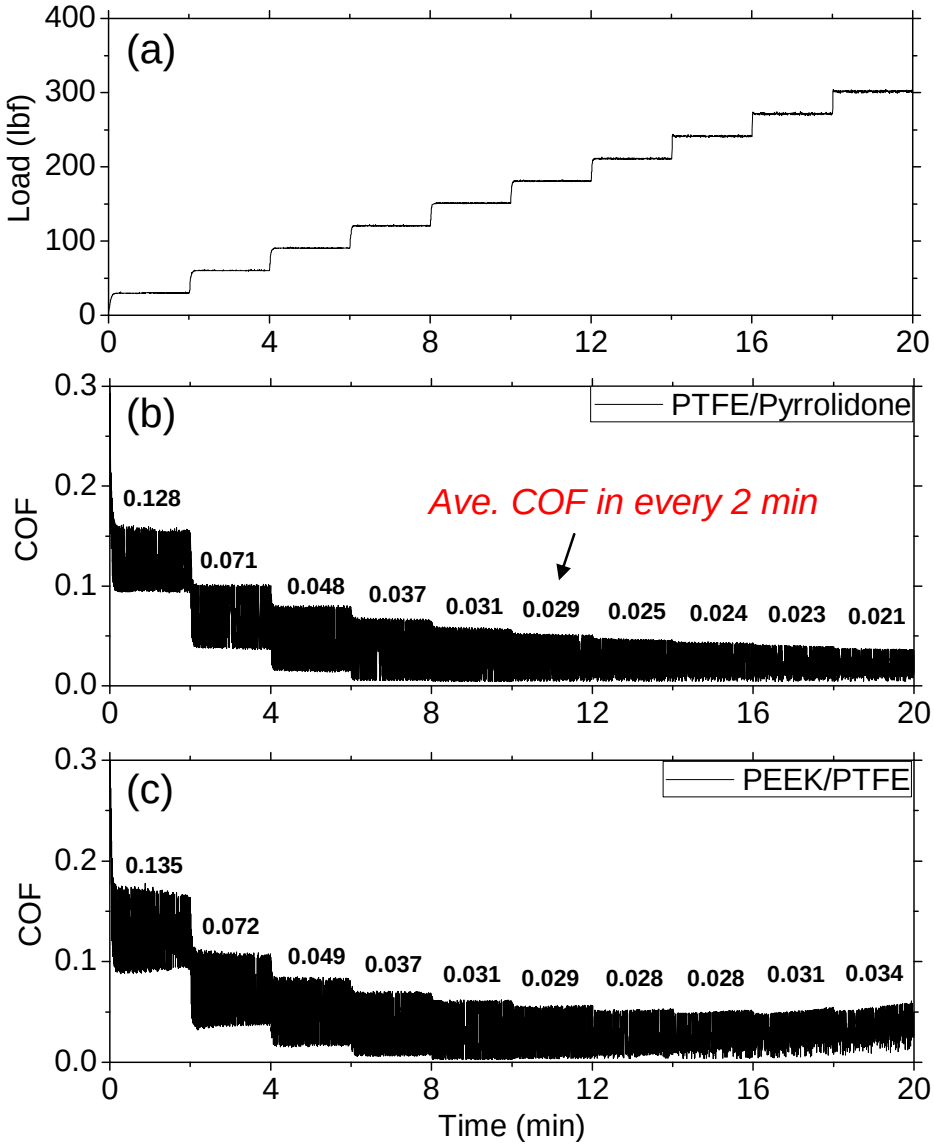

Figure 6.3 Unlubricated scuffing experiments (Table 2, 6.3 mm pin): (a) normal load, (b) friction coefficient, PTFE/Pyrrolidone, (c) friction coefficient, PEEK/PTFE.

Figure 6.3 depicts the in-situ normal load and measured friction coefficient for both coatings under unlubricated fretting contact conditions. The intention of these tests

was to quantify the scuffing resistance (load-to-failure) of these interfaces. However, under the conditions tested, both coatings survived the whole test duration, up to 1334 N normal load (42.8 MPa contact pressure) without showing any catastrophic failure (which is usually associated with abrupt and sharp increase in the COF).

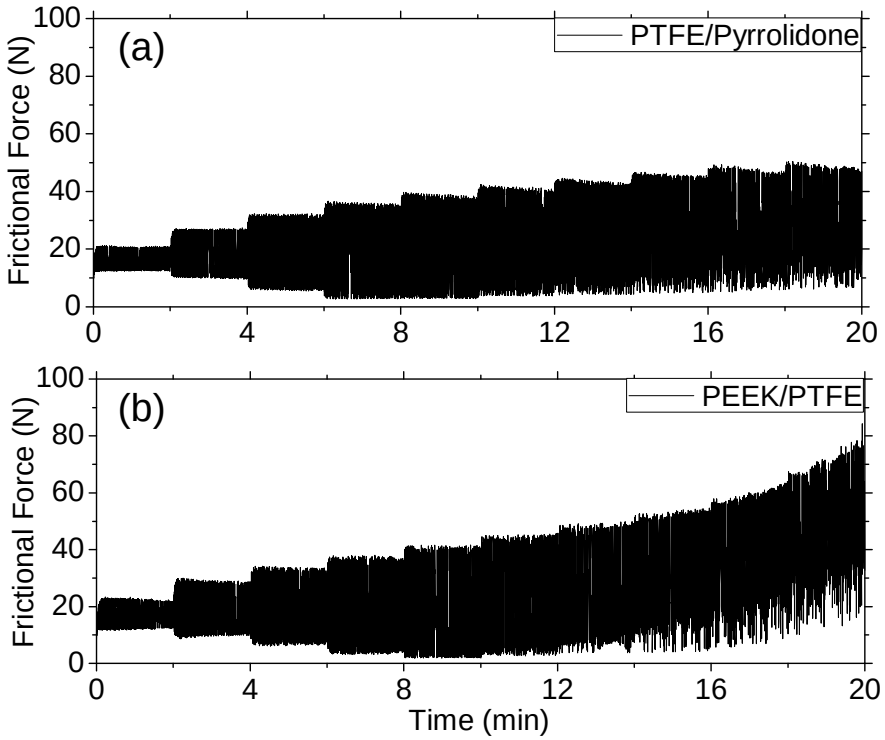

Figure 6.4 *In-situ* friction force for (a) PTFE/Pyrrolidone, and (b) PEEK/PTFE coatings for the experiments shown in Figure 6.3.

As seen in Figure 6.3, both coating interfaces exhibited higher COF during the running in period, decreasing significantly thereafter. Also, in both cases the COF fluctuation is significant due the nature of the fretting tests (few mm sliding distance). Despite these similarities there are specific differences between the two coatings: With increasing normal load, in the case of PTFE/Pyrrolidone, the average COF decreased to 0.021 (this value is half the value under unidirectional high speed sliding experiments reported in Chapter 3). In the case of PEEK/ PTFE the COF decreased to 0.028 after

running in, however, halfway through the test it started to increase reaching a value of 0.034 towards the end of the test. Because these tests were performed under changing normal load with time, it is also important to examine the *in-situ* friction force, which is shown in Figure 6.4. In the case of PTFE/Pyrrolidone, the friction force showed a very slight increase with significant increasing load and thus the apparent reduction in the COF. In the case of PEEK/PTFE the frictional force increases at a faster rate than the normal force, thus the apparent increase in the COF. In both cases, the classic friction "law" stating that there should be a constant COF value violated, which is expected for such polymeric coatings (versus dry metal contacts).

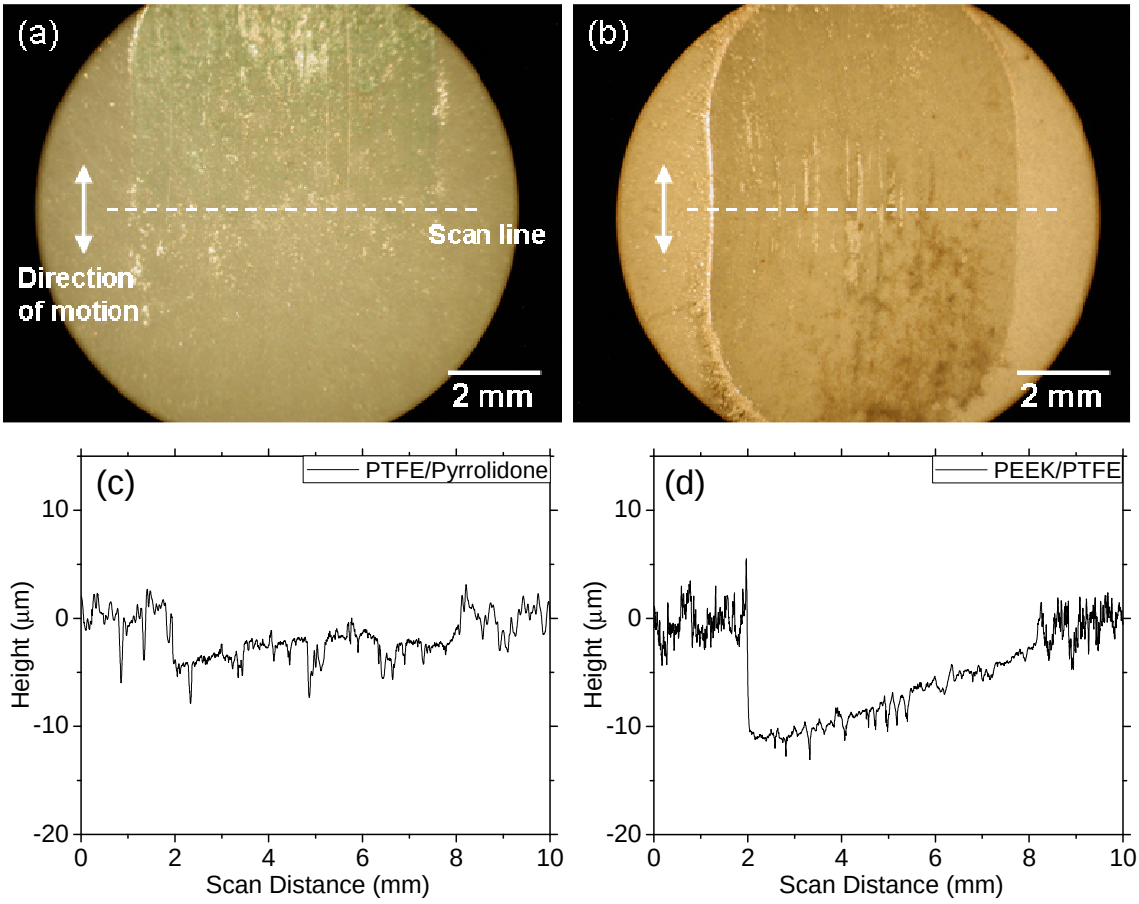

Figure 6.5 Optical images of the worn coating surfaces for (a) PTFE/Pyrrolidone and (b) PEEK/PTFE, and profilometric cross section wear scan measurements for (c) PTFE/Pyrrolidone and (d) PEEK/PTFE (for the experiments shown in Figure 6.3).

Figures 6.5(a) and 6.5(b) show low magnification optical images of the worn coating surfaces, and Figures 6.5(c) and 6.5(d) show profilometric wear track measurements of the same worn surfaces. The optical image of the wear track of PTFE/Pyrrolidone shows mild burnishing, which is confirmed with the profilometric scan showing 3 μm - 4 μm wear depth, Figure 6.5(c). The optical image of the wear track of PEEK/PTFE showed material removal, and confirmed with wear depths higher than 10 μm. This finding, namely that PEEK/PTFE exhibited better wear resistance that PTFE/Pyrrolidone is in accord with the unidirectional sliding experiments reported in Chapter 3. However, both coatings were not completely penetrated even under 42.8 MPa nominal contact pressure, and further stress tests were needed to examine the scuffing resistance of these polymeric coatings under fretting conditions.

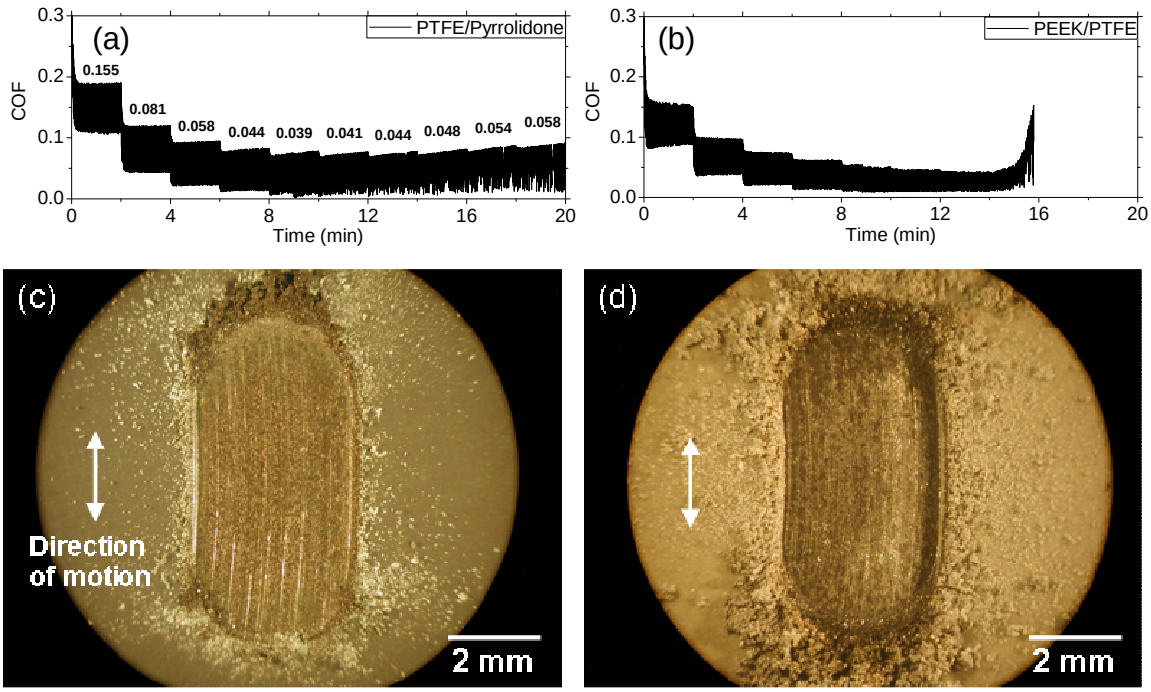

Figure 6.6 *In-situ* friction coefficient of (a) PTFE/Pyrrolidone and (b) PEEK/PTFE coating under unlubricated scuffing experiments (Table 2, 3.2 mm pin). Optical images of worn surfaces of (c) PTFE/Pyrrolidone and (d) PEEK/PTFE.

To obtain higher contact pressure, reduced diameter pins (3.2 mm) were used in another set of fretting tests as shown in Figure 6.6. The same loading profile as used for the regular pins was used, resulting in higher nominal contact pressure up to 165.8 MPa (at the maximum normal load of 1334 N). Even under this high contact pressure condition, the PTFE/Pyrrolidone coating still did not show any scuffing behavior with only smooth and gradual increase of the COF for the last 6 min - 8 min of testing. At the end of the test, its COF was maintained at 0.05-0.06 which was still relatively low. In the case of PEEK/PTFE coating, however, scuffing was clearly observed with a sharp increase of COF at 133 MPa contact pressure as shown in Figure 6.6(b). This sudden increase of the COF was caused by direct metal (pin)-to-metal (substrate) contact when the polymer coating layer was completely penetrated, which is also seen in the worn coating surface in Figure 6.6(d).

Significant amount of wear debris is observed in the vicinity of the wear track of the PEEK/PTFE coating. Although less wear debris was observed in the case of PTFE/Pyrrolidone shown in Figure 6.6(c), this coating was also found to be penetrated after profilometric measurements. Thus, both PTFE/Pyrrolidone and PEEK/PTFE coatings were penetrated under these more aggressive testing conditions, but only the PEEK/PTFE coating exhibited clear scuffing behavior with catastrophic failure at a scuffing pressure of 133 MPa. This implies that in the case PTFE/Pyrrolidone, even though the coating is penetrated, there is a lubricious layer on the interface between the pin and the substrate which prevents direct metal-to-metal contact, thus avoiding scuffing failures. Further investigation of this layer is discussed in section 6.3.2.

6.3.1.2 Liquid lubricated experiments

A practical question that arises is whether the polymeric coatings (which can be viewed as solid lubricants) have similar or better tribological performance compared to currently used state-of-the-art synthetic liquid lubricants. For direct comparison, experiments under identical conditions using both the regular and small diameter pins against uncoated cast iron disks were performed in the presence of 23 mg of synthetic lubricant (RL32-3MAF), shown in Figure 6.7. Using the regular 6.3 mm diameter pin, Figure 6.7(a), the COF values were similar to the polymeric coatings shown in Figure 6.3. Specifically the lowest COF value of 0.040 achieved with lubricant was 90 % and 43 % higher than that of PTFE/Pyrrolidone (0.021) and PEEK/PTFE (0.028) coatings, respectively. In the case of testing with the reduced diameter pin shown in Figure 6.7(b), the liquid lubricant showed superior frictional behavior compared to the two polymeric coatings shown in Figure 6.6. The liquid lubricant did not show any increase in the COF even under 165.8 MPa contact pressure, which maintained a low value of 0.037 until the end of the test. Figures 6.7(c) and 6.7(d) show the wear tracks of the cast iron substrates, which depict mild burnishing only. Therefore, from the lubricant-only conditions experiments, it was found that at lower contact pressures, less than 50 MPa, the polymeric coatings, especially PTFE/Pyrrolidone showed superior frictional behavior with very low COF (0.021). At higher contact pressures over 100 MPa, the liquid lubricant performed better than the polymeric coatings with extremely high scuffing resistance.

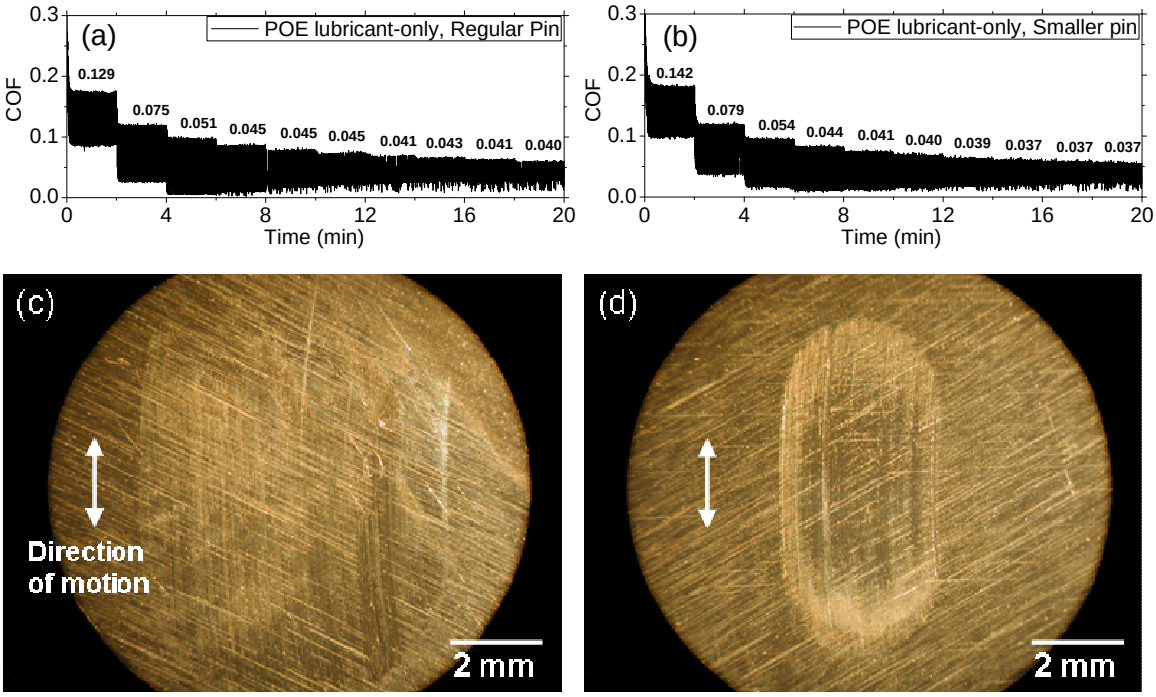

Figure 6.7 *In-situ* friction coefficient of synthetic lubricant-only fretting conditions with (a) 6.3 mm pin and (b) 3.2 mm pin. Optical images of worn disks after experiment using the (c) 6.3 mm pin and (d) the 3.2 mm pin.

6.3.1.3 Polymeric coatings plus liquid lubricated experiments

A second question is the effect of the addition of liquid lubricant at the polymeric coating interface. Such study is practically important since it is unlikely that liquid lubricants will be completely replaced by polymeric coatings (resulting in oil-less compressors) at the outset. More likely there will be a transitional period where the polymeric coatings are introduced into existing compressors that already use liquid lubricants. To answer this question, another set of fretting experiments using the best performing PTFE/Pyrrolidone coating (against the 6.3 mm pin) was performed in the presence of 23 mg RL32-3MAF lubricant. The *in-situ* friction coefficient is shown in Figure 6.8(a) shows that after 12 min, the COF reached the value of 0.030, which is between the COF for the coating-only case, Figure 6.3(b), and liquid lubricant-only case,

Figure 6.7(a). In other words, the frictional behavior under this mixed condition was better than liquid lubricant-only condition, but slightly higher compared to the coating-only case.

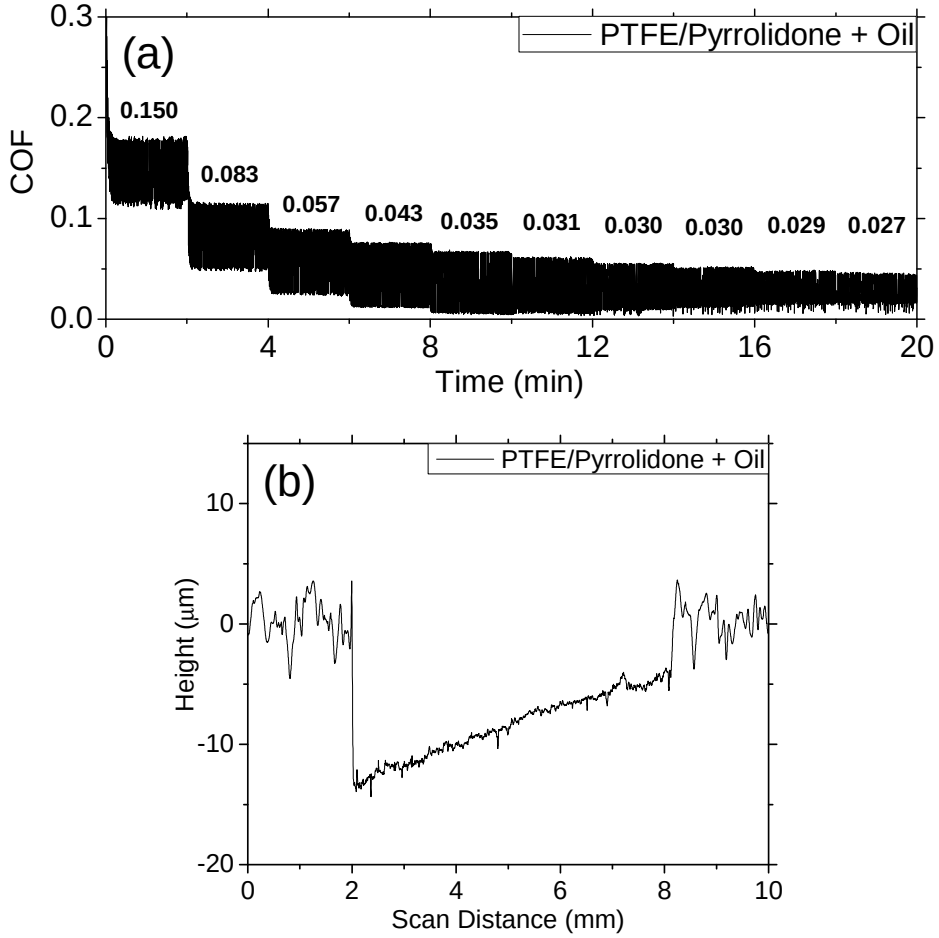

Figure 6.8 (a) *In-situ* friction coefficient of PTFE/Pyrrolidone coating tested under liquid lubricated conditions (Table 2, 6.3 mm pin) and (b) its cross-section wear track profile after testing.

Similarly to the frictional behavior, the wear is lower under coating-only condition (3-4 μm, Figure 6.5(c)), compared to the coating plus lubricant condition (14 μm, Figure 6.8(b)). This somewhat counterintuitive result shows that in the combined presence of two independently beneficial tribo-protecting layers (synthetic liquid

lubricant and polymeric coating), the tribological performance not only is "doubling up" but is worse compared to their individual contributions. Next we investigate the transfer films that are critical for improved tribological performance.

6.3.2 Transfer films

6.3.2.1 Transfer film formation for polymeric coatings

One of the main differences between PTFE/Pyrrolidone and PEEK/PTFE coatings under fretting conditions could be seen by examining the counterpart (pin) surface after testing as seen in Figure 6.9. Even under such low magnification optical images, it could be clearly seen that material transfer from the coated surface to the bare pin surface has occurred in the case of PTFE/Pyrrolidone, Figure 6.9(a), but not in the case of PEEK/PTFE, Figure 6.9(b).

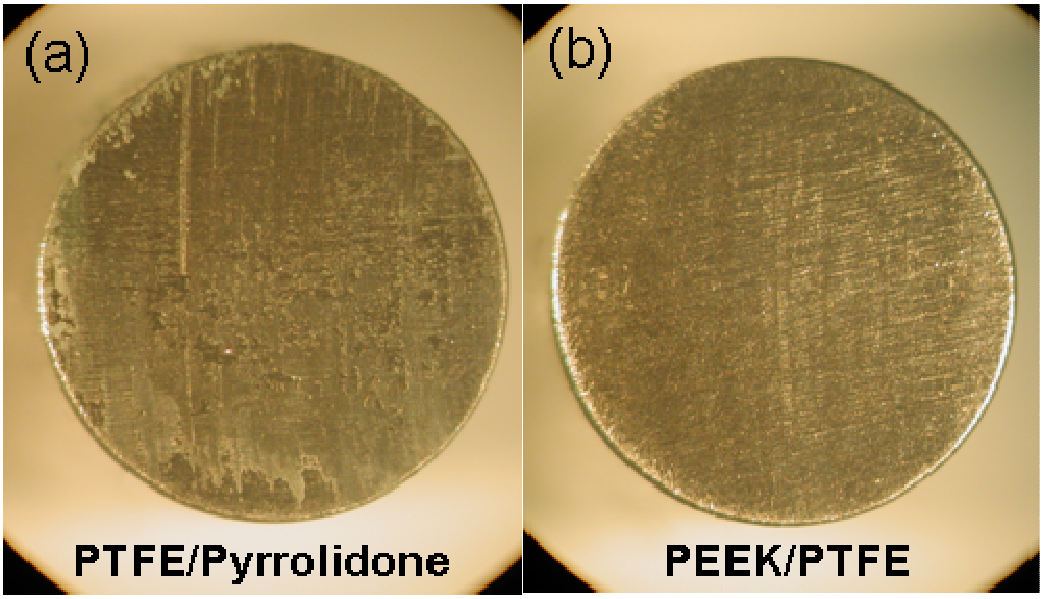

Figure 6.9 Optical images of the 6.3 mm pin surfaces after testing with (a) PTFE/Pyrrolidone and (b) PEEK/PTFE coatings (under dry condition in Figure 6.3).

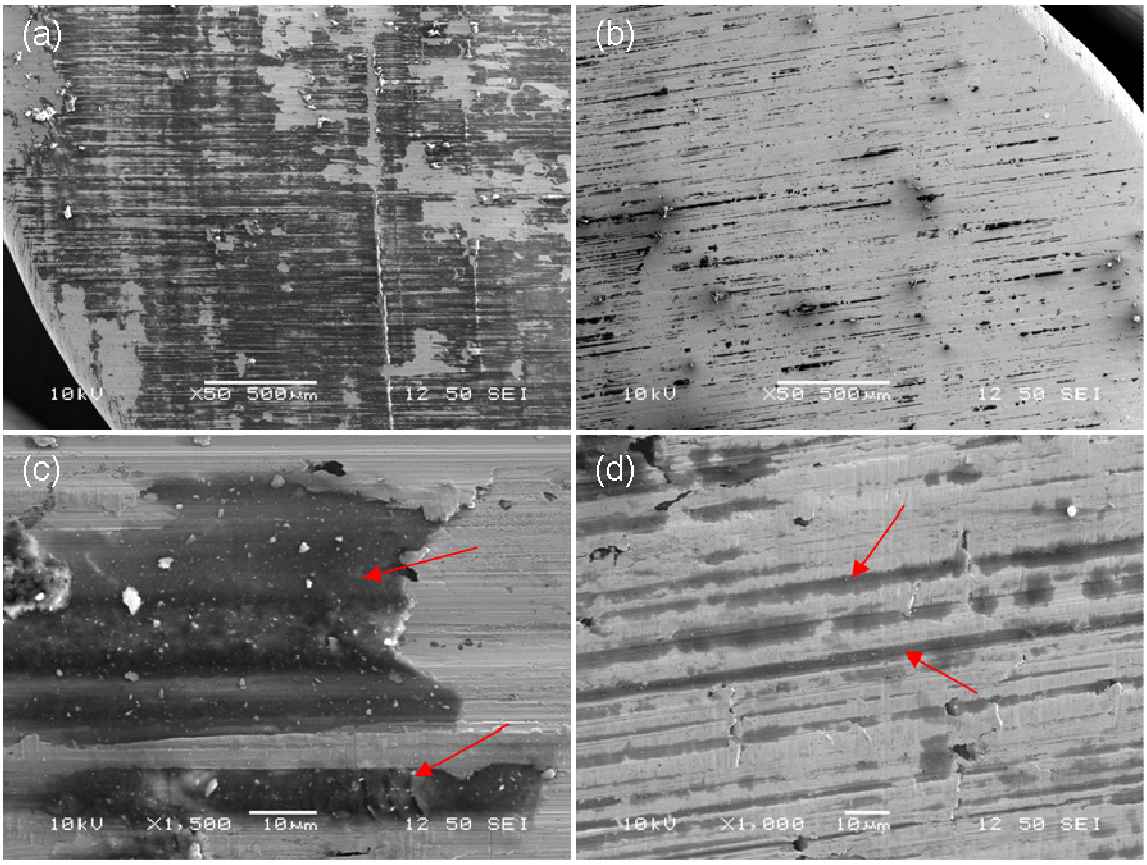

Figure 6.10 SEM images of the pin surfaces (Figure 6.9) tested under dry condition with (a) PTFE/Pyrrolidone and (b) PEEK/PTFE coating, and (c), (d) higher magnification images, respectively, showing the morphology of the transfer films of each coating marked with red arrows.

To further examine the polymeric transfer films, SEM images of the pin surfaces are depicted in Figure 6.10. Figure 6.10(a) shows x50 magnification of the pin surface tested with PTFE/Pyrrolidone, showing that a significant percent of the surface is covered with transferred coating materials (called transfer film). Under the same magnification, in the case of PEEK/PTFE, Figure 6.10(b), there is no evidence of a transfer film. Higher magnification (x1500) SEM images of the same surfaces are shown in Figure 6.10(c) and Figure 6.10(d) for the cases of PTFE/Pyrrolidone and PEEK/PTFE, respectively. These images validate the formation of a relatively thick transfer film in the case of

PTFE/Pyrroline and no obvious transfer film in the case of the PEEK/PTFE film. Note that in the case of PEEK/PTFE there appears to be some spotty transfer films on the valleys of the machining marks of the pin surface, which are not effective under sliding conditions, as the rubbing surface (surface peaks) are bare exposing metal-to-metal contact. Such transfer film formation has also been documented in the case of bulk polymers in contact with a metal counterpart (Wang and Yan, 2007 and Bahadur and Schwartz, 2008). In the present study, it was found that the tribological performance of the polymeric coatings was greatly influenced by the ability of each coating to form a stable and continuous transfer film on the counterface.

6.3.2.2 Mechanism of transfer film

Understanding the mechanism of transfer film formation on the metal counterface will enable us to design better coating systems for improved tribological performance. In general, material transfer of soft polymeric coatings to metal counterface (pin surface) could be attributed to the coupled effects of chemical (adhesion) and mechanical interaction between the two surfaces. In polymer-to-metal contacts, there is a natural propensity for polymer materials to be adhered to metallic counterfaces, which can be the fundamental basis for transfer film formation. There are different mechanisms for adhesion, including Coulomb electrostatic forces, van der Waals forces, and bonding from chemical reactions. In the case of PTFE-based coatings, as the coating is being rubbed against the pin surface, the adhesive junctions are thought to develop due to cohesive bonding between the PTFE-end caps or other free radicals, and the metallic surface (Bahadur, 2000). At the same time, the mechanical transfer of soft coating

materials to the counterface is also initiated at the beginning stages of sliding. In this case, the polymer fragments are sheared by sharp metal asperities of the counterface and interlocked into the crevices and valleys of the pin surface (Bahadur and Schwartz, 2008).

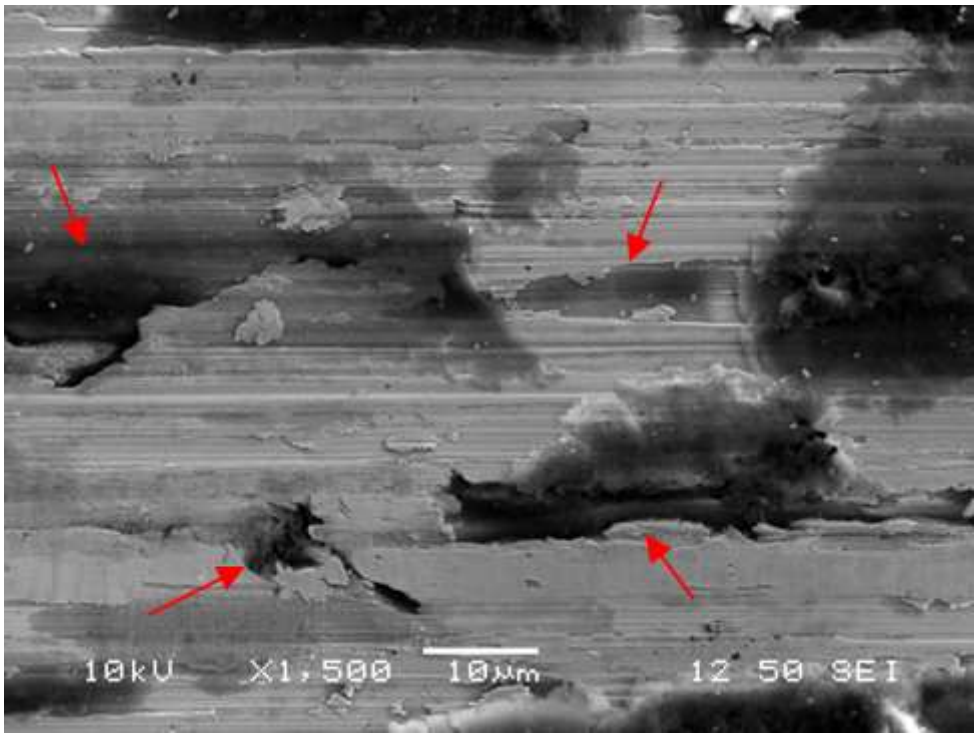

Figure 6.11 SEM image of counterface (pin surface) tested in contact with PTFE/Pyrrolidone coating under dry condition showing the initial formation of transfer film.

The above-mentioned transfer film mechanism can be seen in the x1500 SEM image of the pin surface (6.3 mm) tested with PTFE/Pyrrolidone under dry condition, Figure 6.11. It clearly shows that the pits, holes and crevices of the surface are filled with darker polymer material (also marked with arrows). These small patches of polymer material that initially form on the counterface, agglomerate with repetitive sliding, due to cohesion between mutually compatible polymer fragments, and thus resulting in continuous and large transfer films, as seen in Figure 6.10(a). With increasing number of

fretting cycles, the whole pin surface was covered by the transfer film, and thus protecting the polymer film from damage by sharp and hard metal asperities (i.e., the transfer film acting as a lubricious film at the contact interface).

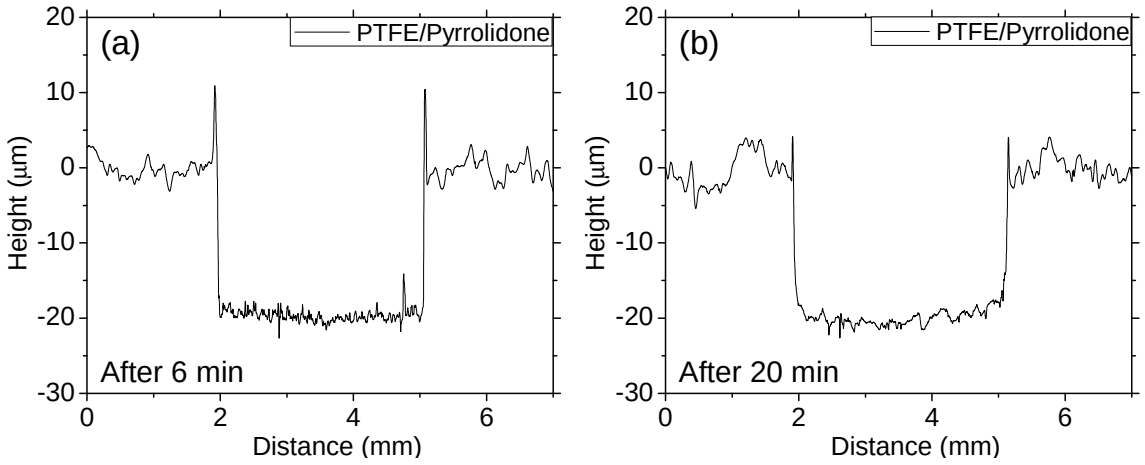

Figure 6.12 Typical profilometric cross-section wear tracks of PTFE/Pyrrolidone coating after (a) 6 min and (b) 20 min of fretting experiments with the 3.2 mm pin.

The process of transfer film formation contributes to the initial transient wear behavior in polymer-on-metal sliding. During this period, higher COF and significant wear are usually observed. Figure 6.12(a) and Figure 6.12(b) show the PTFE/Pyrrolidone coating wear track after 6 min and after 20 min of testing using the 3.2 mm diameter pins, respectively. It is seen that after 6 min of testing, the coating was almost penetrated, showing the same wear depth as that after 20 min of testing. Therefore, the majority of material removal occurs at the beginning of the test, thus resulting in higher friction coefficient and wear rate during this transient period; at the same time the transfer films are formed on the metal counterface. Depending on the roughness of the counterface, this initial transient period could be different, because it

takes more time to fill the rougher surface with a polymer material (Burris *et al.*, 2008). Once a continuous and stable transfer film is formed on the counterface and shields the hard asperities, material removal by mechanical interlocking is significantly reduced, thus exhibiting steady-state frictional behavior for the rest of the test duration.

Further improvement of the transfer film hardness could occur with the accumulation of fretting cycles due to work hardening caused by repeated plastic deformation (Zhang *et al.*, 2006). Wang and Yan (2007) showed that with increasing sliding, continuity and ductility of the transfer film gradually improved, and the transfer film became smoother. Therefore, once the transfer film is firmly formed on the counterface, it can be thought as another hard coating layer lubricating the interface, which results in the so-called "self-lubricating" property to polymer materials. This is the reason that the PTFE/Pyrrolidone coating did not show any catastrophic failure even after the coating was completely penetrated in the fretting experiments with a reduced diameter pin in Figure 6.6(a). However, the PEEK/PTFE coating showed a very sharp increase of COF (Figure 6.6(b)) as soon as the coating was penetrated because there was no uniform transfer film that was formed on the pin surface as seen in Figure 6.10(b). The polymer-to-metal sliding can be summarized in two steps; (1) flattening of the rough metal surface by transferred materials during the transient period, and then (2) self-lubricating effect of transfer film during steady-state sliding.

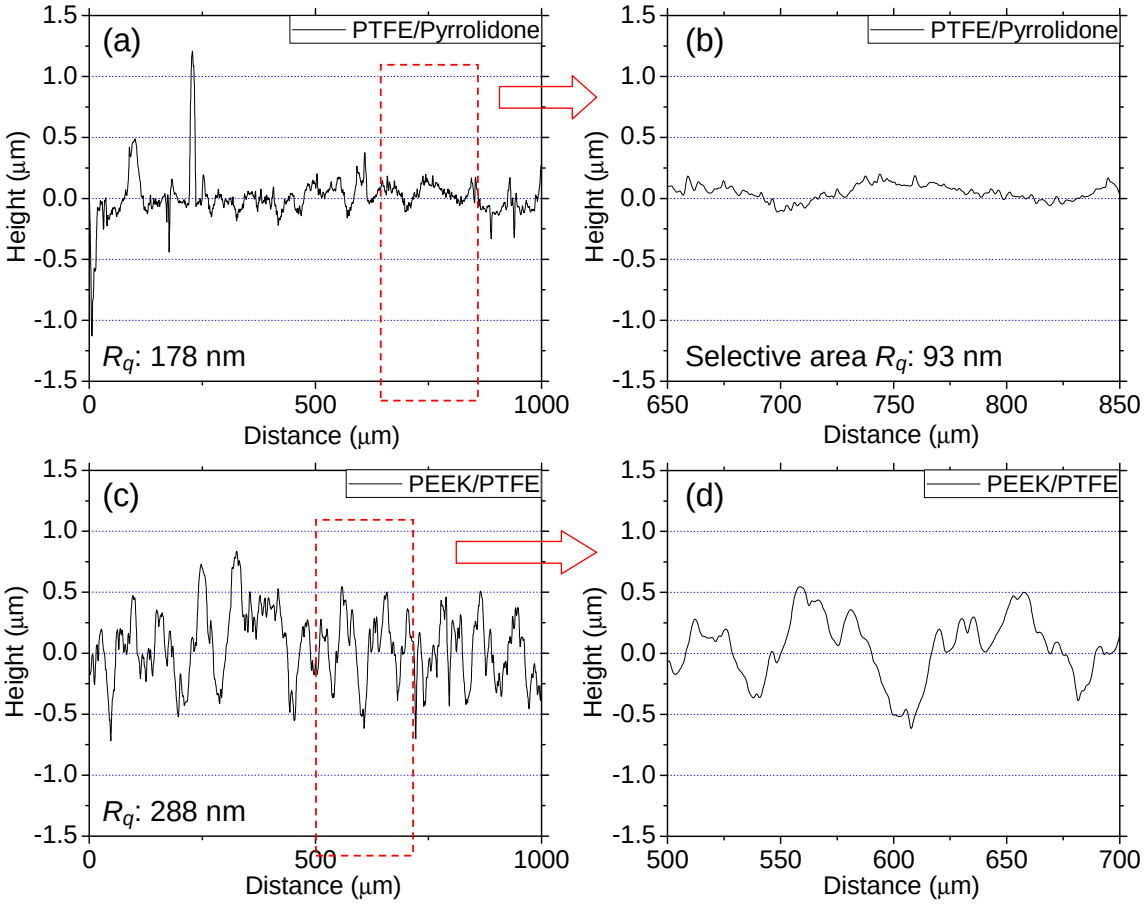

Figure 6.13 Profilometric measurements of 6.3 mm pin surfaces after fretting experiments with (a), (b) PTFE/Pyrrolidone and (c), (d) PEEK/PTFE coatings.

6.3.2.3 Morphology of transfer films

The roughness of the pin surfaces was measured using a stylus profilometer to quantitatively examine the polymer transfer films. Figure 6.13(a) shows a line scan on the pin surface after it was tested against PTFE/Pyrrolidone coating. The root-mean-square (RMS or R_q) roughness is 178 nm, which is 50 % lower than the roughness of original pin surface, 347 nm (using the same length scan size). A selected area from 650 μm to 850 μm shows significantly smoothed pin surface with an RMS roughness of 93 nm, as seen in Figure 6.13(b). This likely resulted from the filling effect of the transferred material onto the asperity crevices. In the case of PEEK/PTFE coating shown

in Figure 6.13(c), the roughness was slightly reduced to 288 nm R_q compared to the original pin surface, but it still showed a much rougher pin surface compared to the PTFE/Pyrrolidone case. Because the transfer film was not effectively formed, the pin surface showed clear asperities and valleys, as seen in Figure 6.13(d). In this case, the hard asperities are continuously wearing out the soft polymeric coating surface with repeated fretting cycles, resulting in higher wear rate and eventually scuffing.

The ability of polymer materials to form a transfer film is known to be greatly dependent on their wear debris shape and size. Studies, e.g., Burris et al. (2008), Wang and Yan (2007) and Bahadur (2000) showed that smaller and fine wear debris were more favorable and helpful to fill the crevices of asperities on the counterface as shown in Figure 6.13. Transferred layers that are formed with larger and flake-like debris are more easily removed from the valleys of metal surfaces with continuous sliding, and need more rapid replenishment, thus resulting in higher wear rate of the polymer surface (Wang and Yan, 2006). The PTFE/Pyrrolidone coating showed very fine wear debris, while the wear debris of PEEK/PTFE coating were larger and flake-like as seen in Figure 6.6 and also in Figure 3.9. Therefore, transferred PTFE/Pyrrolidone is stable on the metal pin surface, and fewer debris are extruded from the contacting region, thus resulting in a smooth metal counterface, as seen in Figure 6.13(b).

6.3.2.4 Transfer films under liquid lubricated conditions

Figure 6.14(a) shows a typical SEM image of the pin surface tested with PTFE/Pyrrolidone coating under liquid lubricated conditions as discussed in Figure 6.8. Compared to the pin surface tested with the same coating under dry conditions in Figure

6.10(a), clearly there seems to be no transferred film in the case of the lubricated condition. The roughness profile of this pin surface shown in Figure 6.14(b) showed even a rougher surface of 333 nm R_q than the case of PEEK/PTFE coating (288 nm R_q), which was similar to the roughness of the original untested pin surface (347 nm R_q). Under lubricated conditions, the formation of polymer transfer film was hindered by the "washing" effect of the liquid lubricant with continuous sliding. Therefore, even though the friction coefficient could be kept low due to the liquid lubricant, higher material removal than under dry conditions was observed because of unfilled sharp metal (pin) asperities as seen in Figure 6.14(b). Thus, the addition of liquid lubricant in a high bearing polymeric coating surface not only did not improve the tribological performance but to the contrary.

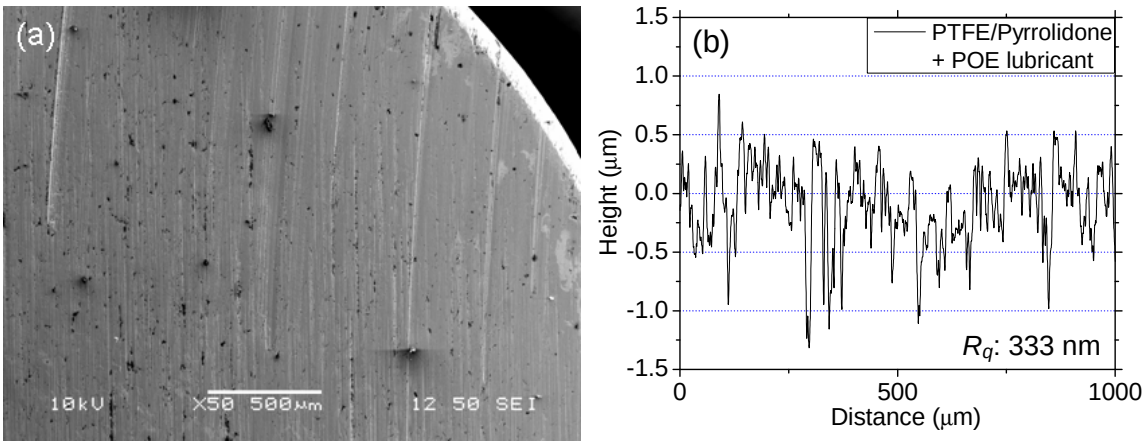

Figure 6.14 (a) SEM image of pin surface tested with PTFE/Pyrrolidone coating under liquid lubricated conditions (6.3 mm pin), and its (b) surface roughness profile.

6.4 Conclusion

Two representative PTFE- and PEEK-based high bearing polymeric coatings were tribologically tested using a specialized tribometer under aggressive fretting contact conditions, and the following conclusions could be drawn:

(a) Both PTFE/Pyrrolidone and PEEK/PTFE coatings showed low friction coefficient in the range of 0.02 – 0.035 under aggressive fretting contact conditions up to 43 MPa nominal contact pressure. Under higher contact pressure, PEEK/PTFE coating scuffed at 133 MPa contact pressure, while PTFE/Pyrrolidone did not show any catastrophic failure up to 166 MPa contact pressure.

(b) The tribological performance of the polymeric coatings under fretting conditions was greatly influenced by the ability of the polymers to form a transfer film on the metal pin counterface. The pin surface tested with PTFE/Pyrrolidone showed a continuous and stable transfer film, while in the case of PEEK/PTFE, only small amount of material was transferred to the counterface, thus exposing hard metal asperities on the contact interface.

(c) Transfer film formation was initiated by interlocking of polymer wear debris within the counterface asperities, thus gradually smoothening and filling the rough pin surface with transferred polymer material. Most of the wear of the polymer film occurred during this initial process of transfer film formation. Once a stable transfer film was formed on the counterface, it acted as a lubricating layer on the interface by protecting the soft polymers from further damage by hard and sharp metal asperities on the counterface. Therefore, PTFE/Pyrrolidone coating which formed a stable transfer film on the counterface did not show any catastrophic failure even after the coating was worn out.

(d) The addition of liquid lubricant on the contact interface in the presence of the polymeric films was not tribologically beneficial. Specifically under such more complex interface conditions, higher wear was measured compared to the

unlubricated case. This is likely due to the fact that the liquid lubricant was washing away the polymer wear debris thus not allowing it to form a transfer film on the metal counter surface.

CHAPTER 7: CONCLUSION AND FUTURE WORK

7.1 Summary of dissertation

Nowadays significant research is conducted in addressing and examining the applicability of polymer materials for use in various industrial sliding/bearing contact surfaces including air-conditioning and refrigeration compressors. Especially, with the development of polymer composite technology, some forms of polymers often have an advantage over other materials such as metals and ceramics showing superior frictional and wear performances. In the past few years, however, majority of research effort was focused only on the bulk form of polymers although the polymer coatings might be more economical and realistic for the actual applications. Therefore, in this dissertation, advanced polymer-based coatings were tribologically characterized for use in aggressive sliding/bearing contact surface applications.

First, several PTFE-, PEEK-, Fluorocarbon- and Resin-based polymer materials were selected and prepared (coated) on gray cast iron substrates (disks). Then, these coatings were comparatively tested using a specialized tribometer to simulate the actual compressor operating conditions including oscillatory motion (simulating piston-type compressors) and unidirectional motion (simulating swash plate compressor operation). It was examined if these polymeric coatings could be used such aggressive sliding/bearing conditions as ACR compressors, and also which coatings between PTFE- and PEEK-based performed better.

Micromechanical properties of these polymeric coatings were examined using instrumented high-load indentation technique. Optimized indentation method was

studied to extract the pure polymeric coating's properties decoupled from the substrate effect. Also, the root causes of tribological performance difference among various coatings were investigated from this material property characterization. Not only mechanical properties such as reduced modulus and hardness, but the micro-structural properties of polymeric coatings could be also explained from their load-displacement behavior during indenting.

Additionally, the polymeric coatings were tested under more aggressive contact conditions such as elevated temperature to investigate the effect of increasing temperature on the tribological behavior of polymeric coatings, as well as to examine the performance limit of PTFE- and PEEK-based polymeric coatings. It was observed that the behavior of polymeric coatings greatly depended on the near contact temperature which eventually determined the visco-elastic property of polymers. Therefore, the visco-elastic property, especially recovery of polymeric coatings was further investigated using instrumented scratch test to directly correlate the recovery property and the frictional behavior of polymeric surfaces.

Finally the tribological performance of two representative PTFE- and PEEK-based polymeric coatings was further evaluated under special conditions, namely, aggressive small amplitude reciprocating (fretting) pin-on-disk conditions. Such a condition is encountered by modern machinery, including air-conditioning and refrigeration compressors, and is sometimes also referred as "dithering" motion. Unlubricated step load-to-failure experiments to determine their scuffing resistance, as well as the effect of liquid lubricant on their friction and wear behavior have been

performed. The morphology of the transfer films on the counterface was observed using SEM and profilometer measurements.

7.2 Main Conclusions

Several conclusions could be made based on the tribological characterization of PTFE- and PEEK-based polymeric coatings performed in this work. These are itemized below:

(1) Unidirectional sliding test of polymeric coatings exhibited acceptable to superior tribological performance with friction coefficient values of 0.04 ~ 0.1 and wear rates of 10^{-7} $mm^3/N \cdot m$ under aggressive oil-less compressor conditions. Therefore, polymeric coatings are likely viable candidates for the next generation of oil-less compressors.

(2) PTFE-based coatings (PTFE/Pyrrolidone and PTFE/MoS_2) generally performed better than PEEK-based coatings (PEEK/PTFE and PEEK/Ceramic) under both piston-type (oscillatory motion) and swash plate (unidirectional motion) compressor conditions, which was not the case for bulk polymer blends (where typically PEEK composites filled with PTFE performed best).

(3) Durability or time-to-failure (3-hour duration) unidirectional testing corresponding to 40.5 km sliding distance showed superb friction and wear behavior of PTFE-based coatings, especially PTFE/Pyrrolidone-2, thus demonstrating its potential applicability for use in oil-less compressors.

(4) Procedures were established for high-load instrumented indentation on polymeric coatings, considering loading profiles (trapezoidal and single loading) and loading rates (10 mN/s) as well as their effect on the measured micromechanical properties.

(5) Using high-load indentations over the thickness of the coating, it was found that at lower contact depths (indenting 1-2 percent of the coating thickness) inconsistent elastic modulus and hardness values were measured due to surface "skin" effects. After that, there was a small plateau region up to a critical contact depth, which was found to be about 10 % of the coating thickness, where substrate effects become evident. This plateau region gives the "true" mechanical properties of the coatings.

(6) PTFE coating exhibited very repeatable load-displacement behavior and extracted micromechanical properties, indicating a uniform and amorphous microstructure, while PEEK coating's load-displacement behavior was quite variable and unpredictable, which was attributed to its semi-crystalline porous microstructure demonstrated from SEM measurements.

(7) Tribological performance of polymeric coatings is not as much directly related to their micromechanical properties, but rather to the coating's structural uniformity, as evident form the instrumented load/unload curves and manifested in their consistent (in the case of PTFE coatings) versus variable (in the case of PEEK coatings) micromechanical properties.

(8) From the frictional behavior of PTFE/Pyrrolidone-2 coating with elevated temperatures, it was observed that COF of amorphous structured polymer surface increased with increasing near contact temperatures (NCT), showing the maximum COF value at its NCT in the vicinity of its glass transition temperature. This is

because, with increasing NCT, polymer surface becomes more plastic resulting in more real contact area, and thus more adhesion on the interfacial zone. Then, as the NCT exceeds the T_g, the COF decreases due to the rapid decline of viscosity and shearing strength on the subsurface zone of polymer caused by the complete scission of molecular chains at temperature higher than T_g. Therefore, it can be summarized that the overall frictional behavior of polymer surface is determined by the viscoelastic property of polymers which directly depends on its near contact temperature.

(9) In order to verify the fact that the polymer surfaces with higher recovery usually had lower COF, the elastic recovery of PTFE-, PEEK-, and ATSP-based polymeric coating surfaces was examined using the scratch testing. As expected, the PTFE/Pyrrolidone-2 coating surface exhibited three times higher elastic recovery (60 %) than PEEK/PTFE coating surface (20 %). Also, ATSP-based coating surface showed the highest recovery around 90 % with the lowest COF values observed directly from the *in-situ* COF measurements during the scratching process.

(10) The tribological performance of the polymeric coatings under fretting conditions was greatly influenced by the ability of the polymers to form a transfer film on the metal pin counterface. The pin surface tested with PTFE/Pyrrolidone showed a continuous and stable transfer film, while in the case of PEEK/PTFE, only small amount of material was transferred to the counterface, thus exposing hard metal asperities on the contact interface.

(11) Transfer film formation was initiated by interlocking of polymer wear debris within the counterface asperities, thus gradually smoothening and filling the rough pin

surface with transferred polymer material. Most of the wear of the polymer film occurred during this initial process of transfer film formation. Once a stable transfer film was formed on the counterface, it acted as a lubricating layer on the interface by protecting the soft polymers from further damage by hard and sharp metal asperities on the counterface.

(12) The addition of liquid lubricant on the contact interface in the presence of the polymeric films was not tribologically beneficial all the time. Specifically under such more complex interface conditions, higher wear rate was measured compared to the unlubricated case. This is likely due to the fact that the liquid lubricant was washing away the polymer wear debris thus not allowing it to form a beneficial transfer film on the metal counter surface.

7.3 Recommendations and Future Work

From the work reported in this dissertation, author has realized that one of the most significant factors affecting the tribological behavior of polymeric coatings might be the microstructure and consequently the wear debris of polymers. Even though Chapter 4 already investigated the microstructure of two representative PTFE- and PEEK-based coatings using indentation and SEM measurements, still there are unanswered questions about more precise and quantitative structural properties of polymeric coatings. Therefore, more preferred and common method to characterize the structure of materials such as transmission electron microscopy (TEM) and X-ray diffraction (XRD) should be used for the polymeric coatings studied in this work. The clear understanding of polymer structure will also explain the formation of wear debris of

polymer surface, and their size and shape as well, which was known to greatly affect the tribological behavior of polymeric coatings. It should be also noted that the structure of polymeric coatings can be significantly affected by the coating process, thus necessitating further investigation of detailed coating process and their effect on the eventual tribological performance of polymeric coatings.

It was shown in Chapter 5 that another important factor determining the tribological behavior of polymeric coatings was the temperature, more specifically near contact temperature (NCT) of polymer interface. Therefore, further study should be focused on the material property characterization under elevated temperature conditions compared to room temperature measurements in this work. Various material properties such as modulus, hardness, scuffing resistance and recovery under varying temperature will give us insight of different tribological behavior of different polymer materials.

Lastly, these polymeric coating can be combined with advanced surface technology such as surface texturing to result in superior lubricity on the contact interface. During the last dozen years the use of surface texturing has been shown to reduce friction and prolonged component life, under primarily lubricated conditions (Etsion, 2004 and Etsion, 2005). Also, initial study of this laser-texturing technique by Mishra and Polycarpou (2011) already showed their significant effect on the tribological performance improvement of compressor-specific surfaces under starved lubrication conditions. Therefore, now, further tribological investigation of textured surface not only with oils but also with polymeric coatings will be needed to better understand their interaction with solid lubricants, consequently resulting in promising tribological performance for compressor use.

BIBLIOGRAPHY

Araki, Y., Stress relaxation of polytetrafluoroethylene in the vicinity of its glass transition temperature at about 130°C, *J. Appl. Polym. Sci.* **9** (1965) 1515-1524.

ATSP Innovations, http://www.atspinnovations.com, accessed in October 27, 2012.

Bahadur, S., The development of transfer layers and their role in polymer tribology, *Wear* **245** (2000) 92-99.

Bahadur, S., C. Sunkara, Effect of transfer film structure, composition and bonding on the tribological behavior of polyphenylene sulfide filled with nano particles of TiO_2, ZnO, CuO and SiC, *Wear* **258** (2005) 1411-1421.

Bahadur, S., C.J. Schwartz, The influence of nanoparticle fillers in polymer matrices on the formation and stability of transfer film during wear, in: K. Friedrich, A.K. Schlarb (Eds.), *Tribology of polymeric nanocomposites – Friction and wear of bulk materials and coatings*, Elsevier, Oxford, UK (2008) 17-34.

Bijwe, J., S. Sen, A. Ghosh, Influence of PTFE content in PEEK–PTFE blends on mechanical properties and tribo-performance in various wear modes, *Wear* **258** (2005) 1536-1542.

Bijwe, J., W. Hufenbach, K. Kunze, A. Langkamp, Polymer composite bearings with engineered tribo-surfaces, in: K. Friedrich, A.K. Schlarb (Eds.), *Tribology of polymeric nanocomposites – Friction and wear of bulk materials and coatings*, Elsevier, Oxford, UK (2008) 17-34.

Bloyce, A., Coatings for high performance pumps and compressors, *World Pumps* **2000**(400) (2000) 43-45.

Bolshakov, A., G.M. Pharr, Influences of pileup on the measurement of mechanical properties by load and depth sensing indentation techniques, *J. Mater. Res.* **13** (1998) 1049-1058.

Brinson, H.F., L.C. Brinson, in: *Polymer Engineering Science and Viscoelasticity, An Introduction*, Springer, New York, NY (2008).

Briscoe, B.J., The tribology of composite materials: A preface, in: K. Friedrich (Eds.), *Advances in composite tribology*, Elsevier, Amsterdam (1993) 3-15.

Briscoe, B.J., L. Fiori, E. Pelillo, Nano-indentation of polymeric surfaces, *J. Phys. D: Appl. Phys.* **31** (1998) 2395-2405.

Briscoe, B.J., S.K. Sinha, Wear of polymers, *Proc. Inst. Mech. Eng., Part J: J. Eng. Tribol.* **216** (2002) 401-413.

Briscoe, B.J., S.K. Sinha, Tribology of polymeric solids and their composites, in: G. Stachowiak (Eds.), *Wear: Materials, Mechanisms and Practice*, John Wiley & Sons, England (2005) 223-267.

Burris, D.L., W.G. Sawyer, A low friction and ultra low wear rate PEEK/PTFE composite, *Wear* **261** (2006) 410-418.

Burris, D.L., W.G. Sawyer, Tribological behavior of PEEK components with compositionally graded PEEK/PTFE surfaces, *Wear* **262** (2007) 220-224.

Burris, D.L, K. Santos, S.L. Lewis, X. Liu, S.S. Perry, T.A. Blanchet, L.S. Schadler, W. Gregory Sawyer, Polytetrafluoroethylene matrix nanocomposites for tribological applications, in: K. Friedrich, A.K. Schlarb (Eds.), *Tribology of polymeric nanocomposites – Friction and wear of bulk materials and coatings*, Elsevier, Oxford, UK (2008) 403-438.

Cannaday, M.L., A.A. Polycarpou, Tribology of unfilled and filled polymeric surfaces in refrigerant environment for compressor applications, *Tribol. Lett.* **19**(4) (2005) 249-262.

Chang, L., Z. Zhang, L. Ye, K. Friedrich, Tribological properties of high temperature resistant polymer composites with fine particles, *Tribol. Int.* **40** (2007) 1170-1178.

Chasiotis, I., Q. Chen, G. M. Odegard, T. S. Gates, Structure-property relationships in polymer composites with micrometer and submicrometer graphite platelets, *Exp. Mech.* **45**(6) (2005) 507-516.

Chen, W.X., F. Li, G. Han, J.B. Xia, L.Y. Wang, J.P. Tu, Z.D. Xu, Tribological behavior of carbon-nanotube-filled PTFE composites, *Tribol. Lett.* **15**(3) (2003) 275-278.

Dascalescu, D., K. Polychronopoulou, A.A. Polycarpou, The significance of tribochemistry on the performance of PTFE-based coatings in CO_2 refrigerant environment, *Surf. Coat. Tech.* **204** (2009) 319-329.

Demas, N.G., A.A. Polycarpou, Ultra high pressure tribometer for testing CO_2 refrigerant at chamber pressures up to 2000 psi to simulate compressor conditions, *Tribol. T.* **49** (2006) 291-296.

Demas, N.G., A.A. Polycarpou, Tribological performance of PTFE-based coatings for air-conditioning compressors, *Surf. Coat. Tech.* **203** (2008) 307-316.

Demas, N.G., J. Zhang, A.A. Polycarpou, J. Economy, Tribological characterization of aromatic thermosetting copolyester (ATSP) blends with PTFE in air conditioning compressor environment, *Tribol. Lett.* **29** (2008) 253-258.

Escobar Nunez, E, S. Yeo, K. Polychronopoulou, A.A. Polycarpou, Tribological study of high bearing blended polymer-based coatings for air-conditioning and refrigeration compressors, *Surf. Coat. Tech.* **205** (2011) 2994-3005.

Etsion, I., Improving tribological performance of mechanical components by laser surface texturing, *Tribol. Lett.* **17**(4) (2004) 733-737.

Etsion, I., State of the art in laser surface texturing, *J. Tribol.* **127** (2005) 248-253.

Friedrich, K., Z. Lu, A.M. Hager, Overview on polymer composites for friction and wear application, *Theor. Appl. Fract. mech.* **19** (1993) 1-11.

Friedrich, K., Z. Zhang, A.K. Schlarb, Effects of various fillers on the sliding wear of polymer composites, *Compos. Sci. Tech.* **65**(15-16) (2005) 2329-2343.

Fusaro, R.L., Self-lubricating polymer composites and polymer transfer film lubrication for space applications, *Tribol. Int.* **23** (1990) 105-122.

Hanchi, J., N.S. Eiss, Jr, Dry sliding friction and wear of short carbon-fiber-reinforced polyetheretherketone (PEEK) at elevated temperatures, *Wear* **203-204** (1997) 380-386.

Hay, J.L., G.M. Pharr, Instrumented Indentation Testing, *ASM Handbook Volume 8: Mechanical Testing and Evaluation,* 10th ed., edited by H. Kuhn and D. Medlin (ASM International, Materials Park, OH, 2000), 231-243.

Hay, J., Measuring substrate-independent modulus of dielectric films by instrumented indentation, *J. Mater. Res.* **24**(3) (2009) 667-677.

Holmberg, K., A. Matthews, in: *Coatings Tribology: Properties, Mechanisms, Techniques and Applications in Surface Engineering*, 2nd edition, edited by B.J. Briscoe, Elsevier B.V., Oxford, UK (2009)

Hufenbach, W., K. Kunze, J. Bijwe, Sliding wear behaviour of PEEK-PTFE blends, *J. Synthetic Lubrication* **20**(3) (2003) 227-240.

Katta, J.K., M. Marcolongo, A. Lowman, K.A. Mansmann, Friction and wear behavior of poly(vinyl alcohol)/poy(vinyl pyrrolidone) hydrogels for articular cartilage replacement, *J. Biomed. Mater. Res. A* **83A**(2) (2007) 471-479.

Klapperich, C., K. Komvopoulos, L. Pruitt, Nanomechanical properties of polymers determined from nanoindentation experiments, *J. Tribol.* **123**(3) (2001) 624-631.

Lal, B., S. Alam, G.N. Mathur, Tribo-investigation on PTFE lubricated PEEK in harsh operating conditions, *Tribol. Lett.* **25**(1) (2007) 71-77.

Lee, Y.Z., S.D. Oh, Friction and wear of the rotary compressor vane-roller surfaces for several sliding conditions, *Wear* **255** (2003) 1168-1173.

Lin, L., G.S. Blackman, R.R. Matheson, A new approach to characterize scratch and mar resistance of automotive coatings, *Prog. Org. Coat.* **40** (2000) 85-91.

Lu, Z.P., K. Friedrich, On sliding friction and wear of PEEK and its composites, *Wear* **181-183** (1995) 624-631.

Mata, M., O. Casals, J. Alcala, The plastic zone size in indentation experiments: The analogy with the expansion of a spherical cavity, *International Journal of Solids and Structures* **43** (2006) 5994-6013.

McCook, N.L., D.L. Burris, G.R. Bourne, J. Steffens, J.R. Hanrahan, W.G. Sawyer, Wear resistant solid lubricant coating made from PTFE and epoxy, *Tribol. Lett.* **18**(1) (2005) 119-124.

Mishra, S.P., A.A. Polycarpou, Tribological studies of unpolished laser surface textures under starved lubrication conditions for use in air-conditioning and refrigeration compressors, *Tribol. Int.* **44** (2011) 1890-1901.

Ohmura, T., S. Matsuoka, K. Tanaka, T. Yoshida, Nanoindentation load-displacement behavior of pure face centered cubic metal thin films on a hard substrate, *Thin Solid Films* **385** (2001) 198-204.

Oliver, W.C., G.M. Pharr, An improved technique for determining hardness and elastic modulus using load and displacement sensing indentation experiments, *J. Mater. Res.* **7**(6) (1992) 1564-1583.

Pergande, S.R., A.A. Polycarpou, T.F. Conry, Nanomechanical properties of aluminum 390-T6 rough surfaces undergoing tribological testing, *J. Tribol.* **126** (2004) 573-582.

Sheiretov, T., W. Van Glabbeek, C. Cusano, Evaluation of the tribological properties of polyimide and poly(amide-imide) polymers in a refrigerant environment, *Tribol. T.* **38**(4) (1995) 914-922.

Solzak, T.A., A.A. Polycarpou, Tribology of WC/C coatings for use in oil-less piston-type compressors, *Surf. Coat. Tech.* **201** (2006) 4260-4265.

Solzak, T.A., A.A. Polycarpou, Tribology of coatings for use in oil-less swashplate compressors, in: *Proceedings of the 9th Biennial ASME Conference on Engineering Systems Design and Analysis*, **ESDA2008-59380**, Haifa, Israel (2008).

Solzak, T.A., A.A. Polycarpou, Tribology of hard protective coatings under realistic operating conditions for use in oilless piston-type and swash-plate compressors, *Tribol. T.* **53**(3) (2010) 319-328.

Stening, T.C., C.P. Smith, P.J. Kimber, Polyaryletherketone: high performance in a new thermoplastic, *Mod. Plast. Int.* **8** (1982) 54–57.

Stolarski, T.A., Tribology of polyetheretherketone, *Wear* **158** (1992) 71-78.

Strojny, A., X. Xia, A. Tsou, W.W. Gerberich, Techniques and considerations for nanoindentation measurements of polymer thin film constitutive properties, *J. Adhes. Sci. Technol.* **12**(12) (1998) 1299-1321.

Suh, A.Y., A.A. Polycarpou, Analytical determination of the surface energy of sub-5 nm head-disk interfaces accounting for multilayer effects, *J. Appl. Phys.* **99** (2006) 08N111.

Suh, N.P., in: *Tribophysics*, Prentice-Hall, Englewood Cliffs, NJ (1986).

Sung, H.C., Tribological characteristics of various surface coatings for rotary compressor vane, *Wear* **221** (1998) 77-85.

Tayebi, N., A.A. Polycarpou, T.F. Conry, Effect of substrate on determination of hardness of thin films by nanoscratch and nanoindentation techniques, *J. Mater. Res.* **19**(6) (2004) 1791-1802.

Wang, Y., F. Yan, Tribological properties of transfer films of PTFE-based composites, *Wear* **261** (2006) 1359-1366.

Wang, Y., F. Yan, A study of tribological behaviour of transfer films of PTFE/bronze composites, *Wear* **262** (2007) 876-882.

Xia, X., A. Strojny, L.E. Scriven, W.W. Gerberich, A. Tsou, C.C. Anderson, Constitutive property evaluation of polymeric coatings using nanomechanical methods, *Mater. Res. Soc. Symp. Proc.* **522** (1998) 199-204.

Yamane, M., T.A. Stolarski, S. Tobe, Wear and friction mechanism of PTFE reservoirs embedded into thermal sprayed metallic coatings, *Wear* **263** (2007) 1364-1374.

Zhang, G., H. Liao, H. Li, C. Mateus, J.-M. Bordes, C. Coddet, On dry sliding friction and wear behaviour of PEEK and PEEK/SiC-composite coatings, *Wear* **260** (2006) 594-600.

Zhang, G., W.-Y. Li, M. Cherigui, C. Zhang, H. Liao, J.-M. Bordes, C. Coddet, Structures and tribological performances of PEEK-based coatings designed for tribological application, *Prog. Org. Coat.* **60** (2007) 39-44.

Zhang, G., H. Yu, C. Zhang, H. Liao, C. Coddet, Temperature dependence of the tribological mechanisms of amorphous PEEK (polyetheretherketone) under dry sliding conditions, *Acta Mater.* **56** (2008) 2182-2190.

Zhang, J., N.G. Demas, A.A. Polycarpou, J. Economy, A new family of low wear low coefficient of friction polymer blend based on polytetrafluoroethylene and an aromatic thermosetting polyester, *Polym. Advan. Technol.* **19** (2008(1)) 1105-1112.

Zhang, J., A.A. Polycarpou, J. Economy, An improved tribological polymer coating system for metal surfaces, *Tribol. Lett.* **38**(3) (2010) 355-365.

Zhao, Q., Y. Liu, H. Müller-Steinhagen, G. Liu, Graded Ni-P-PTFE coatings and their potential applications, *Surf. Coat. Tech.* **155** (2002) 279-284.

APPENDIX: PRELIMINARY RESULTS FOR TRIBOLOGICAL CHARACTERIZATION OF ATSP-BASED COATINGS

A.1 Introduction

Aromatic Thermosetting Copolyesters (ATSP) system was invented by material science Professor J. Economy (UIUC), and newly founded coating development company, ATSP Innovations has recently acquired an exclusive license for the intellectual property to commercialize this technology. Currently, there has been a collaboration work with this company to apply ATSP blended with various functional additives (e.g. PTFE, MoS_2, graphite, PI) as a coating and test them under realistic compressor-specific conditions.

Based on the recent work on bulk ATSP and ATSP/PTFE blends (Zhang *et al.*, 2008(1) and Demas *et al.*, 2008), it was found that pure bulk ATSP experienced "zero wear" but somewhat high friction while ATSP/PTFE blends exhibited excellent tribological performance by combining the harder ATSP "rock-like" structures with the low friction properties of PTFE. Also, some preliminary ATSP coating work has been done under only very mild testing conditions in Zhang *et al.* (2010). In the case of pure ATSP coatings, significantly high friction coefficient (around 1.0) and wear rate (1.62×10^{-4} $mm^3/N \cdot m$) were observed. However, the ATSP coating blended with fluoroadditive powder lubricant (Zonyl® TE-5069AN) showed significantly reduced frictioin coefficient (around 0.2) and wear rate (7.36×10^{-7} $mm^3/N \cdot m$). To directly compare the improved tribological performance of ATSP/Fluoroadditive coatings with commercially available PTFE-based coatings, PTFE/Pyrrolidone-1 coating was tested under the exact same conditions, and its friction coefficient was similar to that of ATSP/Fluoroadditive coating,

but the wear rate was estimated to be 1.23×10^{-4} $mm^3/N \cdot m$, which was over 150 times higher than for ATSP/Fluoroadditive coatings.

Coating processes and blend compositions are being developed and optimized to find out the best performing coatings, and some preliminary tribo-testing of these new coatings was performed to examine their frictional and wear behaviors under aggressive sliding/bearing contact conditions. Therefore, in this section, 5% (wt%) ATSP/PTFE coating solution-casted on the cast iron substrate was tested under aggressive and realistic compressor specific conditions, namely the conditions under which PTFE- and PEEK-based coating were already tested in Chapter 3, which enables the direct comparison of tribological performance between ATSP- and PTFE/PEEK-based coatings.

A.2 Results and discussion

A.2.1 Dry-unidirectional testing under room temperature

For the swash plate compressor simulation, the unidirectional sliding tests were performed with a rotating speed of 1500 rpm and an average wear track diameter of 43.2 mm which corresponded to a linear speed of 3.75 m/s. Environmental conditions include 445 N normal load, room temperature without any feedback control, 172 kPa (25 psi) of CO_2 refrigerant with no lubricant, and 30 min duration, corresponding to 6.75 km sliding distance. The crowned 52100 steel shoes with 9.6 mm diameter were used as a counter part. More details about the experimental setup can be found in Section 3.2 and Table 3.2 as well.

Figure A.1(a) and (b) show the *in-situ* measurements of the friction coefficient and near contact temperature, respectively, of 5% ATSP/PTFE coating during 30 min

dry-unidirectional testing. Three strange bumps in the COF plot in Figure A.1(a) are thought to be the machine noise as no such behaviors are observed in 60 min tests later. 5% ATSP/PTFE coating showed relatively stable and low friction coefficient with average value of 0.077 which is quite similar to the COF of PEEK/PTFE coating tested under the same conditions in Section 3.3.2 (Table 3.3). Even though, higher COF of 5% ATSP/PTFE than PTFE-based coatings, its near contact temperature was very similar to the NCT of PTFE-based coating at around 160°C (Figure A.1(b)) showing its good heat dissipation capability compared to PEEK-based coatings.

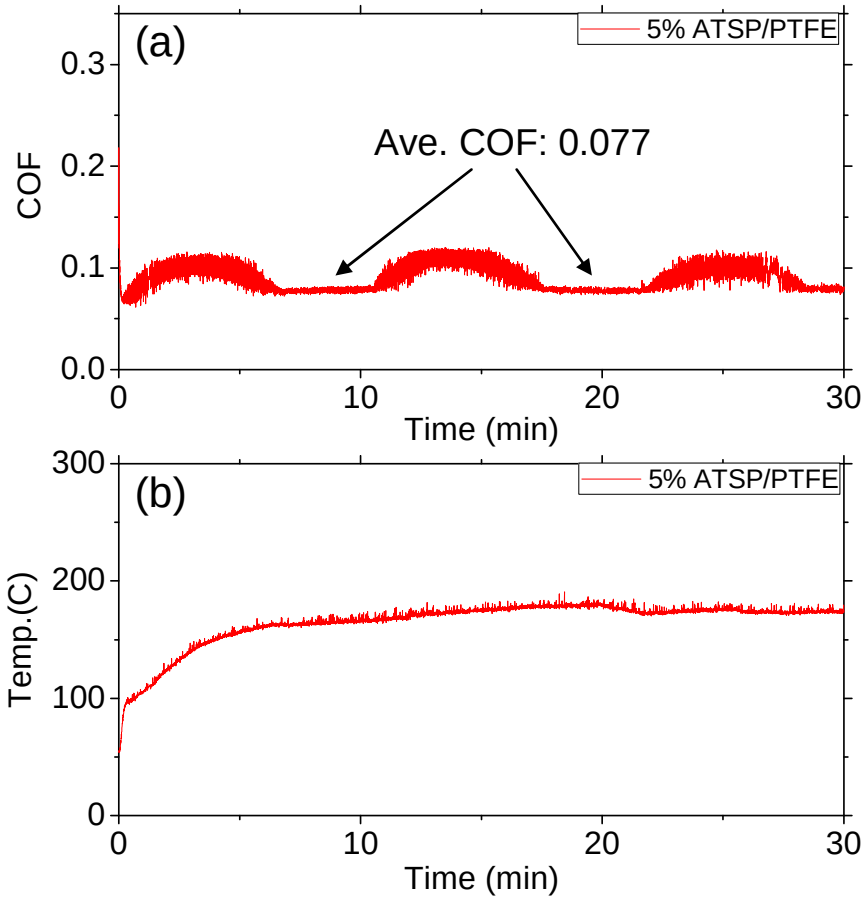

Figure A.1 *In-situ* (a) friction coefficient (COF) and (b) near contact temperature (NCT) of 5% ATSP/PTFE coating during 30 min dry-unidirectional testing.

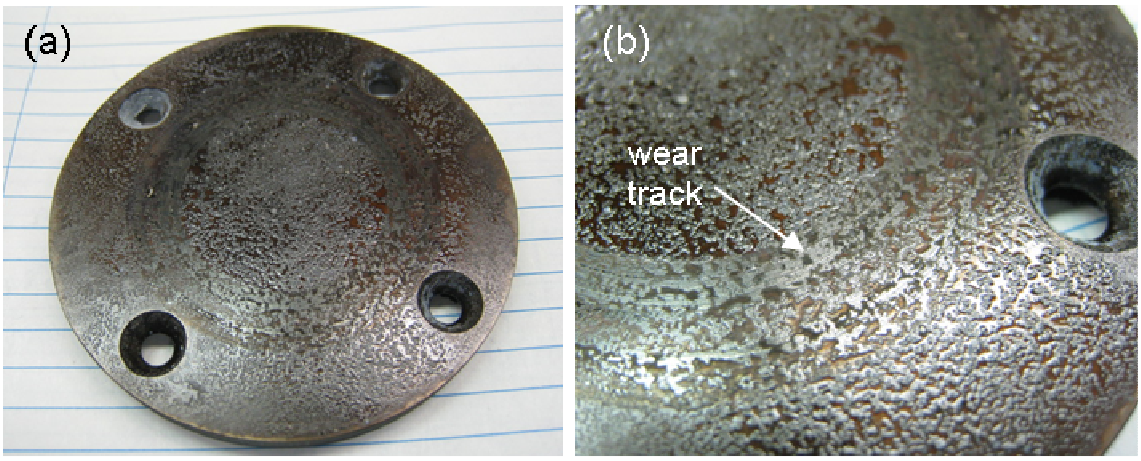

Figure A.2 (a) Optical image of 5% ATSP/PTFE coating surface after 30 min dry-unidirectional testing in Figure A.1, and (b) its zoomed-in image showing the wear track.

Figure A.2 shows the coating surface and wear track after 30 min dry-unidirectional testing. Initially, the coating surface was relatively rough compared to other commercially available PTFE- and PEEK-based coatings due to PTFE powders which were not well distributed in this Phase-I coating system. Interestingly, this coating showed almost zero wear (material removal) without any wear debris observed, and only mild burnishing was seen in Figure A.2(b).

The cross-section line profile of this wear track was measured using a stylus profilometer as seen in Figure A.3. As already seen in the optical images, Figure A.3 showed significantly rough surface of 5% ATSP/PTFE coating with many tall asperities of about 20 μm height. It was observed that only top parts of these tall asperities were removed by the sliding without any severe wear of sub-surface coating layers, thus resulting in almost zero wear in the optical images. Now, therefore, longer duration (60 min) testing was performed for this coating system to see if this superior wear performance is its actual steady-state property.

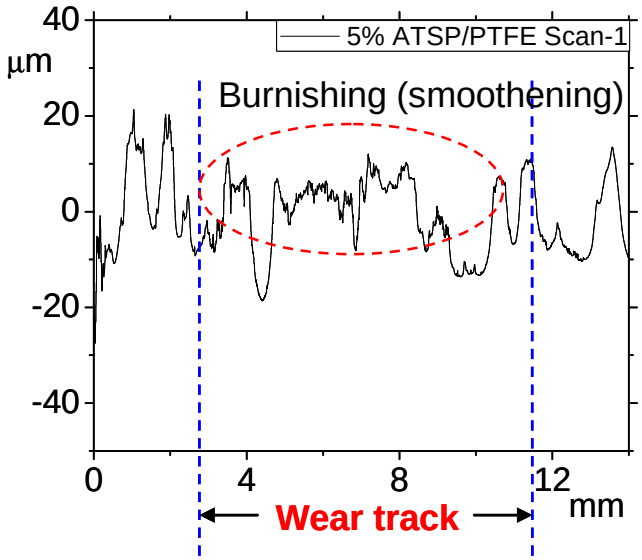

Figure A.3 Profilometric wear track measurement of 5% ATSP/PTFE coating after 30 min dry-unidirectional testing.

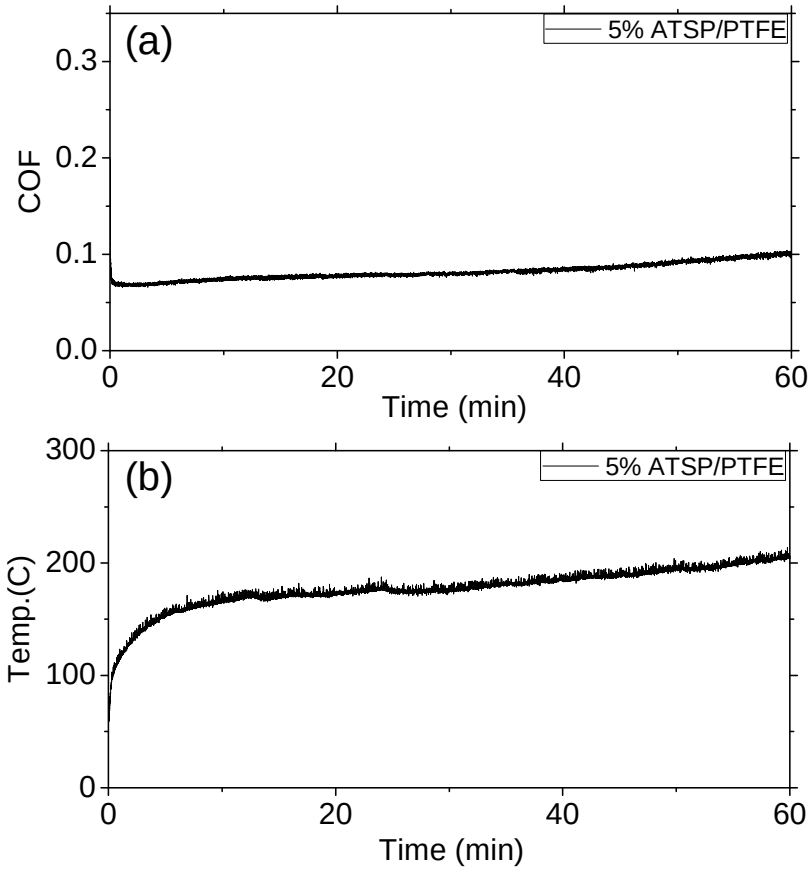

Figure A.4 *In-situ* (a) friction coefficient (COF) and (b) near contact temperature (NCT) of 5% ATSP/PTFE coating during 60 min dry-unidirectional testing.

Figure A.4(a) and (b) show the *in-situ* friction coefficient and near contact temperature, respectively, of 5% ATSP/PTFE coating during 60 min dry-unidirectional testing. Testing was performed under exactly same conditions as in Figure A.1 except the testing duration. We can clearly see that the behaviors of both COF and NCT are pretty repeatable with previous 30 min testing results (note that there is no machine noise in COF at this time). Even though the COF slightly increased through the whole testing duration, it still exhibited extremely stable behavior with 0.1 at the end of the test. NCT also gradually increased up to 200 °C at the end of the test. Compared to commercially available coatings under longer duration testing in Section 3.3.2.3 (in Figure 3.12), 5% ATSP/PTFE coating clearly showed much better frictional and heat dissipation behavior than PEEK-based coatings, but not as good as PTFE-based coatings.

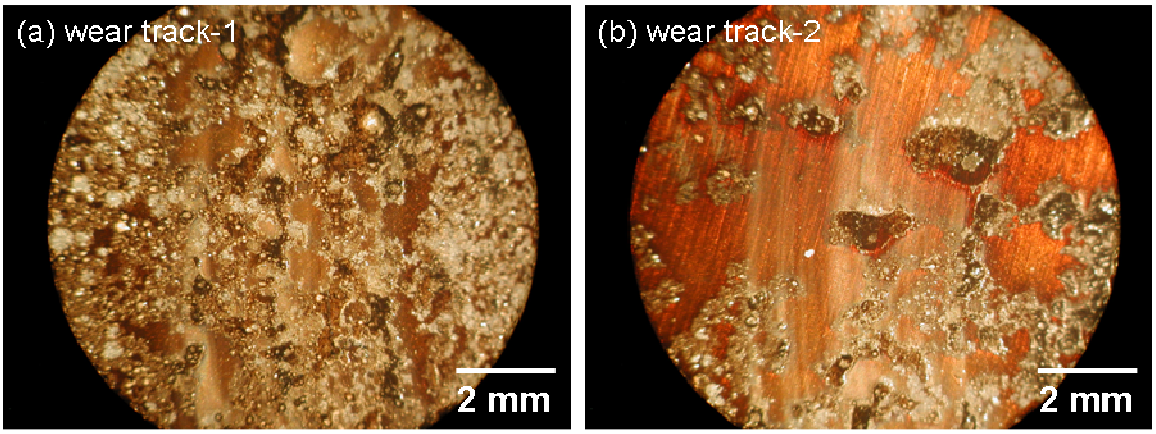

Figure A.5 Optical images of two different locations of wear track on the 5% ATSP/PTFE coating surface after 60 min dry-unidirectional testing (in Figure A.4) with (a) lots of PTFE powders and (b) less PTFE powders.

After testing, the wear track was observed under the optical microscope as seen in Figure A.5. Figure A.5(a) shows the wear track of the location where lots of PTFE powders were placed compared to the location in Figure A.5(b). The location with much

PTFE powders in Figure A.5(a) showed almost zero material removal, while the location with less PTFE powder showed clearer wear mark but still only mild burnishing level. Therefore, it can be seen that the good and even distribution of PTFE powder affects the wear behavior of coating surface.

The wear track was also measured under the profilometer to see its cross-section line profile as seen in Figure A.6(a), and Figure A.6(b) shows the optical image of shoe surface after testing. Even after 60 min testing, the wear track profile was similar to the one after 30 min testing showing only smoothening of the top parts of tall asperities. On the other hand, interestingly, the shoe surface (52100 steel) exhibited mild burnishing as seen in Figure A.6(b), which had never been observed for the case of PTFE- and PEEK-based coatings. Therefore, extremely strong wear resistance of 5% ATSP/PTFE coating surface was observed.

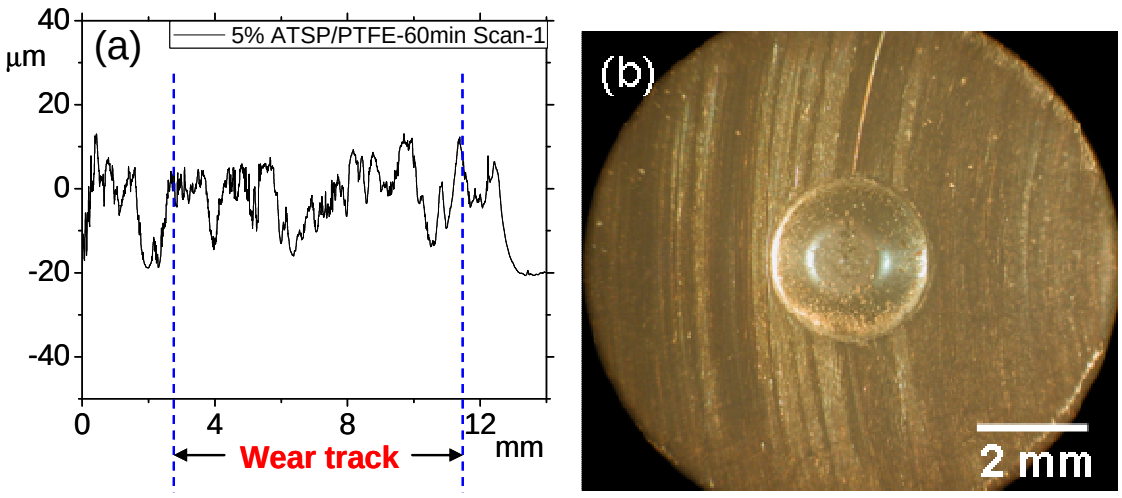

Figure A.6 (a) Profilometric wear track measurement of 5% ATSP/PTFE coating, and (b) shoe surface showing mild burnishing after 60 min dry-unidirectional testing.

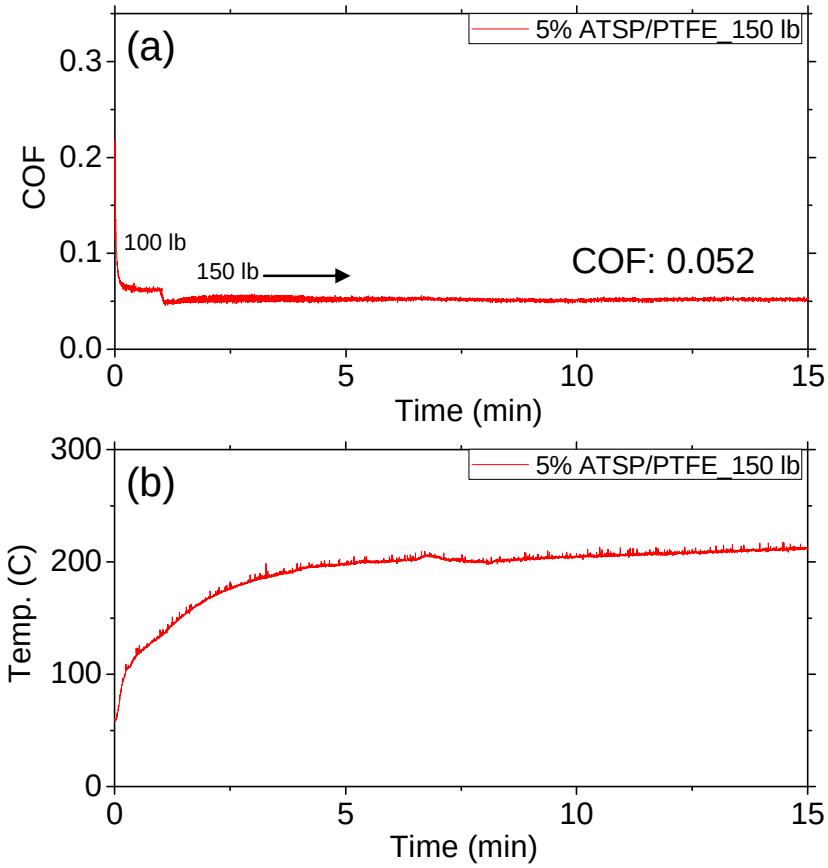

Figure A.7 *In-situ* (a) friction coefficient (COF) and (b) near contact temperature (NCT) of 5% ATSP/PTFE coating during 15 min dry-unidirectional testing under 150 lb normal load.

On the same coating surface previously tested in Figure A.4 (due to the limited samples provided at the time, and also zero wear even after 60 min testing), higher normal load testing was performed with 668 N (150 lb) in Figure A.7 and 890 N (200 lb) in Figure A.8. Each testing was performed under the same testing conditions as in Figure A.4 (only except the normal load condition) during only 15 min to examine the scuffing resistance of 5% ATSP/PTFE coating. Under 668 N normal load condition in Figure A.7, this coating showed still very stable friction coefficient with even lower value of 0.052 than COF under 445 N normal load condition, 0.077. However, its NCT increased fast up to 200 °C even after 5 min of testing. Under 890 N normal load condition in Figure

A.8, even lower COF of 0.048 was observed with significantly stable behavior through the whole testing duration.

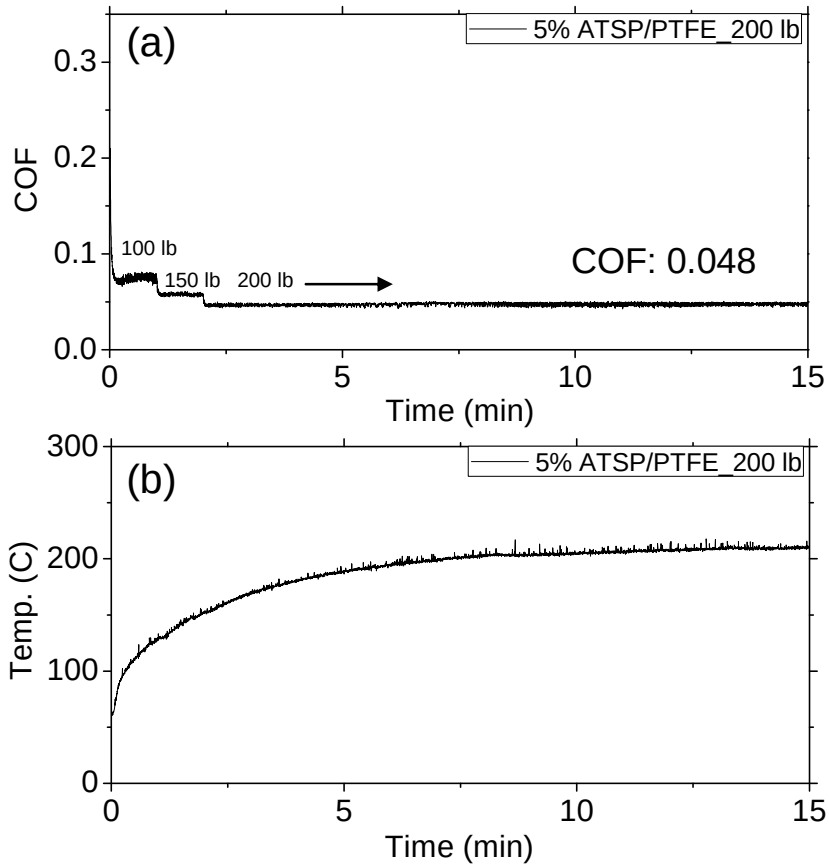

Figure A.8 *In-situ* (a) friction coefficient (COF) and (b) near contact temperature (NCT) of 5% ATSP/PTFE coating during 15 min dry-unidirectional testing under 200 lb normal load.

Figure A.9(a) and (b) show the coating surface with wear track after 668 N (150 lb) and 890 N (200 lb) normal load testing, respectively. In the case of 668 N normal load testing, the wear track still showed only very mild burnishing as seen in Figure A.9(a), but after 890 N normal load testing, eventually the clearly visible wear track was observed as seen in Figure A.9(b).

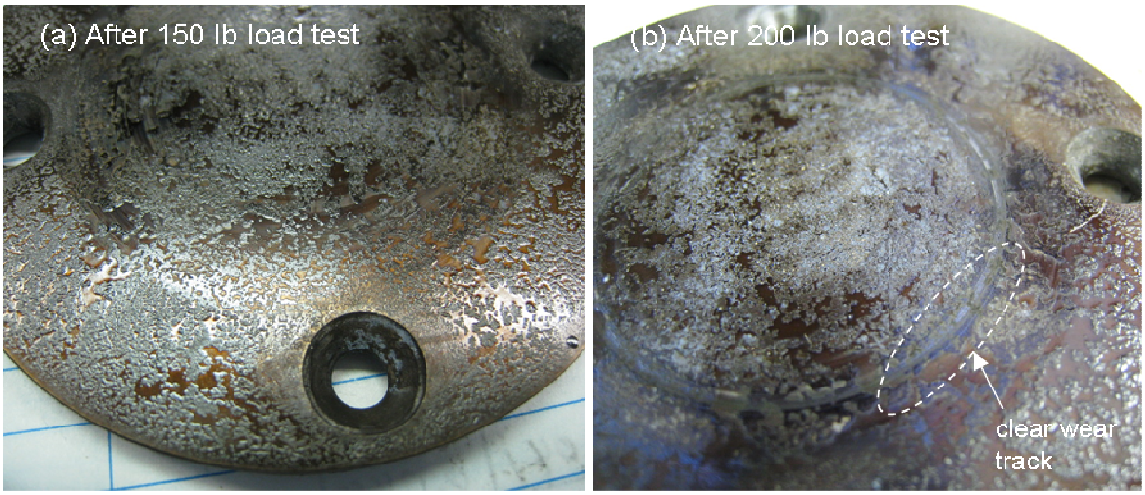

Figure A.9 5% ATSP/PTFE coating surface with wear track after (a) 668 N (150 lb) and (b) 890 N (200 lb) normal load condition dry-unidirectional testing during 15 min.

A.2.2 Dry-unidirectional testing under varying temperatures

In previous section, 5% ATSP/PTFE coating showed relatively low friction coefficient similar to PEEK-based commercial coatings, and superior wear performance to any other coatings tested in this dissertation under room temperature testing. In this section, therefore, their tribological behavior was examined again under varying temperature conditions, namely under 3, 23, and 80 °C. Except temperature condition, all the other testing conditions are the same as in Figure A.4, 445 N normal load, dry-unidirectional and 25 psi of CO_2 environment.

Figure A.10(a) and (b) show the *in-situ* friction coefficient and near contact temperature of 5% ATSP/PTFE coating during 60 min dry-unidirectional testing under 3 different temperature conditions. It should be noted that for 3 °C condition, the testing was intentionally stopped by the operator after 20 min and it was not a failure of testing. At low temperature (3 °C) condition, slightly lower COF of about 0.065 than COF in room temperature condition (0.077) was observed, while the COF under high temperature

condition showed almost same behavior as COF under room temperature. As for the near contact temperature, depending on the setting temperature, their increasing speed was a little different at the beginning of the testing, but we could see that they were eventually closing to 200 °C at the end of the testing.

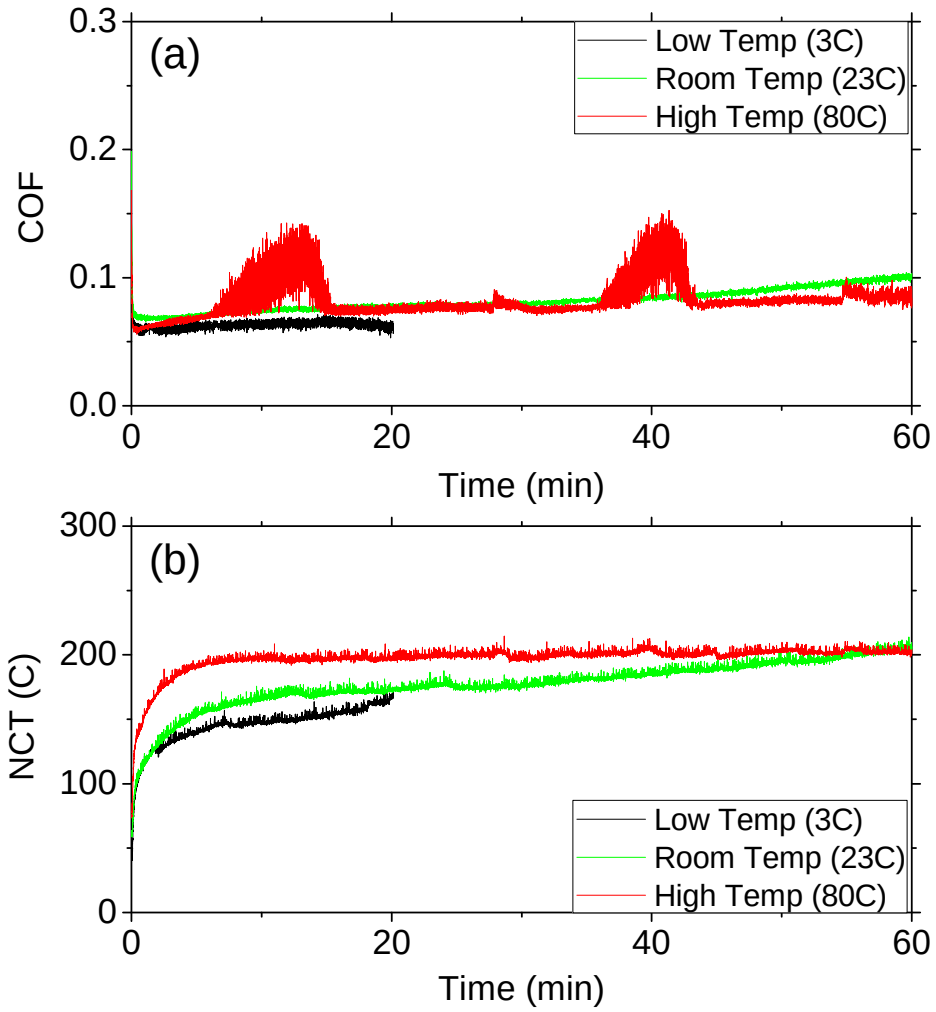

Figure A.10 *In-situ* (a) friction coefficient (COF) and (b) near contact temperature (NCT) of 5% ATSP/PTFE coating during 60 min dry-unidirectional testing under three different temperature conditions.

After each testing, the coating surface and the wear track were optically examined as seen in Figure A.11. Under 3°C condition, still very mild burnishing was observed on

the coating surface in Figure A.11(a) even though there was only one clear wear scar as seen in zoomed-in image in Figure A.11(b). Under 80 °C condition, much clearer wear track was observed in Figure A.11(b) and (d). Therefore, compared to room temperature testing with almost zero wear in Figure A.5, slightly higher wear was observed under higher temperature condition. However, still the wear resistance of this 5% ATSP/PTFE coating is incomparably superior to any other commercially available PTFE- and PEEK-based coatings only except PTFE/Pyrrolidone-2 coating.

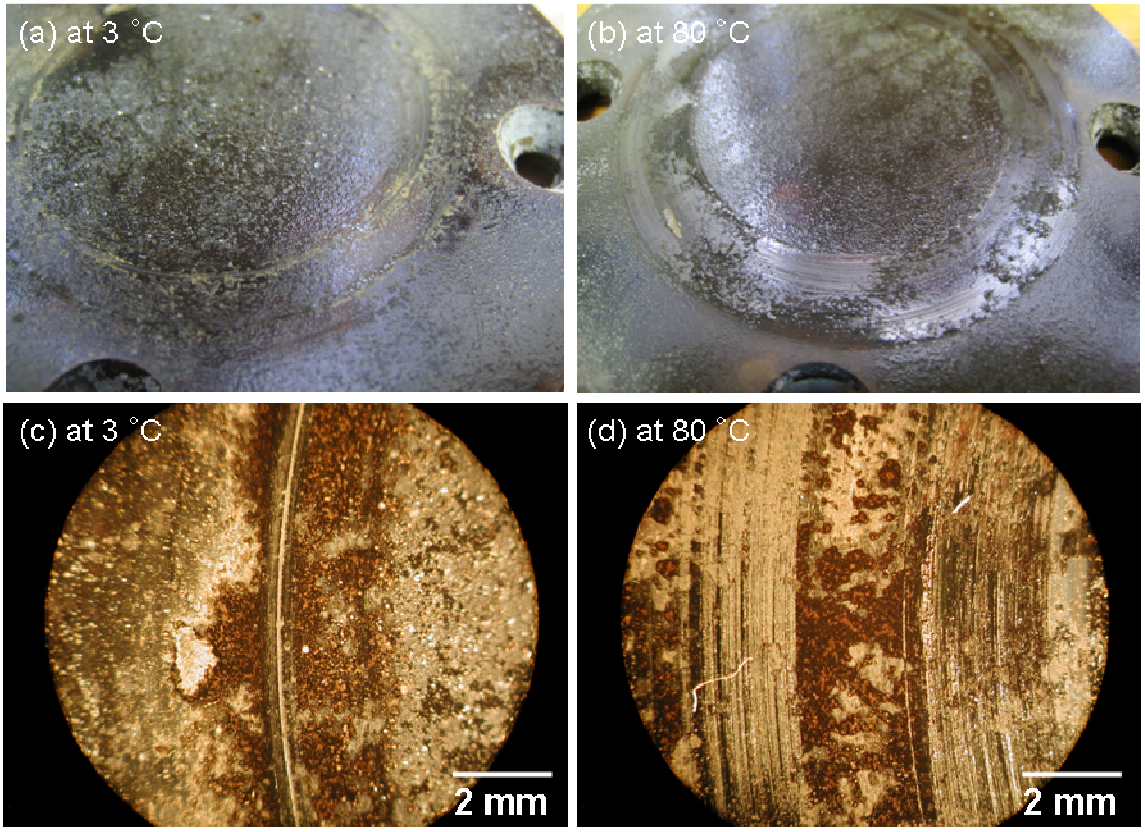

Figure A.11 Optical images of 5% ATSP/PTFE coating surface with wear track after dry-unidirectional testing under (a) 3 °C and (b) 80 °C conditions, and (c) zoom-in image of (a) and zoom-in image of (b).

A.3 Conclusion

5% ATSP/PTFE material coated on the cast iron substrate was preliminarily tested under aggressive compressor-specific conditions and the following conclusions could be drawn,

(a) 5% ATSP/PTFE coating showed relatively low friction coefficient of 0.077 under room temperature and 445 N normal load conditions, which was similar to the COF of PEEK/PTFE, but much more stable behavior than PEEK/PTFE coating. Also, 5% ATSP/PTFE coating showed almost zero wear without any wear debris observed on the coating surface even after 60 min duration testing.

(b) Higher normal load tests (15 min duration) with 668 N (150 lb) and 890 N (200 lb) exhibited the exceptional scuffing resistance of 5% ATSP/PTFE coating with low and stable friction coefficient (0.052 for 668 N and 0.048 for 890 N) and negligible amount of wear.

(c) Low (3 °C) and high (80 °C) temperature testing performed on 5% ATSP/PTFE coating showed very similar frictional behavior to its room temperature result, but some clear wear marks under high temperature testing was observed compared to almost zero wear under room temperature condition.